Backward Bifurcation in *SIR* endemic models

This thesis is presented in partial fulfillment of the requirements for the Degree of

Masters of Information Science
in
Mathematics

at Massey University, Albany, Auckland,
New Zealand.

Sameeha Qaiser Siddiqui

2008

Abstract

In the well known *SIR* endemic model, the infection-free steady state is globally stable for $\mathcal{R}_0 < 1$ and unstable for $\mathcal{R}_0 > 1$. Hence, we have a forward bifurcation when $\mathcal{R}_0 = 1$. When $\mathcal{R}_0 > 1$, an asymptotically stable endemic steady state exists. The basic reproduction number $\mathcal{R}_0$ is the main threshold bifurcation parameter used to determine the stability of steady states of *SIR* endemic models.

In this thesis we study extensions of the *SIR* endemic model for which a backward bifurcation may occur at $\mathcal{R}_0 = 1$. We investigate the biologically reasonable conditions for the change of stability. We also analyse the impact of different factors that lead to a backward bifurcation both numerically and analytically. A backward bifurcation leads to sub-critical endemic steady states and hysteresis.

We also provide a general classification of such models, using a small amplitude expansion near the bifurcation. Additionally, we present a procedure for projecting three dimensional models onto two dimensional models by applying some linear algebraic techniques. The four extensions examined are: the *SIR* model with a susceptible recovered class; nonlinear transmission; exogenous infection; and with a carrier class.

Numerous writers have mentioned that a nonlinear transmission function in relation to the infective class, can only lead to a system with an unstable endemic steady state. In spite of this we show that in a nonlinear transmission model, we have a function depending on the infectives and satisfying certain biological conditions, and leading to a sub-critical endemic equilibriums.

Acknowledgments

I would like to thank my supervisor Professor Mick Roberts for his patience, for always being there and providing many relevant suggestions and worthy opinions throughout all stages of this thesis.

I also would like to thank to the department of IIMS at the Massey University (Albany) for giving me the opportunity to pursue my postgraduate studies and wish to thank Haydn Cooper for his valuable comments.

I am also grateful to my family, my husband Arsh and my baby Talish, for without their help and support this study would have been impossible.

Contents

List of Tables

List of Figures

1 Introduction

1.1 The Basic *SIR* Model

There are many infections for which the recovered individuals attain an immunity against the infection. This type of infection can be modeled by the *SIR* model, which is based on the classic epidemic theory of Kermack and McKendrick [7]. This model has played an important role in mathematical epidemiology. In this model, a closed population of constant size is subdivided into three classes: susceptible (S) individuals that may suffer infection; infected (I) individuals that transmit infection to the susceptibles; and removed (R) individuals who are recovered and immune or dead.

The proportions in each class at time t are denoted as $s(t)$, $i(t)$ and $r(t)$ respectively. The differential equations representing this system are

$$\begin{aligned} \frac{ds}{dt} &= \mu - \beta si - \mu s, \\ \frac{di}{dt} &= \beta si - (\gamma + \mu)i, \\ \frac{dr}{dt} &= \gamma i - \mu r. \end{aligned} \tag{1}$$

As $r(t)$ = 1 - $s(t)$ - $i(t)$, the system is two dimensional. The parameters are birth and death rate ($\mu > 0$), recovery rate ($\gamma > 0$) and contact rate ($\beta > 0$) (See Table 1). The basic reproduction number $\mathcal{R}_0 = \frac{\beta}{\mu+\gamma}$, is defined to be the expected number of secondary cases generated from an infective case in a susceptible population [12].

Now, if $\mu << \gamma$, then this system becomes the *SIR* epidemic model, which describes the sudden rise and fall of an infection in a closed population, for example influenza, plague etc [3]. If, on the other hand, $\mu \approx \gamma$, then we have the *SIR* endemic model, where an infection tends to persist in a population for a longer period, for example leprosy or tuberculosis. Endemic models focus on when there is no net change in the number of individuals in the infective class, so prevalence of infection remains constant [11].

Thesis Outline

In this thesis, we review properties of the *SIR* epidemic model in Sect. 1.2 briefly, and the endemic model in Sect. 1.3 in detail as this model is the primary subject of this thesis. In Chapters 2 and 4 we present the two and three dimensional extensions of the *SIR*

Variables	Description	Proportions
S	Number of susceptibles	$s(t)$
I	Number of infectives	$i(t)$
R	Number of recovered people with immunity	$r(t)$
Parameters	**Description**	**Dimensions**
μ	Birth and death rate	time^{-1}
γ	Recovery rate	time^{-1}
β	Transmission or contact rate	time^{-1}
$\mathcal{R}_0$	Basic reproduction number	-

Table 1: Summary of the notations used in the *SIR* Model

endemic model respectively discovering different dynamics, using $\mathcal{R}_0$ as the main bifurcation parameter and showing that an endemic infection may persist for some values of $\mathcal{R}_0 < 1$. To prove these dynamics, we calculate the steady states of these models and their stability by analysing the Jacobian matrices using the **Maple** [5]. We also analyse bifurcation and phase-plane diagrams using the **MATLAB** [10]. In short, we set up a model, using nonlinear ordinary differential equations, which is analysed mathematically and simulated numerically.

In Chapters 3 and 5 we give an account of the general analysis for these extensions and investigate the different dynamics by applying Taylor and Binomial expansions using a perturbation variable near the bifurcation point i.e. near $\mathcal{R}_0 = 1$. We also examine what types of bifurcations occur at $\mathcal{R}_0 = 1$. Backward bifurcation, multiple endemic steady states and hysteresis phenomena involve a type of bifurcation, that shows an exchange of stability between infection-free and endemic steady states. We also check if the results at the critical points are consistent with the results in Chapters 2 and 4. Moreover, we put our analysis in the models which have been discussed in [14]. Finally, we discuss our results in Chapter 6.

1.2 The *SIR* Epidemic Model

The *SIR* epidemic model was proposed to explain the rapid rise and fall in the number of infected patients observed in epidemics such as the examples of plague (London 1665-1666, Bombay 1906) and cholera (London 1865). In this model, it is assumed that the population size is effectively constant, that means there are no births, deaths or migration. The incubation period of the infectious agent is considered to be instantaneous, thus the durations of infectivity and disease are equal. It is also assumed that the population interacts homogeneously; with no restriction of age, mobility or other social factors [1].

Starting with the system (1) of the *SIR* epidemic model; we assume that $\mu = 0$, then we have

$$\begin{aligned} \frac{ds}{dt} &= -\beta si, \quad (2) \\ \frac{di}{dt} &= \beta si - \gamma i, \quad (3) \\ \frac{dr}{dt} &= \gamma i. \end{aligned}$$

As we assume that the population is of constant size we have $r(t) = 1$ - $s(t)$ - $i(t)$. The rate parameters for the transition between the three classes are β and γ (see Sect. 1.1). The term $-\beta si$ describes a transmission of infection due to the interaction between susceptibles and infectives. The term $-\gamma i$ describes the recovery from an infection [3].

Observe that if $\frac{di}{dt} \leq 0$ at $t = 0$, then there is no epidemic, while if $\frac{di}{dt} > 0$ at $t = 0$, then an epidemic occurs i.e. an increase in infective individuals. Also, equation (2) implies that if the term $-\beta si = 0$, then we get either $s = 0$ or $i = 0$. If $i = 0$, then $\frac{di}{dt} = 0$, which means an infection-free population will remain infection-free forever, on the contrary if $i \neq 0$ and $s > \frac{\gamma}{\beta}$, then $\frac{di}{dt} > 0$, which is a threshold condition [11]. Therefore an epidemic occurs for $s_0 > \frac{\gamma}{\beta}$ where s_0 is the initial number of susceptibles. Thus, the expected number of infections produced by one infected individual is $\mathcal{R}_0 = \frac{\beta}{\gamma}$ and $s(0) = s_0$ [11].

The basic reproduction number $\mathcal{R}_0$ determines whether an epidemic is expected to occur in the population or not, thus an epidemic arises when $\mathcal{R}_0 s_0 > 1$ as shown in [2]. Moreover, equations (2) & (3) show that

$$\frac{d(s+i)}{dt} = -\gamma i,$$

demonstrating that $s + i$ is decreasing when $i > 0$ (see Fig. 1). We derive an expression for the final size of an epidemic. Firstly, we combine equations (2) & (3) to get

$$\begin{aligned} \frac{di}{ds} &= \frac{\beta si - \gamma i}{-\beta si} = -1 + \frac{\gamma}{\beta s} \\ \Rightarrow di &= \left(-1 + \frac{\gamma}{\beta s}\right) ds = \left(-1 + \frac{1}{\mathcal{R}_0 s}\right) ds. \end{aligned}$$

Integrating, using the initial conditions, and then taking limits gives,

$$i = -s + \frac{1}{\mathcal{R}_0} \log s + K,$$

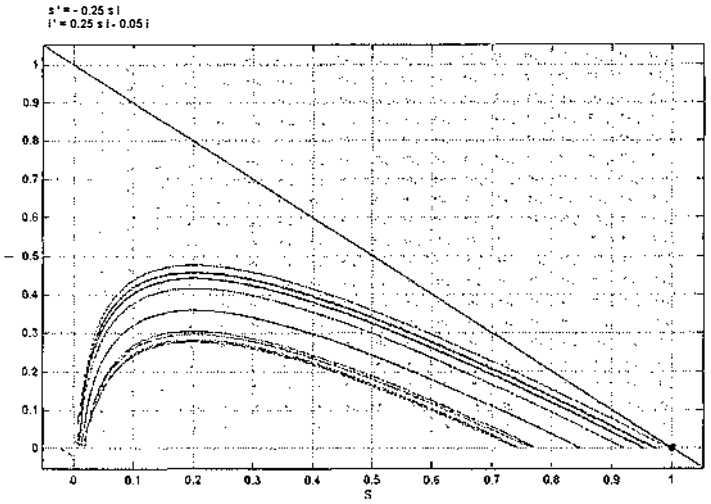

Figure 1: Phase-Plane for *SIR* epidemic model when $\mathcal{R}_0 = 5$.

$$K = i_0 + s_0 - \frac{1}{\mathcal{R}_0}\log s_0 = i_\infty + s_\infty - \frac{1}{\mathcal{R}_0}\log s_\infty. \tag{4}$$

where K is constant and s_∞ is the proportion of susceptibles at the end of the epidemic [1].

Using equation (4), we plot the solutions to equation (3) in the (s, i) phase-plane (Fig. 1). In this figure, the epidemic is shown as a curve from the point $(s_0, 0)$ to the point $(s_\infty, 0)$. Thus, by setting $i = 0$ as $t \to +\infty$ in equation (4), we get $z = s_0 - s_\infty$, the proportion of the population infected in an epidemic and then equation (4) equivalently becomes

$$s_0 - s_\infty + \frac{1}{\mathcal{R}_0}\log\frac{s_\infty}{s_0} = 0.$$

or

$$z + \frac{1}{\mathcal{R}_0}\log\left(\frac{s_0 - z}{s_0}\right) = 0.$$

Rearranging and assuming that the population is initially fully susceptible $s_0 = 1$, we have

$$z + \frac{1}{\mathcal{R}_0}\log(1 - z) = 0.$$

or

$$\mathcal{R}_0 + \frac{1}{z}\log(1 - z) \;=\; 0. \tag{5}$$

Equation (5) is known as the *Final Size Equation*. In this equation if $\mathcal{R}_0 > 1$, we have solutions in the range $0 < z < 1$. Note that z may be determined approximated numeri-

cally, or using Taylor expansions [3].

In Sect. 1.3, we will discuss the *SIR* endemic model, our main subject of interest.

1.3 The *SIR* Endemic Model

The main focus of this thesis will be on the *SIR* endemic model. In epidemiology an endemic infection is technically defined as an infection with comparatively small variations in monthly case counts, and only a slow rise and fall over years, such as the case with leprosy and tuberculosis [3]. In this section, we present the *SIR* endemic model, and reproduce qualitative results for different values of $\mathcal{R}_0$, as reported in [12].

Consider the system (1) in which a constant size of population is maintained by a balance between birth and death rates (μ), given as follows:

$$\begin{aligned} \frac{ds}{dt} &= \mu - \beta si - \mu s, \\ \frac{di}{dt} &= \beta si - \gamma i - \mu i, \\ \frac{dr}{dt} &= \gamma i - \mu r, \end{aligned} \tag{6}$$

with $r(t) = 1$ - $s(t)$ - $i(t)$. By observing these equations, we conclude that the average time of an infection is $\frac{1}{\gamma+\mu}$, and as infectious individuals infect others at rate β, the basic reproduction number $\mathcal{R}_0 = \frac{\beta}{\gamma+\mu}$.

At this point we cover the important parts of the analysis of this model. We do this by firstly establishing the global stability of each of the steady states of this system. Consequently we find these steady states and their stability and then analyse them using bifurcation and phase-plane diagrams.

We prove the global asymptotic stability of the steady state using the classical Poincaré-Bendixson theorem. Observe that if $s = 0$, then $\frac{ds}{dt} = \mu > 0$ and if $i = 0$, then $\frac{di}{dt} = 0$ and all other higher derivatives of i are zero. If the region $\mathcal{X} = \{s(t) > 0, i(t) > 0, s + i \leq 1\}$, then $\frac{d(s+i)}{dt} = -\gamma i < 0$ when $s + i = 1$, hence biologically we can imagine a triangle to prove the non-existence of periodic solutions only in the region $\mathcal{X}$ (see Fig. 2). In Fig. 2, arrows along the boundary of $\mathcal{X}$ point inward, this shows that any solution beginning within $\mathcal{X}$, stays within $\mathcal{X}$. Therefore we may use Dulac's criteria to rule out the periodic solutions. Consider the expression

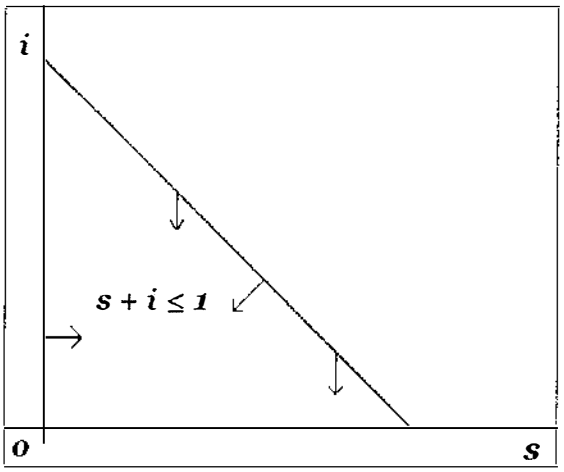

Figure 2: Triangle Invariance of *SIR* endemic model.

$$\frac{\partial}{\partial s}\left(\frac{\mu - \beta si - \mu s}{si}\right) + \frac{\partial}{\partial i}\left(\frac{\beta si - \gamma i - \mu i}{si}\right) = -\frac{\mu}{s^2 i}.$$

This equation shows that as $-\frac{\mu}{s^2 i} < 0$, no closed orbits may exist in $\mathcal{X}$. Thus, there exists a globally asymptotically stable steady state in $\mathcal{X}$.

1.3.1 Steady State Solutions

There are two steady states that can be obtained by setting the right hand side of the system (6) to zero:

$$\mu - \beta si - \mu s = 0 \tag{7}$$

$$\beta si - \gamma i - \mu i = 0 \tag{8}$$

Equation (8) gives two steady state conditions, one infection-free when $i = 0$ and another endemic, when $\beta s = \gamma + \mu$. We solve these conditions to get the infection-free and endemic steady states respectively

$$(s, i) = (1, 0),$$

and

$$(s, i) = (s^*, i^*) = \left(\frac{1}{\mathcal{R}_0}, \frac{\mu(\mathcal{R}_0 - 1)}{\beta}\right).$$

An infection-free equilibrium exists for any values of $\mathcal{R}_0$ while the endemic steady states exist only in the biological feasible region if $\mathcal{R}_0 > 1$.

1.3.2 Stability

In this section, we calculate the local stability of these steady states by linearising the system (6). The Jacobian matrix is found to be

$$J = \begin{pmatrix} -\mu - \beta i & -\beta s \\ \beta i & \beta s - (\gamma + \mu) \end{pmatrix}; \tag{9}$$

and when $(s, i) = (1, 0)$, we have

$$J_{\text{infection-free}} = \begin{pmatrix} -\mu & -\beta \\ 0 & \beta - (\gamma + \mu) \end{pmatrix} \tag{10}$$

By looking at the eigenvalues of $J_{\text{infection-free}}$, it is quite obvious that the infection-free equilibrium is stable when $\beta < (\mu + \gamma)$ or equivalently $\mathcal{R}_0 < 1$.

The stability of an endemic steady state

$$(s^*, i^*) = \left(\frac{1}{\mathcal{R}_0}, \frac{\mu(1 - s^*)}{\gamma + \mu}\right) = \left(\frac{1}{\mathcal{R}_0}, \frac{\mu(\mathcal{R}_0 - 1)}{\beta}\right)$$

is derived from the Jacobian matrix (9):

$$J_{\text{endemic}} = \begin{pmatrix} -\mu\mathcal{R}_0 & -(\mu + \gamma) \\ \mu(\mathcal{R}_0 - 1) & 0 \end{pmatrix} \tag{11}$$

One can easily see that the trace (τ) of this matrix is negative and the determinant (Δ) is positive as long as $\mathcal{R}_0 > 1$. This implies that this endemic steady state is stable whenever it exists. Observing these results, we see that a bifurcation can take place at $\mathcal{R}_0 = 1$. An endemic equilibrium exists only when $\mathcal{R}_0 > 1$, this gives a forward bifurcation. Thus the endemic infection only persists for $\mathcal{R}_0 > 1$.

1.3.3 Bifurcation Analysis

In the Fig. 3, we have an infection-free steady state i globally stable when $\mathcal{R}_0 < 1$ and unstable when $\mathcal{R}_0 > 1$. It is also clear that a unique stable endemic equlibrium arises from the bifurcation point $\mathcal{R}_0 = 1$ and increases as $\mathcal{R}_0$ increases, thus it shows that the infection free steady state exists for all $\mathcal{R}_0$, while an endemic infection only exists for $\mathcal{R}_0 > 1$. Fig. 3 gives forward bifurcation, so this phenomenon involves a transcritical bifurcation, thus we conclude that endemic infection only persist for $\mathcal{R}_0 > 1$.

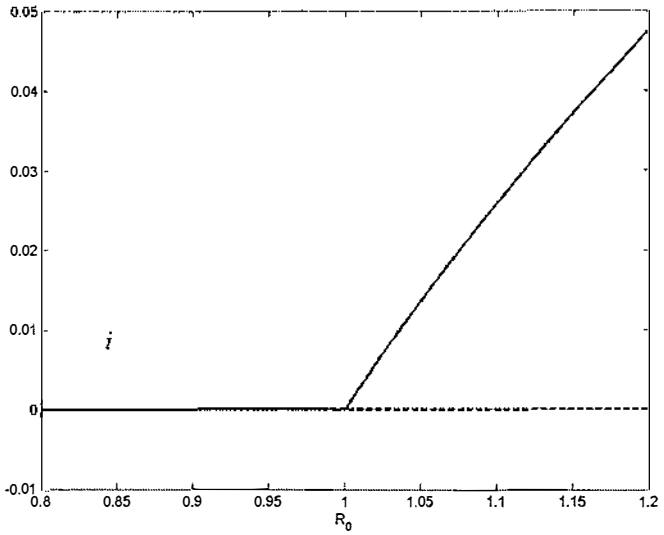

Figure 3: Bifurcation analysis for *SIR* endemic model. Stable infection-free steady state for $\mathcal{R}_0 < 1$; unstable infection-free i and stable endemic steady state i^* for $\mathcal{R}_0 > 1$.

1.3.4 Phase-Plane Analysis

We analyse equations of the system (6), in the (s, i) phase-plane, for different values of $\mathcal{R}_0$ (see Fig. 4). The arrows represent the direction of solutions and a dark black dot represents the equilibrium point. Dashed lines show nullclines and the dark black line shows the triangle $\mathcal{X}$. Some plotted curves show solutions of system (6). Observe that the qualitative behaviour changes at $\mathcal{R}_0 = 1$.

- If $\mathcal{R}_0 < 1$: The infection-free steady state is globally asymptotically stable i.e. globally attracting and biologically feasible endemic solutions do not exist in Fig. 4 (a).
- If $\mathcal{R}_0 > 1$: The infection-free steady state is unstable and a unique endemic equilibrium exists, and is globally asymptotically stable in Fig. 4 (b).

1.3.5 Summary

In this section we have shown that if $\mathcal{R}_0 > 1$, then an epidemic will occur. We have also proved that, biologically, an endemic infection can only continue to exist in a population for $\mathcal{R}_0 > 1$. Hence, we conclude that for $\mathcal{R}_0 < 1$, the infection-free equilibrium is globally attracting, this means that if the average number of secondary infections caused by an

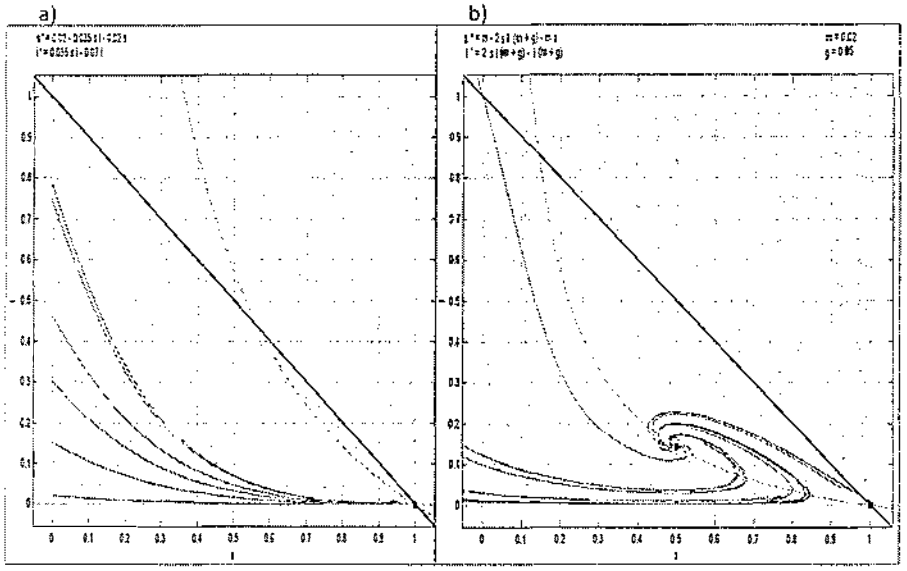

Figure 4: Phase-Plane for *SIR* endemic model when: (a) $\mathcal{R}_0 = 0.5 < 1$; (b) $\mathcal{R}_0 = 2 > 1$. Other parameter values are $\mu = 0.02$ and $\gamma = 0.05$.

infective is less than one, then the infection will no longer persist. If $\mathcal{R}_0 > 1$, then the infection-free steady state is unstable. Thus the endemic steady state $(s^\star, i^\star)$ is globally attracting only for $\mathcal{R}_0 > 1$.

In the following chapter we will consider four extensions of the *SIR* endemic models. These four models have an endemic infection that persists for some values of $\mathcal{R}_0 < 1$ (which are close enough to one) that leads to phenomena of backward bifurcation, multiple endemic steady states and hysteresis.

2 2D Extensions

In this chapter, we will study four extensions of *SIR* endemic models, their potential for a backward bifurcation and the presence of sub-critical endemic steady states. We will also examine the dynamics of these models by varying parameters values.

In these models an endemic infection is maintained in the population when $\mathcal{R}_0 > 1$ and when $\mathcal{R}_0$ equals certain values less than one. The main bifurcation parameter $\mathcal{R}_0$ is also considered as a fundamental epidemiological parameter; while $\mathcal{P}$, as mentioned previously, is a secondary parameter, whose definition varies between the different models.

2.1 The *SIR* model with Susceptible *R* Class

In this model, the recovered R class is susceptible, and possibly even more susceptible, to infection than the susceptible class, as examined in the paper by Safan et al. [13]. This model has been used for treatment effects in case of tuberculosis; the infective class in a population is treated at a constant rate and then proceeds to a recovered class, described as treatment T in Feng et al. [4]. The system of differential equations is

$$\begin{aligned} \frac{ds}{dt} &= \mu - \beta si - \mu s, \\ \frac{di}{dt} &= \beta si + \mathcal{P}\beta ri - (\mu + \gamma)i. \end{aligned} \tag{12}$$

with $r(t) = 1 - s(t) - i(t)$. The parameters β, μ, γ and $\mathcal{R}_0 = \frac{\beta}{\gamma+\mu}$ are as in Sect. 1. The parameter $\mathcal{P}$ is defined as the ratio of transmission probabilities from the recovered and susceptible classes. In this model, if $\mathcal{P} = 0$, then we have the *SIR* model, in which the population has zero susceptibility after recovering from one infection; and if $\mathcal{P} = 1$, then we have the *SIS* model, in which the infected class returns to the susceptible class on removal or recovery, see [13].

In a similar manner to Sect. 1.3, we calculate the global stability of the steady states by applying the classical Poincaré-Bendixson theorem. Periodic solutions are ruled out using Dulac's criterion in $(s, i) \in \mathcal{X}$ region. Here $\frac{d(s+i)}{dt} = \mathcal{P}\beta ri - \gamma i = -\gamma i < 0$ when $s + i = 1$ and $r(t) = 0$, thus any trajectory that starts in $\mathcal{X}$ stays in $\mathcal{X}$.

$$\frac{\partial}{\partial s}\left(\frac{\mu - \beta si - \mu s}{si}\right) + \frac{\partial}{\partial i}\left(\frac{\mathcal{P}\beta ri - \gamma i - \mu i}{si}\right) = -\frac{\mu}{s^2 i} - \frac{\mathcal{P}\beta}{s} < 0. \tag{13}$$

Equation (13) implies that this model does not have any limit cycles in the region $\mathcal{X}$, thus

the steady state for $\mathcal{R}_0 > 1$ is globally stable if it exists.

2.1.1 Steady State Solutions

We begin a qualitative approach to study steady states solutions. In order to get the equilibrium condition, we set the right hand side of equations in the system (12) to zero. By factorising these equation we find that the infection-free equilibrium occurs at $(s, i) = (1, 0)$.

The endemic condition satisfies $\beta s + \mathcal{P}\beta(1 - s - i) - (\gamma + \mu) = 0$. Now, we have two types for endemic steady states: $\mathcal{P} = 0$; and $\mathcal{P} \neq 0$. For $\mathcal{P} = 0$ the endemic steady states are $(s^\star, i^\star) = \left(\frac{1}{\mathcal{R}_0}, \frac{\mu(\mathcal{R}_0 - 1)}{\beta}\right)$, as in Sect. 1.3.1. If $\mathcal{P} \neq 0$, then we find the endemic steady states for $s^\star = \frac{\mu}{\mu + \beta i^\star}$ where $i^\star$ is found by solving the quadratic equation

$$f(i^\star) = \mathcal{P}\mathcal{R}_0 i^{\star 2} + (1 + \mathcal{P}\Gamma - \mathcal{P}\mathcal{R}_0)\, i^\star + \Gamma\left(\frac{1}{\mathcal{R}_0} - 1\right) \;=\; 0, \tag{14}$$

where $\Gamma = \frac{\mu}{\mu + \gamma}$. If $\mathcal{R}_0 > 1$ and $\mathcal{P} > 0$, then $f(0) < 0$ and there is a unique positive solution $i^\star > 0$ with $f(i^\star) = 0$. For $\mathcal{R}_0 < 1$, we need to solve equations (14) to have better understanding of the roots for $f(i^\star)$. We have

$$i^\star_\pm = \frac{1}{2}\frac{(-1 - \mathcal{P}\Gamma + \mathcal{P}\mathcal{R}_0) \pm \sqrt{(1 + \mathcal{P}\Gamma - \mathcal{P}\mathcal{R}_0)^2 - 4\mathcal{P}\Gamma\,(1 - \mathcal{R}_0)}}{\mathcal{P}\mathcal{R}_0}.$$

We consider the discriminant of $f(i^\star)$ when $\mathcal{R}_0 < 1$, we have three possibilities for the solutions of $f(i^\star)$: if the discriminant of $f(i^\star)$ is negative, then we have no real roots; if the discriminant of $f(i^\star)$ is positive, then we have two real roots; and if the discriminant of $f(i^\star)$ is zero, then we have one real root. Graphically, the parabola of $f(i^\star)$ is concave up and is tangential to the $i^\star$-axis whenever $\mathcal{R}_0 = \mathcal{R}_{\text{saddle}}$ and if $\mathcal{R}_0 > \mathcal{R}_{\text{saddle}}$, then the parabola intersects the $i^\star$-axis. There is still another situation to consider, which characterises the critical or turning points for $\mathcal{P}$ and $\mathcal{R}_0$.

2.1.2 Saddle Node Equation

The following is an elaborate from equation (14) to obtain the critical value for $\mathcal{P}$. For this treating $\mathcal{R}_0$ as a function of $i^\star$ and differentiating equation (14). Hence we get

$$i^\star = \frac{\mathcal{P}\mathcal{R}_0 - \mathcal{P}\Gamma - 1}{2\mathcal{R}_0\mathcal{P}}.$$

μ	0.02
γ	0.05
Γ	0.286
$\mathcal{R}_{\text{saddle}}$	0.871699
$\mathcal{P}_{\text{crit}}$	1.4

Table 2: Parameter values for susceptible R class.

at the critical point we obtain $\frac{d\mathcal{R}_0}{di^*}\big|_{(1,0)} = \frac{\gamma}{\mu+\gamma}\mathcal{P} - 1$. This gives

$$\mathcal{P}_{\text{crit}} = 1 + \frac{\mu}{\gamma}$$

when $\frac{d\mathcal{R}_0}{di^*}\big|_{(1,0)} = 0$.

Now decreasing $\mathcal{R}_0$ on the horizontal axis in order to find the saddle node equation for $\mathcal{R}_0$ when $\mathcal{P} > \mathcal{P}_{\text{crit}}$. Putting this value of i^* back into equation (14), the saddle node solution, for the value of $\mathcal{R}_0$, becomes

$$\mathcal{P}^2\mathcal{R}_0^2 + ((2-\mathcal{P})\Gamma - 1)\,2\mathcal{P}\mathcal{R}_0 + (1-\mathcal{P}\Gamma)^2 = 0.$$

The solution of this equation gives $\mathcal{R}_{\text{saddle}}$, the value of $\mathcal{R}_0$ where two endemic steady states with $i-$component $i_- = i_+ = i^*$ coincide in the turning point (see Fig. 5) only when $\mathcal{P} > \mathcal{P}_{\text{crit}}$. For more details see [13].

2.1.3 Stability

In this subsection, we investigate the stability of these steady states by linearising equation (12). The Jacobian matrix for this model is

$$J = \begin{pmatrix} -\mu - \beta i & -\beta s \\ \beta i(1-\mathcal{P}) & \beta s + \mathcal{P}\beta(1-s-2i) - (\mu+\gamma) \end{pmatrix}. \tag{15}$$

At the infection-free steady state, $(s,i) = (1,0)$, we have a Jacobian matrix as in matrix (10), and from which we have already found that if $\mathcal{R}_0 < 1$, then an infection-free equilibrium is locally stable for all values of $\mathcal{P}$. If $\mathcal{R}_0 > 1$, then we have an unstable infection-free equilibrium.

Using the endemic steady state for s^* and i^*, when $\mathcal{P} = 0$, the matrix (15) becomes matrix (11). When $\mathcal{R}_0 > 1$, we have $\tau < 0$ and $\Delta > 0$, thus the endemic steady state is stable for $\mathcal{P} = 0$.

For the stability of the endemic steady state when $\mathcal{P} \neq 0$, we have quadratic solutions for $s_+^\star = \frac{\mu}{\mu+\beta i_+^\star}$ and $i_+^\star$ (see equation (14)). Simplifying the matrix (15) in terms of $i_+^\star$ to get the matrix

$$J_{\text{endemic}+} = \begin{pmatrix} -\mu - \beta i_+^\star & -\frac{\beta\mu}{\mu+\beta i_+^\star} \\ \beta i_+^\star(1-\mathcal{P}) & -\mathcal{P}\beta i_+^\star \end{pmatrix}, \tag{16}$$

which has

$$\tau_+ = -\mu - \mathcal{R}_0(\mu+\gamma)(1+\mathcal{P})i_+^\star,$$

and

$$\Delta_+ = \left[(\mu + \mathcal{R}_0(\mu+\gamma)i_+^\star)\mathcal{P} + \frac{\mu\mathcal{R}_0(\mu+\gamma)(1-\mathcal{P})}{\mu+\mathcal{R}_0(\mu+\gamma)i_+^\star}\right]\mathcal{R}_0(\mu+\gamma)i_+^\star.$$

We substitute the value of $i_+^\star$ (see Sect. 2.1.1) in τ_+ and Δ_+. We calculate that for $\mathcal{P} > \mathcal{P}_{\text{crit}}$ and for the region between $\mathcal{R}_{\text{saddle}} < \mathcal{R}_0 < 1$, a stable endemic steady state exists when $\tau_+ < 0$ and $\Delta_+ > 0$. For $\mathcal{R}_0 > 1$, as $\tau_+ < 0$ and $\Delta_+ > 0$, we have stable endemic steady state for any value of $\mathcal{P}$.

Writing matrix (15) in terms of $i_-^\star$ we get

$$J_{\text{endemic}-} = \begin{pmatrix} -\mu - \beta i_-^\star & -\frac{\beta\mu}{\mu+\beta i_-^\star} \\ \beta i_-^\star(1-\mathcal{P}) & -\mathcal{P}\beta i_-^\star \end{pmatrix}, \tag{17}$$

this gives

$$\tau_- = -\mu - \mathcal{R}_0(\mu+\gamma)(1+\mathcal{P})i_-^\star,$$

and

$$\Delta_- = \left[(\mu + \mathcal{R}_0(\mu+\gamma)i_-^\star)\mathcal{P} + \frac{\mathcal{R}_0(\mu+\gamma)(1-\mathcal{P})\mu}{\mu+\mathcal{R}_0(\mu+\gamma)i_-^\star}\right]\mathcal{R}_0(\mu+\gamma)i_-^\star.$$

Now, we substitute the value of $i_-^\star$ into τ_- and Δ_-. For $\mathcal{P} > \mathcal{P}_{\text{crit}}$ and for the region between $\mathcal{R}_{\text{saddle}} < \mathcal{R}_0 < 1$ we have $\tau_- < 0$ and $\Delta_- < 0$, which indicates the presence of an unstable steady state. If $\mathcal{R}_0 > 1$, the trace $\tau_- < 0$ and $\Delta_- > 0$ for $\mathcal{P}$ is both greater and less than $\mathcal{P}_{\text{crit}}$, so we have a unique globally stable endemic steady state.

Thus, we have two endemic steady states, $(s_+^\star, i_+^\star)$ and $(s_-^\star, i_-^\star)$, in addition to a stable infection-free steady state (s, i). This shows that this model exhibits backward bifurcation when $\mathcal{P} > \mathcal{P}_{\text{crit}}$ and for $\mathcal{R}_{\text{saddle}} < \mathcal{R}_0 < 1$.

Now in the following subsections, we study bifurcation and phase-plane analyses using **MATLAB** [10] to prove the stability of infection-free and endemic steady states.

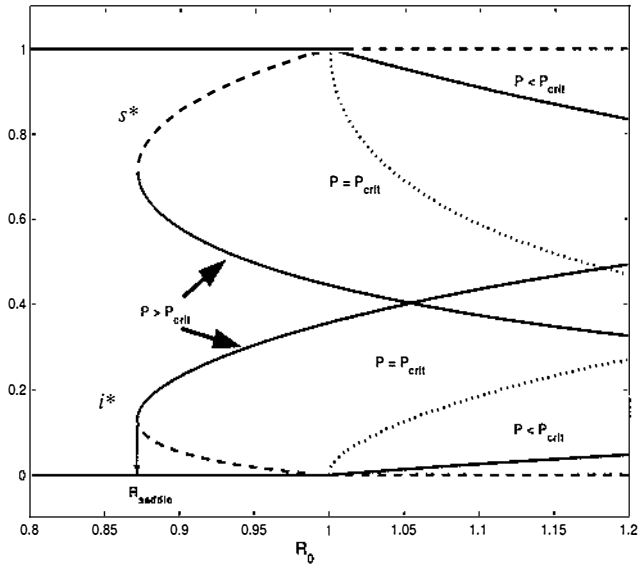

Figure 5: Bifurcation diagram for the *SIR* model with susceptible R class giving curves $(\mathcal{R}_0, s^*)$ and $(\mathcal{R}_0, i^*)$. Broken lines signify unstable steady state while unbroken & dotted lines are stable ones. Light dark arrow points downward at $\mathcal{R}_0 = \mathcal{R}_{\text{saddle}}$ where two endemic equilibriums coincide. The $(\mathcal{R}_0, s^*)$ and $(\mathcal{R}_0, i^*)$ curves have backward bifurcations when $P > P_{\text{crit}}$ where $P_{\text{crit}} = 1 + \frac{\mu}{\gamma}$.

2.1.4 Bifurcation Analysis

As we can see the infection-free steady state is globally stable for $\mathcal{R}_0 < 1$ and unstable for $\mathcal{R}_0 > 1$, for all the values of $\mathcal{P}$. If $\mathcal{P} < \mathcal{P}_{\text{crit}} = 1 + \frac{\mu}{\gamma}$, then there is a bifurcation at $\mathcal{R}_0 = 1$ into a globally stable endemic steady state and an unstable infection-free steady state. For $\mathcal{P} > \mathcal{P}_{\text{crit}}$ the bifurcation that occurs at $\mathcal{R}_0 = 1$ is 'backward'. For $\mathcal{R}_{\text{saddle}} < \mathcal{R}_0 < 1$, there is a pair of endemic steady states, one stable and the other unstable. After this value the curve defining an unstable endemic steady state changes direction and becomes stable. So, at $\mathcal{R}_0 = 1$, an endemic steady state bifurcates from an infection-free steady state. If $\mathcal{P} < \mathcal{P}_{\text{crit}}$ the endemic steady state is stable. At this point, i^* increases with increasing $\mathcal{R}_0$. At $\mathcal{P} = \mathcal{P}_{\text{crit}}$ (represents as dotted line in Fig. 5), the curve leaves vertically at $\mathcal{R}_0 = 1$ and divides two qualitatively different dynamics, see Fig. 5.

This model also demonstrates the phenomenon of hysteresis. In Fig. 5, if $\mathcal{R}_0$ increases from $\mathcal{R}_0 < 1$, then at $\mathcal{R}_0 = 1$ and $\mathcal{P} > \mathcal{P}_{\text{crit}}$, the stable infection-free steady state *jumps straight up* to i^* and *down* to s^*, the stable endemic steady state. If $\mathcal{R}_0$ subsequently decreases, i^* decreases and s^* increases to $\mathcal{R}_0 = \mathcal{R}_{\text{saddle}}$, then a stable endemic steady state *jumps straight down* for i^* and *up* for s^* to a stable infection-free equilibrium.

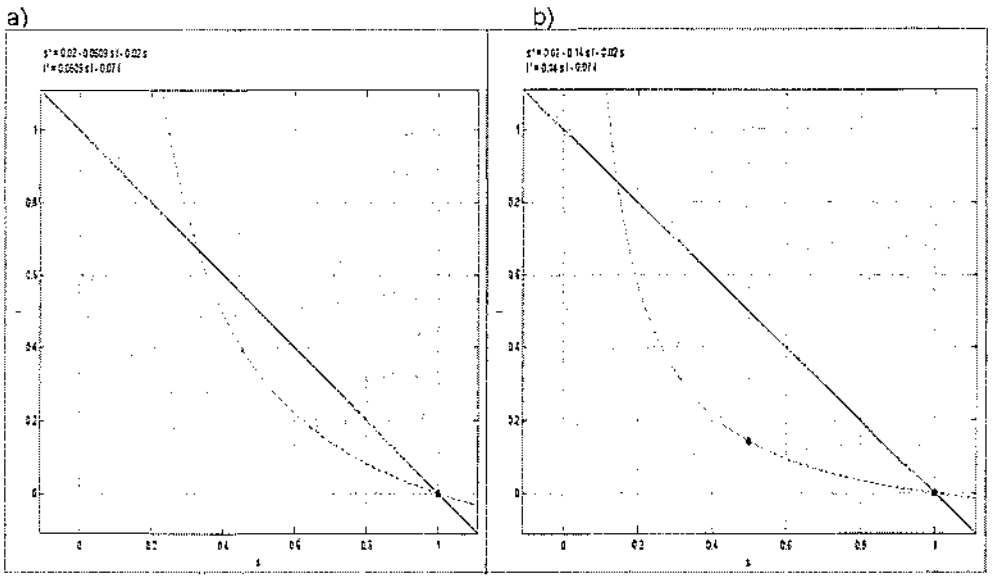

Figure 6: Phase-Plane for the *SIR* model with susceptible R Class for $\mathcal{P} = 0 < \mathcal{P}_{\text{crit}}$ when: (a) $\mathcal{R}_0 = 0.8 < 1$; (b) $\mathcal{R}_0 = 1.2 > 1$.

2.1.5 Phase-Plane Analysis

We now investigate the above results by plotting phase-plane diagrams for different $\mathcal{R}_0$ and $\mathcal{P}$, using equations (12). We separate $\mathcal{R}_0$ into four different regions: $\mathcal{P} = 0$; $\mathcal{P} = \frac{\mathcal{P}_{\text{crit}}}{2}$; $\mathcal{P} = \mathcal{P}_{\text{crit}} = 1 + \frac{\mu}{\gamma}$; and $\mathcal{P} > \mathcal{P}_{\text{crit}}$. In these phase-planes, we specify the solutions in the triangle region $\mathcal{X}$. Small arrows in the following figures show the direction field; dashed lines are nullclines; the black dot represents the equilibrium point; dotted arrow shows $\mathcal{R}_{\text{saddle}}$; dashes lines are unstable; and continuous lines are stable. Notice that for $\mathcal{P} = 0$, we have the same phase-planes as in Sect. 1.3 this is because the susceptible R class degenerates the classical *SIR* model.

1. $\mathcal{P} = 0$

   - $\mathcal{R}_0 < 1$: A stable infection-free steady state is present as in Sect. 1.3.4, see Fig. 6 (a).
   - $\mathcal{R}_0 > 1$: An unstable infection-free equilibrium and a stable endemic steady state are present as in Sect. 1.3.4, see Fig. 6 (b).

2. $\mathcal{P} = \frac{\mathcal{P}_{\text{crit}}}{2}$

   - $\mathcal{R}_0 < 1$: A stable infection-free steady state exists in Fig. 7 (a).
   - $\mathcal{R}_0 > 1$: An unstable infection-free and a stable endemic steady states in Figure 7 (b). Thus we have found that for some values of $\mathcal{P} < \mathcal{P}_{\text{crit}}$, these dynamics are similar to dynamics for $\mathcal{P} = 0$.

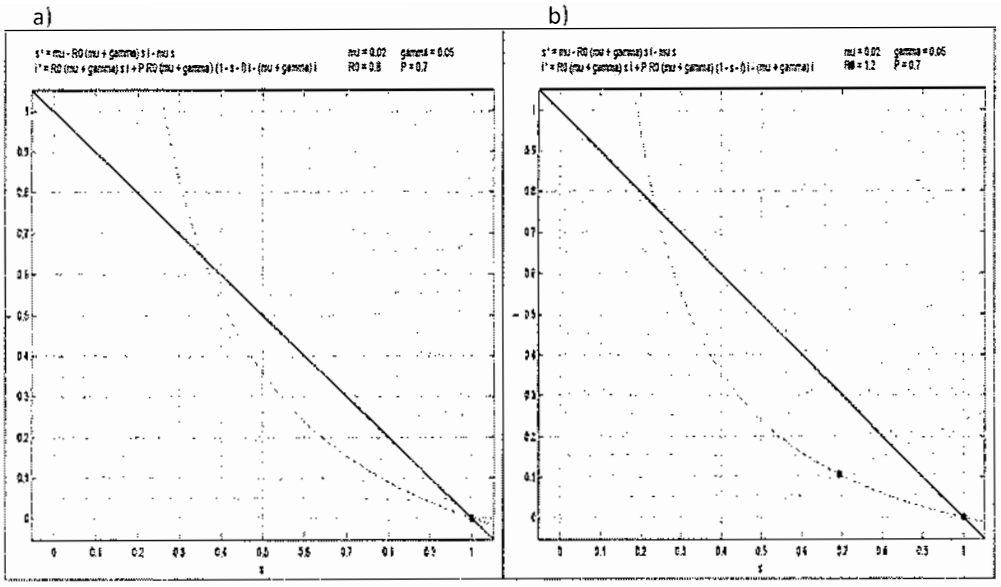

Figure 7: Phase-Planes for susceptible R class for $\mathcal{P} = \frac{\mathcal{P}_{\text{crit}}}{2}$ when: (a) $\mathcal{R}_0 = 0.8 < 1$; (b) $\mathcal{R}_0 = 1.2 > 1$.

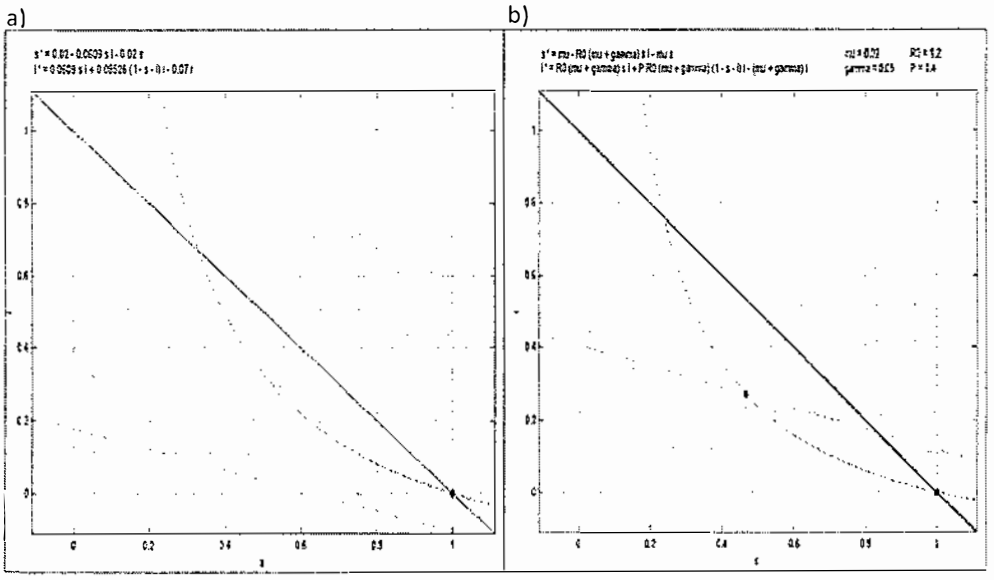

Figure 8: Phase-Planes for susceptible R class for $\mathcal{P} = \mathcal{P}_{\text{crit}}$ when: (a) $\mathcal{R}_0 = 0.8 < 1$; (b) $\mathcal{R}_0 = 2 > 1$.

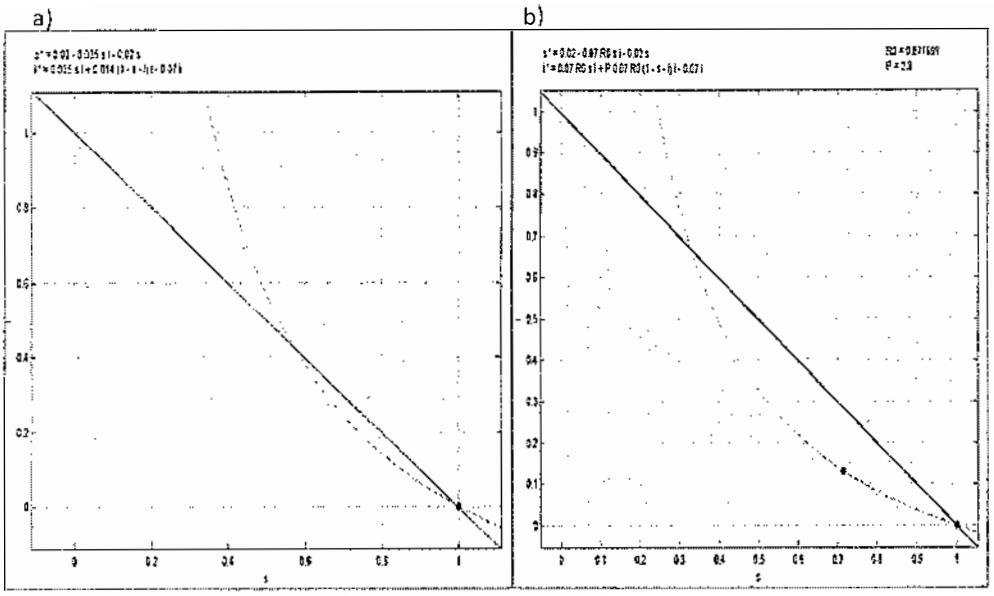

Figure 9: Phase-Planes for susceptible R class for $\mathcal{P} = 2.8 > \mathcal{P}_{\text{crit}}$ when: (a) $\mathcal{R}_0 = 0.5 < \mathcal{R}_{\text{saddle}}$; (b) $\mathcal{R}_0 = \mathcal{R}_{\text{saddle}}$.

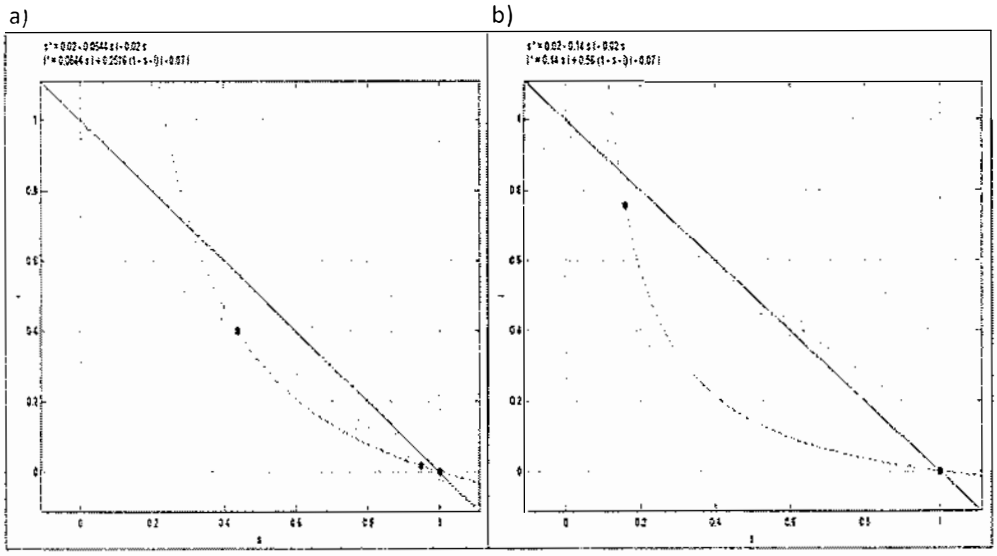

Figure 10: Phase-Planes for susceptible R class for $\mathcal{P} = 2.8 > \mathcal{P}_{\text{crit}}$ when: (a) $\mathcal{R}_{\text{saddle}} < \mathcal{R}_0 = 0.92 < 1$; (b) $\mathcal{R}_0 = 2$.

3. $\mathcal{P} = \mathcal{P}_{\text{crit}}$

   - $\mathcal{R}_0 < 1$: Only a stable infection-free equilibrium is present in Fig. 8 (a)
   - $\mathcal{R}_0 > 1$: An unstable infection-free steady state and stable endemic steady states are present in Fig 8 (b).

4. $\mathcal{P} > \mathcal{P}_{\text{crit}}$

   - $\mathcal{R}_0 < \mathcal{R}_{\text{saddle}}$: Only a stable infection-free equilibrium is present in Fig. 9 (a).
   - $\mathcal{R}_0 = \mathcal{R}_{\text{saddle}} = 0.871699$: A stable infection-free steady state exists. Another equilibrium point shows two endemic steady states which are top of each other at this value of $\mathcal{R}_{\text{saddle}}$. The nullclines are tangential to each other.
   - $\mathcal{R}_{\text{saddle}} < \mathcal{R}_0 < 1$: An stable infection-free, two endemic both stable and unstable exist in Fig. 10 (a).
   - $\mathcal{R}_0 > 1$: An unstable infection-free steady state and one stable endemic steady state are present in Fig. 10 (b).

2.2 The *SIR* model with Nonlinear Transmission Class

The *SIR* model with nonlinear transmission of infection is explained in detail in Gomes et al. [6]. In this model, we show that the transmission function of any infection satisfies the biological conditions that lead to the system with an asymptotically stable steady state [8]. The differential equations are written as

$$\begin{aligned} \frac{ds}{dt} &= \mu - \lambda s - \mu s, \\ \frac{di}{dt} &= \lambda s - (\mu + \gamma) i. \end{aligned} \tag{18}$$

with $r(\text{t}) = 1$ - $s(\text{t})$ - $i(\text{t})$ as above. Take $\lambda = \beta i(1 + h(i))$ as a nonlinear force of infection for some increasing function h. This function $h(i)$ is defined as the increase in risk of infection with the intensity of exposure, and if $h(i) \equiv 0$, then we have a standard force of infection $\lambda = \beta i$ as analysed in [6]. We have assumed that $h^{'}(i) \geq 0$. Thus considering $h(i)$ using a functional form $h(i) = \frac{\mathcal{P}i}{1+\mathcal{P}i}$ in order to get *useful* illustrations; here we use $\mathcal{P}$ as a secondary bifurcation parameter. The basic reproduction number $\mathcal{R}_0 = \frac{\beta}{\mu+\gamma}$ is unchanged.

In order to find the global stability, we consider the triangle $\mathcal{X}$ as an invariant set such that $\mathcal{X} = \left\{s, i \in \mathbf{R}^2 | (s, i) > 0; (s + i \leq 1)\right\}$, then $\frac{d(s+i)}{dt} = \mu - \mu(s + i) - \gamma i < 0$ when $s + i = 1$. We use Dulac's criterion [2] that states that if the sign of $\frac{\partial \dot{s}}{\partial s} + \frac{\partial \dot{i}}{\partial i}$ is constant

in a simply connected region $\mathcal{X}$, of the phase space, then limit cycles cannot exist in the region.

$$\frac{\partial}{\partial s}\left(\frac{\mu-\lambda s-\mu s}{si}\right)+\frac{\partial}{\partial i}\left(\frac{\lambda s-\gamma i-\mu i}{si}\right)=-\frac{\mu}{s^2 i}+\frac{\mathcal{P}\beta}{(1+\mathcal{P}i)^2} \tag{19}$$

As the above expression changes sign in the region $\mathcal{X}$, by using Dulac's criterion and the Poincaré-Bendixson theorem. Thus, we cannot exclude limit cycles and cannot say if the nontrivial steady state is globally asymptotically stable for the function $h(i)=\frac{\mathcal{P}i}{1+\mathcal{P}i}$. Thus, any conclusion about the existence of limit cycle, cannot be drawn and, in this case Dulac's criterion fails.

Note that in some cases, we do not apply Dulac's criterion to this model, as there are some functions $h(i)$ that may lead to limit cycles surrounding the nontrivial equilibrium, as demonstrated in Gomes et al. [6]. Gomes provide a theorem stating that there may exist at least one limit cycle derivable from the function $h(i)$. Correspondingly if $h''(i)<0$ and $h''(i)>0$, then we have at least one limit cycle surrounding the equilibrium provided $h'(0)<\frac{(\mu+\gamma)}{\mu}$ and $h''(0)>\frac{81(\mu+\gamma)}{4\mu}-\frac{3h'(0)(\mu+\gamma)}{\mu}$.

We apply this theorem for the function $h(i)=\frac{\mathcal{P}i}{1+\mathcal{P}i}$. If $h'(0)=\mathcal{P}<\frac{(\mu+\gamma)}{\mu}$, then $h''(0)<\frac{81(\mu+\gamma)}{4\mu}-\frac{3h'(0)(\mu+\gamma)}{\mu}$; and if $h'(0)=\mathcal{P}>\frac{(\mu+\gamma)}{\mu}$, then $h''(0)>\frac{81(\mu+\gamma)}{4\mu}-\frac{3h'(0)(\mu+\gamma)}{\mu}$, this shows that this theorem fails. This theorem is helpful if any limit cycle exists for the function $h(i)$, however, the theorem does not say what happens if this theorem fails. Thus the nonexistence of any limit cycles for any value of the parameter $\mathcal{P}$, when $\mathcal{R}_0>1$ remains in question.

2.2.1 Steady State Solutions

A steady state can be found by solving the system (18), with the right hand sides set to zero.

$$\mu-\beta(1+h(i))si-\mu s=0,$$

$$\beta(1+h(i))si-(\mu+\gamma)i=0.$$

We get an infection-free equilibrium at $(s,i)=(1,0)$ as in Sect. 2.1. For all $\mathcal{P}$, the endemic steady state is the solution of:

$$s^\star = \frac{1}{\mathcal{R}_0(1+h(i^\star))}; \tag{20}$$

$$1 = \frac{1}{\mathcal{R}_0(1+h(i^\star))}+\frac{(\mu+\gamma)i^\star}{\mu}. \tag{21}$$

We may find either a unique positive solution or multiple solutions for equation (21), depending on the function $h(i)$. Now, if $\mathcal{P} = 0$, then we have the same endemic steady state as in Sect. 2.1. And for any other values for $\mathcal{P}$, we have endemic steady states for i^* and s^*. We solve equation (21) in quadratic form, using $h(i) = \frac{\mathcal{P}i}{1+\mathcal{P}i}$.

$$f(i^*) = 2\mathcal{P}\mathcal{R}_0 i^{2*} + (\mathcal{R}_0 - 2\mathcal{P}\mathcal{R}_0\Gamma + \mathcal{P}\Gamma)i^* + \Gamma(1 - \mathcal{R}_0) = 0, \tag{22}$$

$$s^* = \frac{1 + \mathcal{P}i^*}{\mathcal{R}_0(1 + 2\mathcal{P}i^*)},$$

where $\Gamma = \frac{\mu}{\mu+\gamma}$ as in Sect. 2.1. For the function $h(i) = \frac{\mathcal{P}i}{1+\mathcal{P}i}$, we find that $f(i^*)$ has a unique positive solution $i^* > 0$ for $f(0) < 0$ whenever $\mathcal{R}_0 > 1$. But if $\mathcal{R}_0 < 1$, then we have a more complex situation so in order to get a better analysis, we solve equation (22) to get

$$i^*_{\pm} = \frac{1}{4}\frac{(2\mathcal{P}\mathcal{R}_0\Gamma - \mathcal{R}_0 - \mathcal{P}\Gamma) \pm \sqrt{(\mathcal{R}_0 - 2\mathcal{P}\mathcal{R}_0\Gamma + \mathcal{P}\Gamma)^2 - 8\mathcal{P}\mathcal{R}_0\Gamma(1 - \mathcal{R}_0)}}{\mathcal{P}\mathcal{R}_0}.$$

Whenever $\mathcal{R}_0 < 1$, we have three possibilities for the solutions of $f(i^*)$. If the discriminant of $f(i^*)$ is positive then we have two real roots and if negative then we have no real roots. If it is zero then graphically, we have a concave up parabola of $f(i^*)$ which is tangential to the i^*-axis. At this point we have $\mathcal{R}_{\text{saddle}}$ that makes the parabola tangential on the i^*-axis.

In the following subsection, we will calculate the critical values for $\mathcal{P}$ and $\mathcal{R}_{\text{saddle}}$. Also we analyse the turning points where the backward bifurcation occurs.

2.2.2 Saddle Node Equation

To determine the direction of bifurcation at the critical point, we solve equation (21) treating $\mathcal{R}_0$ as a function of i^*, giving a value for

$$i^* = \frac{2\mathcal{P}\mathcal{R}_0\Gamma - \mathcal{R}_0 - \mathcal{P}\Gamma}{4\mathcal{P}\mathcal{R}_0}.$$

If we set $\mathcal{R}_0 = 1$, $i^* = 0$, then $\frac{d\mathcal{R}_0}{di^*}\big|_{(1,0)} = \frac{\mu+\gamma}{\mu} - h'(0)$. As $\frac{d\mathcal{R}_0}{di^*} \leq 0$, thus

$$h'(0) > \mathcal{P}_{\text{crit}} = 1 + \frac{\gamma}{\mu}$$

μ	0.02
γ	0.05
Γ	0.286
$\mathcal{R}_{\text{saddle}}$	0.9519197
$\mathcal{P}_{\text{crit}}$	3.5

Table 3: Parameter values for nonlinear transmission class.

This gives the critical value of $\mathcal{P}_{\text{crit}}$ and for $\mathcal{P} > \mathcal{P}_{\text{crit}}$, we calculate the saddle node equation for $\mathcal{R}_0$. Putting the value of i^* back into equation (22) to get

$$\mathcal{R}_0 = (2\mathcal{P}\Gamma + 1)^2\mathcal{R}_0^2 - 2\mathcal{P}\Gamma(2\mathcal{P}\Gamma + 3)\mathcal{R}_0 + \mathcal{P}^2\Gamma^2 = 0.$$

This equation solves for the value of $\mathcal{R}_{\text{saddle}}$. Thus, when $\mathcal{P} > \mathcal{P}_{\text{crit}}$ and $\mathcal{R}_{\text{saddle}} < \mathcal{R}_0 < 1$, a backward bifurcation occurs. We will calculate the stability of infection-free and endemic steady states in next subsection.

2.2.3 Stability

We linearise the system (18) in order to study stability of these steady states. The Jacobian matrix is given by

$$J = \begin{pmatrix} -\mu - \beta i(1 + h(i)) & -\beta s(1 + ih'(i) + h(i)) \\ \beta i(1 + h(i)) & \beta s(1 + ih'(i) + h(i)) - (\mu + \gamma) \end{pmatrix}. \tag{23}$$

For the infection-free steady state $(s, i) = (1, 0)$, this Jacobian matrix is the same as the matrix (10). Thus, for $\mathcal{R}_0 < 1$, $(s, i) = (1, 0)$ is stable and; for $\mathcal{R}_0 > 1$, it is unstable. To study the stability of the endemic steady state for $\mathcal{P} = 0$, we set $(s^*, i^*) = \left(\frac{1}{\mathcal{R}_0}, \frac{\mu(\mathcal{R}_0 - 1)}{\beta}\right)$. The Jacobian matrix (24) is same as the matrix (11) and possess the same stability for $\mathcal{R}_0 > 1$ i.e. we have stable endemic steady state for $\mathcal{R}_0 > 1$ for the parameter values given in Table 3.

When $\mathcal{P} \neq 0$, we have the endemic steady states (see equations (20)), (21)). We find the Jacobian matrix and solve it for the function $h(i^*)$. Thus we have

$$J_{\text{endemic}+} = \begin{pmatrix} -\mu - \frac{\mathcal{R}_0 i_+^*(\mu+\gamma)(1+2\mathcal{P}i_+^*)}{1+\mathcal{P}i_+^*} & -\frac{(\mu+\gamma)(1+4\mathcal{P}i_+^* + 2\mathcal{P}^2 i_+^{*2})}{(1+\mathcal{P}i_+^*)(1+2\mathcal{P}i_+^*)} \\ \frac{\mathcal{R}_0 i_+^*(\mu+\gamma)(1+2\mathcal{P}i_+^*)}{1+\mathcal{P}i_+^*} & \frac{(\mu+\gamma)\mathcal{P}i_+^*}{(1+\mathcal{P}i_+^*)(1+2\mathcal{P}i_+^*)} \end{pmatrix}, \tag{24}$$

with

$$\tau_+ = -\mu - \frac{\mathcal{R}_0 i_+^*(\mu+\gamma)(1+2\mathcal{P}i_+^*)}{1+\mathcal{P}i_+^*} + \frac{(\mu+\gamma)\mathcal{P}i_+^*}{(1+\mathcal{P}i_+^*)(1+2\mathcal{P}i_+^*)},$$

and determinant

$$\Delta_+ = \frac{(\mu+\gamma)i_+^*[4\mathcal{R}_0 i_+^*\mathcal{P}^2(\mu+\gamma) + 4\mathcal{R}_0 i_+^*\mathcal{P}(\mu+\gamma) + \mathcal{R}_0(\mu+\gamma) - \mu\mathcal{P}]}{(1+2\mathcal{P}i_+^*)(1+\mathcal{P}i_+^*)}.$$

Substituting the value of i_+^* and the parameter values from Table 3 in τ_+ and Δ_+ to evaluate $J_{\text{endemic}+}$ (24). We find that for $\mathcal{P} > \mathcal{P}_{\text{crit}}$ and $\mathcal{R}_{\text{saddle}} < \mathcal{R}_0 < 1$, a stable endemic steady state i_+^* exists. For $\mathcal{R}_0 > 1$, we have only one stable endemic steady state as $J_{\text{endemic}+}$ (24) has only real negative eigenvalue for any $\mathcal{P}$.

Putting the endemic steady state i_-^* in the matrix (23) to get

$$J_{\text{endemic}-} = \begin{pmatrix} -\mu - \frac{\mathcal{R}_0 i_-^*(\mu+\gamma)(1+2\mathcal{P}i_-^*)}{1+\mathcal{P}i_-^*} & -\frac{(\mu+\gamma)(1+4\mathcal{P}i_-^*+2\mathcal{P}^2 i_-^{*2})}{(1+\mathcal{P}i_-^*)(1+2\mathcal{P}i_-^*)} \\ \frac{\mathcal{R}_0 i_-^*(\mu+\gamma)(1+2\mathcal{P}i_-^*)}{1+\mathcal{P}i_-^*} & \frac{(\mu+\gamma)\mathcal{P}i_-^*}{(1+\mathcal{P}i_-^*)(1+2\mathcal{P}i_-^*)} \end{pmatrix}, \tag{25}$$

We get

$$\tau_- = -\mu - \frac{\mathcal{R}_0 i_-^*(\mu+\gamma)(1+2\mathcal{P}i_-^*)}{1+\mathcal{P}i_-^*} + \frac{(\mu+\gamma)\mathcal{P}i_-^*}{(1+\mathcal{P}i_-^*)(1+2\mathcal{P}i_-^*)},$$

and

$$\Delta_- = \frac{(\mu+\gamma)i_-^*[4\mathcal{R}_0 i_-^*\mathcal{P}^2(\mu+\gamma) + 4\mathcal{R}_0 i_-^*\mathcal{P}(\mu+\gamma) + \mathcal{R}_0(\mu+\gamma) - \mu\mathcal{P}]}{(1+2\mathcal{P}i_-^*)(1+\mathcal{P}i_-^*)}.$$

By substituting i_-^* into τ_- and Δ_-, we find that $\tau_- < 0$ and $\Delta_- < 0$ whenever $\mathcal{P} > \mathcal{P}_{\text{crit}}$ and $\mathcal{R}_{\text{saddle}} < \mathcal{R}_0 < 1$, hence an unstable endemic steady state i_-^* exists. Additionally, if $\mathcal{R}_0 > 1$, then we have stable endemic steady states for any $\mathcal{P}$. Thus, for $\mathcal{P} > \mathcal{P}_{\text{crit}}$ and $\mathcal{R}_{\text{saddle}} < \mathcal{R}_0 < 1$, we have multiple endemic steady states.

2.2.4 Bifurcation Analysis

The dynamics of this system are similar to those of the susceptible R class described in the previous Sect. 2.1. So for the bifurcation analysis we refer the read to that Sect. 2.1. Fig. 11 illustrates same dynamics as Fig. 5 that a backward bifurcation occurs at $\mathcal{R}_0 = 1$, this refers to sub-critical endemic steady states (shown as dashed and solid black lines) and a stable infection-free equilibrium.

2.2.5 Phase-Plane Analysis

In this section, we analyse the system (18) using a (s, i) phase-plane, the methodology is similar to that of Sect. 2.1. We find the force of infection (λ) by calculating the

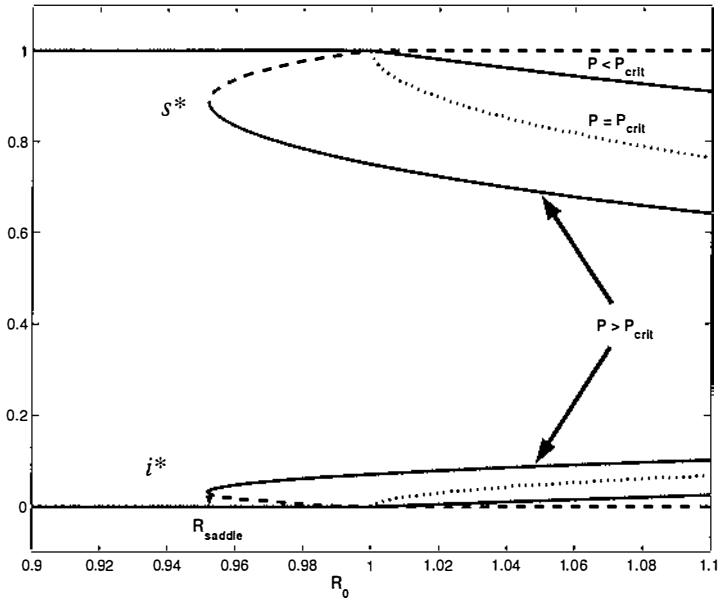

Figure 11: Bifurcation diagram for the *SIR* model with nonlinear transmission class. Labels are as in Fig. 5. For this class, $\mathcal{P}_{\text{crit}} = 1 + \frac{\gamma}{\mu}$.

function $h(i) = \frac{\mathcal{P}i}{(1+\mathcal{P}i)}$ to plot the phase-planes. We have plotted several phase-planes by categorising $\mathcal{R}_0$ in different regions and using different values for $\mathcal{P}$.

1. $\mathcal{P} = 0 < \mathcal{P}_{\text{crit}}$
   - $\mathcal{R}_0 < 1$: A stable infection-free steady state $(s, i) = (1, 0)$ exists in Fig. 12 (a).
   - $\mathcal{R}_0 > 1$: An unstable infection-free and a stable endemic steady states exist in Fig. 12 (b).
2. $\mathcal{P} = \frac{\mathcal{P}_{\text{crit}}}{2}$
   - $\mathcal{R}_0 < 1$: A stable infection-free steady state exists in Fig. 13 (a).
   - $\mathcal{R}_0 > 1$: An unstable infection-free and a stable endemic steady states exist in Fig. 13 (b).
3. $\mathcal{P} = \mathcal{P}_{\text{crit}}$
   - $\mathcal{R}_0 < 1$: A stable infection-free steady state is present in Fig. 14 (a).
   - $\mathcal{R}_0 > 1$: An unstable infection-free steady state and a stable (spiral sink) endemic steady state $(s^\star, i^\star)$ are present in Fig. 14 (b).
4. $\mathcal{P} > \mathcal{P}_{\text{crit}}$

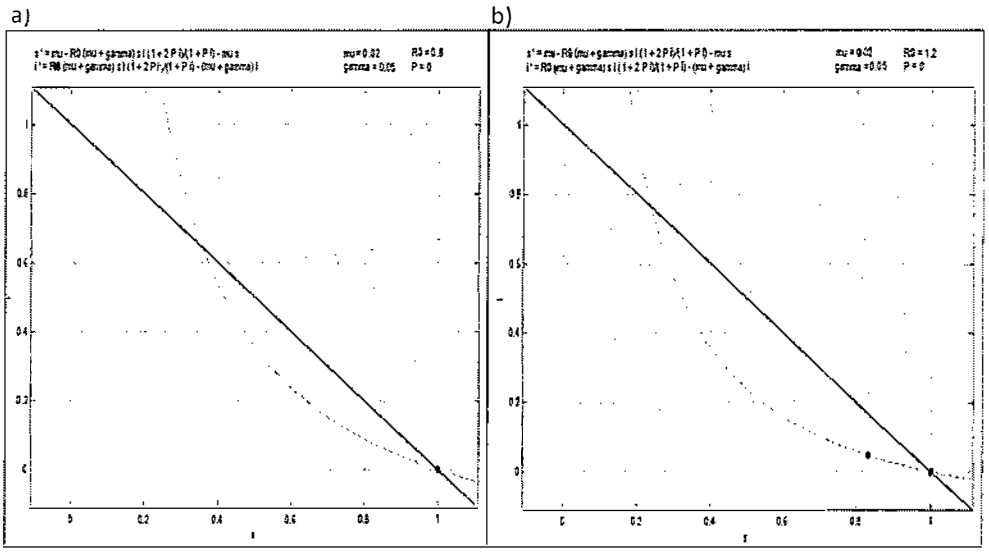

Figure 12: Phase-Planes for the *SIR* model with nonlinear transmission class for $\mathcal{P} = 0 < \mathcal{P}_{\text{crit}}$ when: (a) $\mathcal{R}_0 = 0.8 < 1$; (b) $\mathcal{R}_0 = 1.2 > 1$.

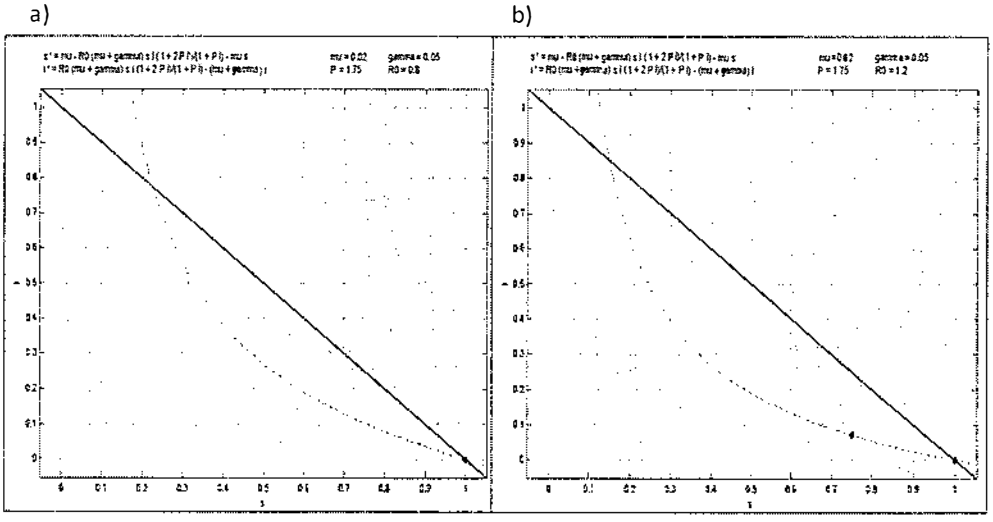

Figure 13: Phase-Planes for nonlinear transmission class for $\mathcal{P} = \frac{\mathcal{P}_{\text{crit}}}{2}$ when: (a) $\mathcal{R}_0 = 0.8 < 1$; (b) $\mathcal{R}_0 = 1.2 > 1$.

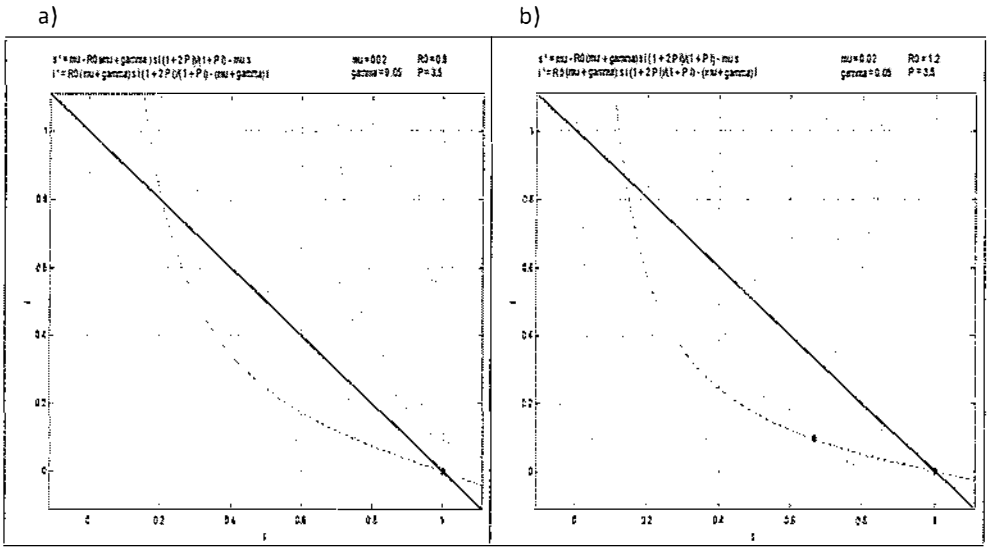

Figure 14: Phase-Planes for nonlinear transmission class for $\mathcal{P} = 3.5 = \mathcal{P}_{\text{crit}}$ when: (a) $\mathcal{R}_0 = 0.8 < 1$; (b) $\mathcal{R}_0 = 1.2 > 1$.

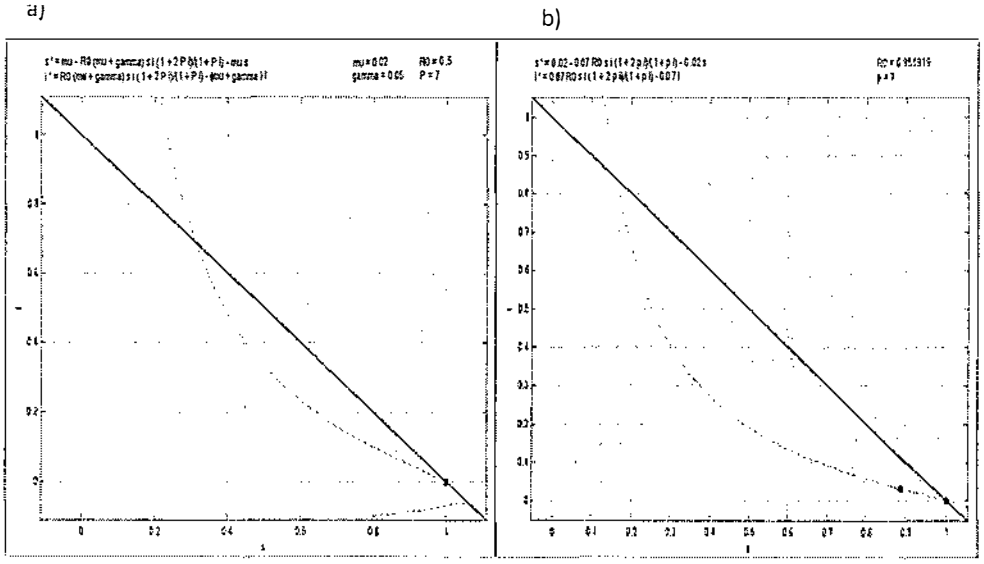

Figure 15: Phase-Plane for nonlinear transmission class for $\mathcal{P} > \mathcal{P}_{\text{crit}}$ when: (a) $\mathcal{R}_0 = 0.5$; (b) $\mathcal{R}_0 = \mathcal{R}_{\text{saddle}} = 0.951919$.

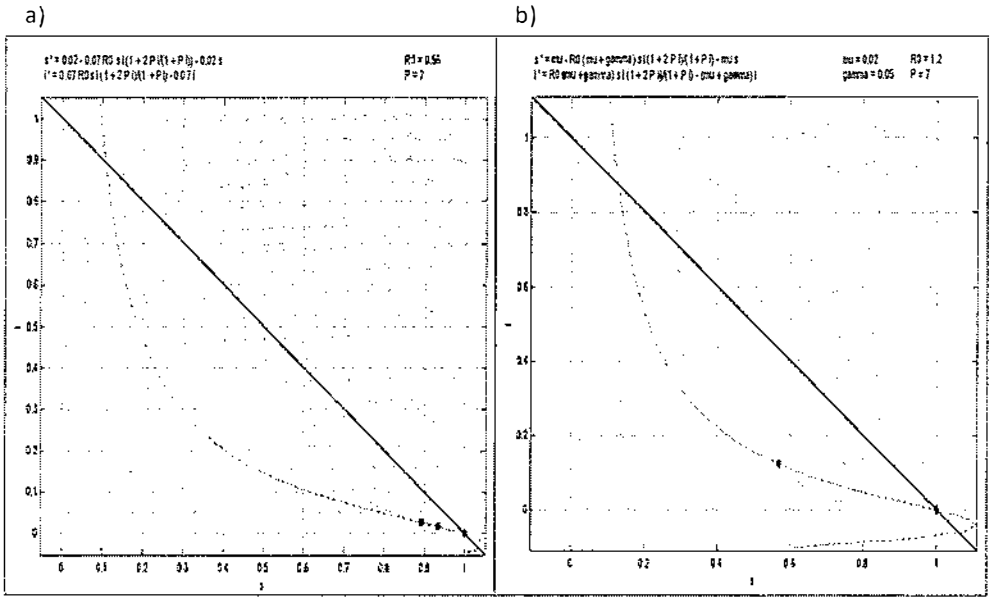

Figure 16: Phase-Plane for nonlinear transmission class for $\mathcal{P} > \mathcal{P}_{\text{crit}}$ when: (a) $\mathcal{R}_{\text{saddle}} < \mathcal{R}_0 = 0.96 < 1$; (b) $\mathcal{R}_0 = 1.2 > 1$.

- $\mathcal{R}_0 < \mathcal{R}_{\text{saddle}}$: Only a stable infection-free steady state is present in Fig. 15 (a).
- $\mathcal{R}_0 = \mathcal{R}_{\text{saddle}} = 0.951919$: A stable infection-free steady state and two endemic steady states (represent as a single black dot) that are on top of each other, exist in Fig. 15 (b). The endemic steady states change their stability at this point.
- $\mathcal{R}_{\text{saddle}} < \mathcal{R}_0 = 0.96 < 1$: A stable infection-free steady state and two endemic steady states (both stable and unstable) exist in Fig. 16 (a).
- $\mathcal{R}_0 > 1$: An unstable infection-free steady state is present in Fig. 16 (b).

2.3 The *SIR* model with Exogenous Infection Class

This model is one of the special cases proposed in a paper by Feng et al. [4]. In model, a new class is included, the Exposed *(E)* which represents those that are infected but not yet infectious. The proportion of the exposed class is denoted by $e(t)$. To keep this model two dimensional, we assume that those in the infectious class will remain in the infectious class, hence we do not need the removed class (R) and its proportion $r(t) = 0$.

This model is defined by

$$\begin{aligned} \frac{ds}{dt} &= \mu - \beta si - \mu s, \\ \frac{de}{dt} &= \beta si - \mathcal{P}\beta ei - (\mu + \nu)e, \\ \frac{di}{dt} &= \mathcal{P}\beta ei + \nu e - \mu i. \end{aligned} \tag{26}$$

with $e(t) = 1 - s(t) - i(t)$. If $\mathcal{P} = 0$, then this model is a standard *SEI* model [12]. The parameters β and μ are the same as in the Sect. 2.1 and Sect. 2.2. The parameter ν is a rate at which an individual, who has been exposed to infection, becomes infectious in the absence of reinfection. The expression $\mathcal{P}\beta ei$ models the exogenous reinfection rates with parameter $\mathcal{P}$ that represents the level of reinfection. In this model, the basic reproduction number is $\mathcal{R}_0 = \frac{\beta\nu}{\mu(\mu+\nu)}$.

In the Sect. 4.1, later we will cover the *SEIR* model, a three dimensional model where we have four classes: Susceptibles (S); Infectives (I); Removed (R) and; Exposed (E).

Now studying the global asymptotic stability of the system (26) using Dulac' s criterion in the region $\mathcal{X}$. If $s = 0$, then $\frac{ds}{dt} = \mu > 0$; if $i = 0$ and $s = 1$, then $\frac{di}{dt}, \frac{de}{dt} = 0$. Thus the invariant region $\mathcal{X} = \{0 < s(t), i(t) < 1, e(t) = 0, s + i \leq 1\}$. Dulac's criterion for this model is

$$\frac{\partial}{\partial s}\left(\frac{\mu - \beta si - \mu s}{si}\right) + \frac{\partial}{\partial i}\left(\frac{\mathcal{P}\beta(1 - s - i)i - \nu i - \mu i}{si}\right) = -\frac{\mu}{s^2 i} - \frac{\mathcal{P}\beta}{s} - \frac{\nu(1 - s)}{si^2}.$$

This expression is less than zero for positive $0 < s < 1$, hence, the steady state is globally asymptotically stable for $\mathcal{R}_0 > 1$.

2.3.1 Steady State Solutions

We determine the infection-free and endemic steady states by setting the right hand side of equations (26) to zero. The infection-free steady state is the same as before, that is $(s, i) = (1, 0)$. For the endemic equilibrium, when $\mathcal{P} = 0$; we have $(s^*, i^*) = \left(\frac{1}{\mathcal{R}_0}, \frac{\mu(\mathcal{R}_0 - 1)}{\beta}\right)$ and when $\mathcal{P} \neq 0$; we have the endemic steady state for $s^* = \frac{\mu}{\mu + \beta i^*}$, where i^* is in quadratic form.

$$f(i^*) = \mathcal{P}\mathcal{R}_0^2 i^{*2} + \Psi\mathcal{P}\mathcal{R}_0 i^* + \frac{\nu^2(1 - \mathcal{R}_0)}{\mu(\mu + \nu)} = 0, \tag{27}$$

μ	0.02
ν	0.05
$\mathcal{R}_{\text{saddle}}$	0.9838
$\mathcal{P}_{\text{crit}}$	8.75

Table 4: Parameter values for exogenous infection class.

where $\Psi = \left(\frac{\nu}{\mu} + \mathcal{P}\frac{\nu}{\nu+\mu} - \mathcal{P}\mathcal{R}_0\right)$. In equation (27), $f(i^*)$ gives a unique positive solution for $i^* > 0$ whenever $\mathcal{R}_0 > 1$, as $f(0) < 0$. If $\mathcal{R}_0 < 1$, then we solve $f(i^*)$ for a better understanding. A quadratic solution for i^*

$$i^*_{\pm} = \frac{-\Psi\mathcal{P}\mu(\mu+\nu) \pm \sqrt{\Psi^2\mathcal{P}^2\mu^2(\mu+\nu)^2 + (\mathcal{R}_0 - 1)4\mathcal{P}\mu\nu^2(\mu+\nu)}}{2\mathcal{P}\mathcal{R}_0\mu(\mu+\nu)}.$$

We calculate the discriminant of $f(i^*)$ to determine the behaviour of $f(i^*)$. If the discriminant of $f(i^*)$ is negative, then no real roots exist; while there are two real roots, when it is positive. If it is zero then we have one real root which is tangential to the i^*-axis. At this point we solve for $\mathcal{R}_{\text{saddle}}$ from the saddle node equation of $\mathcal{R}_0$ which we will calculate in the next subsection, along with the critical value of the parameter $\mathcal{P}$.

2.3.2 Saddle Node Equation

To find a critical value of $\mathcal{P}$, we differentiate equation (27), treating $\mathcal{R}_0$ as a function of i^*, we get

$$i^* = \frac{\mathcal{P}\mathcal{R}_0 - \mathcal{P}\frac{\nu}{\mu+\nu} - \frac{\nu}{\mu}}{2\mathcal{P}\mathcal{R}_0},$$

and setting $(\mathcal{R}_0, i^*) = (1, 0)$. Then, we have

$$\mathcal{P}_{\text{crit}} = \frac{\nu(\nu+\mu)}{\mu^2}.$$

Thus we have the critical value of $\mathcal{P}$. Now to find two endemic steady states when $\mathcal{P} > \mathcal{P}_{\text{crit}}$, for some values of $\mathcal{R}_0 < 1$; we estimate the saddle node equation by differentiating equation (27) with respect to $\mathcal{R}_0$, getting i^* provided $\frac{d\mathcal{R}_0}{di^*} = 0$, that gives

$$\mathcal{P}^2\mathcal{R}_0^2 + \left(2\frac{\nu^2}{\mu(\mu+\nu)} - \frac{\nu}{\mu} - \mathcal{P}\frac{\nu}{\mu+\nu}\right)2\mathcal{P}\mathcal{R}_0 + \left(\frac{\nu}{\mu} - \mathcal{P}\frac{\mu}{\mu+\nu}\right)^2 = 0.$$

This equation solves for $\mathcal{R}_{\text{saddle}}$, that makes the parabola of $f(i^*)$ tangential on the i^*-axis. Next we review, in detail, the local stability of these steady states.

2.3.3 Stability

In this subsection to investigate the stability of the infection-free and endemic steady states, we linearise equations in system (26) to find the Jacobian matrix

$$J = \begin{pmatrix} -\mu - \beta i & -\beta s \\ -\mathcal{P}\beta i - \nu & \mathcal{P}\beta - \mathcal{P}\beta s - 2\mathcal{P}\beta i - (\mu + \nu) \end{pmatrix}. \tag{28}$$

For the infection-free steady state $(s, i) = (1, 0)$, the Jacobian matrix becomes

$$J_{\text{infection-free}} = \begin{pmatrix} -\mu & -\beta \\ -\nu & -(\mu + \nu) \end{pmatrix}. \tag{29}$$

Now this matrix have $\tau = -2\mu - \nu$, and $\Delta = (1 - \mathcal{R}_0)(\mu\nu + \mu^2)$ respectively. If $\mathcal{R}_0 < 1$, then trace is negative and the determinant is positive, meaning that the infection-free steady state is stable. If $\mathcal{R}_0 > 1$, then the infection-free steady state is unstable as $\tau, \Delta < 0$.

The Jacobian matrix for the endemic steady state, when $\mathcal{P} = 0$, is

$$J_{\text{endemic}} = \begin{pmatrix} -\mu\mathcal{R}_0 & -\frac{\mu}{\nu(\mu + \nu)} \\ -\nu & -(\mu + \nu) \end{pmatrix}. \tag{30}$$

This matrix has $\tau = -\mu(\mathcal{R}_0 + 1) - \nu$ and $\Delta = (\mathcal{R}_0 - 1)(\mu\nu + \mu^2)$ respectively. If $\mathcal{R}_0 > 1$, then $\tau < 0$ with $\Delta > 0$. Thus the endemic steady state is stable for $\mathcal{R}_0 > 1$.

To study the endemic steady state for $\mathcal{P} \neq 0$, we put the value for $s^\star$ in the Jacobian matrix (28) in terms of $i^\star$,

$$J_{\text{endemic}+} = \begin{pmatrix} -\mu - \beta i_+^\star & -\frac{\beta\mu}{\mu + \beta i_+^\star} \\ -\mathcal{P}\beta i_+^\star - \nu & \mathcal{P}\beta - (2\mathcal{P}\beta i_+^\star + \frac{\mu\mathcal{P}\beta}{\mu + \beta i_+^\star} + \mu + \nu) \end{pmatrix}.$$

This has

$$\tau_+ = \frac{\mathcal{P}\beta^2 i_+^\star - (2\mathcal{P} + 1)\beta^2 i_+^\star - 2\mathcal{P}\beta i_+^\star \mu - \nu\beta i_+^\star - \mu\nu - 3\mu\beta i_+^\star - 2\mu^2}{\mu + \beta i_+^\star},$$

$$\Delta_+ = (2\mathcal{P}\beta i_+^\star \mu - 2\mathcal{P}\beta^2 i_+^{\star 2} - \mathcal{P}\beta^2 i_+^\star + \nu\beta i_+^\star + \mu\nu + \mu\beta i_+^\star + \mu^2) - \frac{\beta\mu(\mathcal{P}\beta i_+^\star + \nu)}{\mu + \beta i_+^\star}.$$

Evaluating the above Jacobian matrix by substituting the value for $i_+^\star$ and using Table 4 for parameter values, we find that $\tau_+ < 0$ and $\Delta_+ > 0$ for $\mathcal{P} > \mathcal{P}_{\text{crit}}$ and $\mathcal{R}_{\text{saddle}} <$

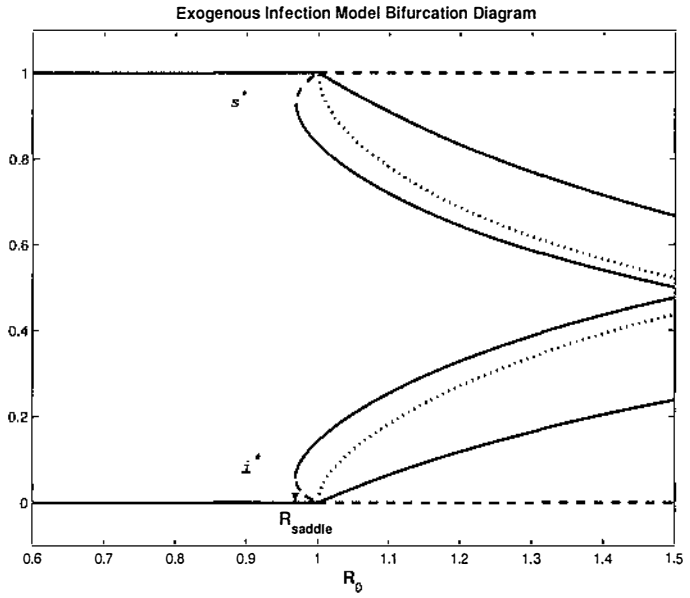

Figure 17: Bifurcation diagram for the *SIR* model with exogenous infection class. Labels are as in Fig. 5. The critical value of $\mathcal{P}$ for this class is $\frac{\nu(\nu+\mu)}{\mu^2}$.

$\mathcal{R}_0 < 1$. Hence, we have a stable endemic steady state i^*_+. For $\mathcal{R}_0 > 1$ and all $\mathcal{P}$, the endemic steady state is stable.

$$J_{\text{endemic}-} = \begin{pmatrix} -\mu - \beta i^*_- & -\frac{\beta\mu}{\mu+\beta i^*_-} \\ -\mathcal{P}\beta i^*_- - \nu & \mathcal{P}\beta - (2\mathcal{P}\beta i^*_- + \frac{\mu\mathcal{P}\beta}{\mu+\beta i^*_-} + \mu + \nu) \end{pmatrix}.$$

This has

$$\tau_- = \frac{\mathcal{P}\beta^2 i^*_- - (2\mathcal{P}+1)\beta^2 i^*_- - 2\mathcal{P}\beta i^*_-\mu - \nu\beta i^*_- - \mu\nu - 3\mu\beta i^*_- - 2\mu^2}{\mu + \beta i^*_-},$$

and

$$\Delta_- = (2\mathcal{P}\beta i^*_-\mu - 2\mathcal{P}\beta^2 i^{*2}_- - \mathcal{P}\beta^2 i^*_- + \nu\beta i^*_- + \mu\nu + \mu\beta i^*_- + \mu^2) - \frac{\beta\mu(\mathcal{P}\beta i^*_- + \nu)}{\mu + \beta i^*_-}.$$

We find that for $\mathcal{P} > \mathcal{P}_{\text{crit}}$ and $\mathcal{R}_{\text{saddle}} < \mathcal{R}_0 < 1$, an unstable endemic steady state i^*_- is present as $\tau_-, \Delta_- < 0$, while endemic steady state is stable for $\mathcal{R}_0 > 1$ and for any $\mathcal{P}$.

Thus we have multiple endemic steady states for $\mathcal{P} > \mathcal{P}_{\text{crit}}$ and $\mathcal{R}_{\text{saddle}} < \mathcal{R}_0 < 1$ and only a stable endemic steady state for all $\mathcal{P}$ and $\mathcal{R}_0 > 1$.

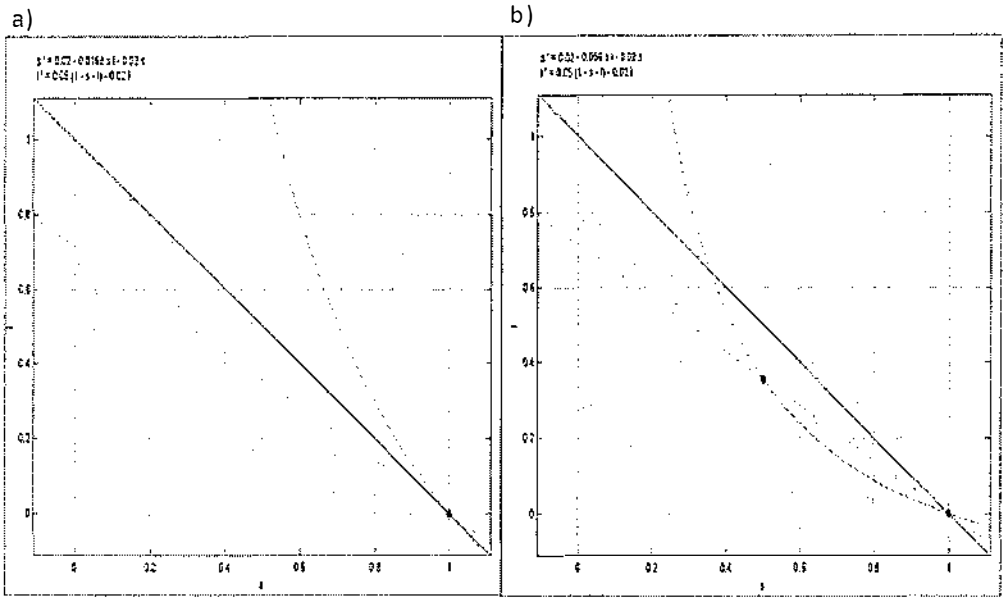

Figure 18: Phase-Planes for the *SIR* model with exogenous infection class for $\mathcal{P} = 0 < \mathcal{P}_{\text{crit}}$ when: (a) $\mathcal{R}_0 = 0.6 < \mathcal{R}_{\text{saddle}}$; (b) $\mathcal{R}_0 = 2$ within triangle $s + i = 1$.

2.3.4 Bifurcation Analysis

The stability of the infection-free and endemic steady states for all values of $\mathcal{R}_0$ and $\mathcal{P}$ is the same as in Sect. 2.1 and Sect. 2.2. Figure 17 illustrates the asymptotic behaviour of these solutions to the system of equations (26). Again, the dynamics are similar to those in Sect. 2.1.

2.3.5 Phase-Plane Analysis

Now, consider the triangular region $\mathcal{X}$ and plot phase-planes so that we can develop a better understanding of the above results. Again we categorise based on different values of $\mathcal{R}_0$ and $\mathcal{P}$. Arrows show the flow of the solutions; dashed lines represent nullclines; and black dots are steady states. This model gives similar results to those in Sect. 2.

1. $\mathcal{P} = 0$

   - $\mathcal{R}_0 < 1$
     A stable infection-free steady state is present in Fig. 18 (a).
   - $\mathcal{R}_0 > 1$
     There is an unstable infection-free steady state and a stable endemic equilibrium in Fig. 18 (b).

2. $0 < \mathcal{P} < \mathcal{P}_{\text{crit}}$

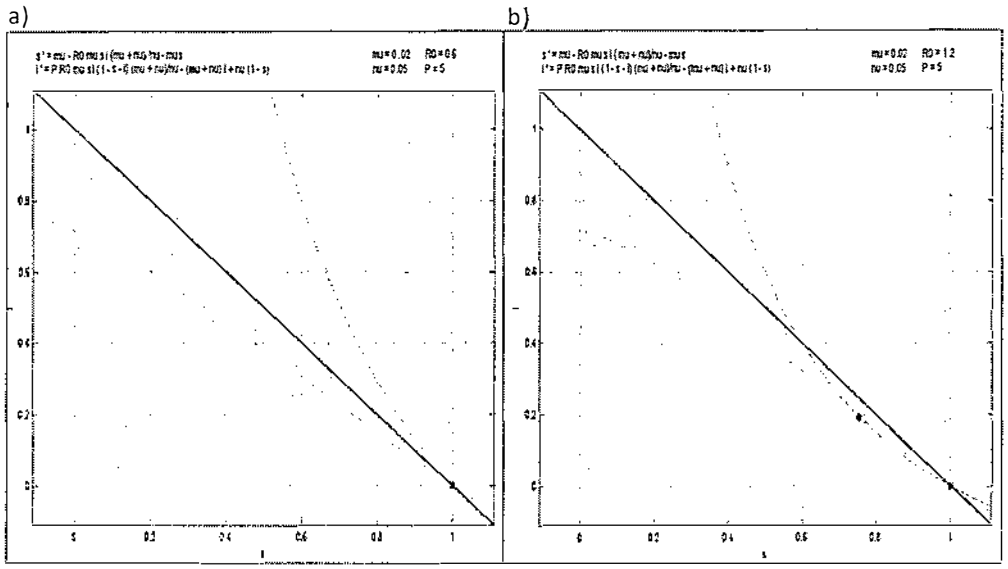

Figure 19: Phase-Planes for exogenous infection class for $\mathcal{P} = 5 < \mathcal{P}_{\text{crit}}$ when: (a) $\mathcal{R}_0 = 0.6 < \mathcal{R}_{\text{saddle}}$; (b) $\mathcal{R}_0 = 1.2$.

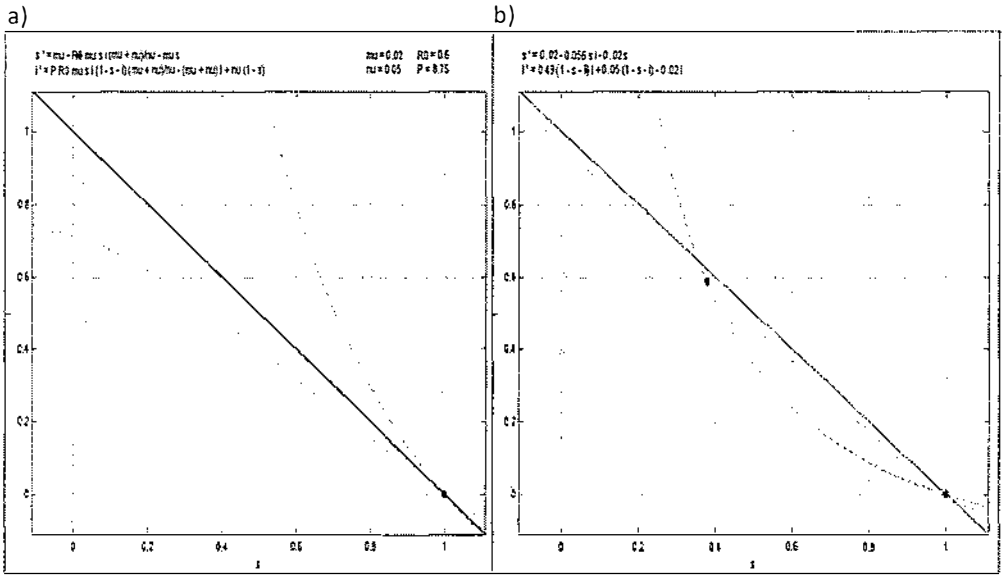

Figure 20: Phase-Planes for exogenous infection class for $\mathcal{P} = \mathcal{P}_{\text{crit}} = 8.75$ when: (a) $\mathcal{R}_0 = 0.6 < \mathcal{R}_{\text{saddle}}$; (b) $\mathcal{R}_0 = 2$.

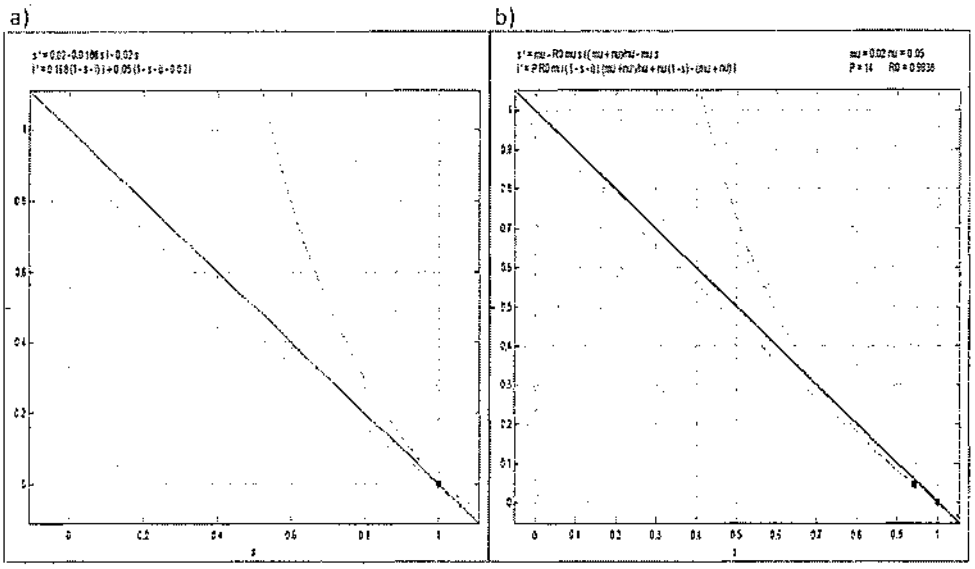

Figure 21: Phase-Planes for exogenous infection class for $\mathcal{P} = 14 > \mathcal{P}_{\text{crit}}$ when: (a) $\mathcal{R}_0 = 0.6 < \mathcal{R}_{\text{saddle}}$; (b) $\mathcal{R}_0 = 0.9838 = \mathcal{R}_{\text{saddle}}$.

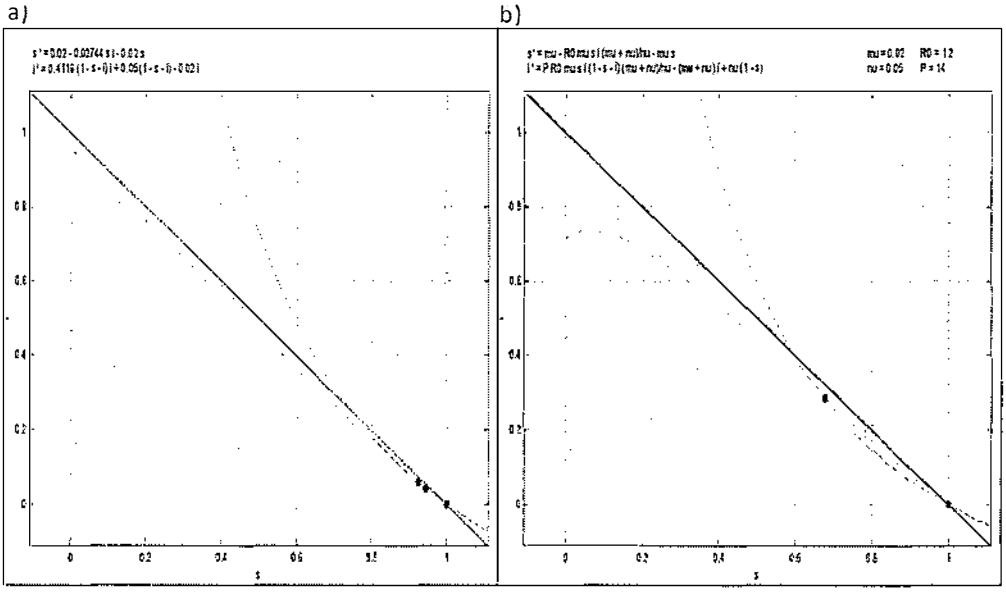

Figure 22: Phase-Planes for exogenous infection class for $\mathcal{P} = 14 > \mathcal{P}_{\text{crit}}$ when: (a) $\mathcal{R}_{\text{saddle}} < \mathcal{R}_0 = 0.99 < 1$; (b) $\mathcal{R}_0 = 1.2 > 1$ is of interest.

- $\mathcal{R}_0 < 1$
  A stable infection-free steady state in Fig. 19 (a).
- $\mathcal{R}_0 > 1$
  A stable endemic and an unstable infection-free steady states are present in Fig. 19 (b).

3. $\mathcal{P} = \mathcal{P}_{\text{crit}}$
   - $\mathcal{R}_0 < 1$
     A stable infection-free steady state is present in Fig. 20 (a).
   - $\mathcal{R}_0 > 1$
     There are two equilibriums: an unstable infection-free and a stable endemic steady states in Fig. 20 (b) .
4. $\mathcal{P} > \mathcal{P}_{\text{crit}}$
   - $\mathcal{R}_0 < \mathcal{R}_{\text{saddle}}$
     Only an infection-free equilibrium is present in Fig. 21 (a).
   - $\mathcal{R}_0 = \mathcal{R}_{\text{saddle}} = 0.9838$
     A stable infection-free steady state exists while there are two endemic steady states exist which coincide with each other in Fig. 21 (b).
   - $\mathcal{R}_{\text{saddle}} < \mathcal{R}_0 < 1$
     There are stable and unstable endemic steady states and a stable infection-free equilibrium in Fig. 22 (a).
   - $\mathcal{R}_0 > 1$
     An unstable infection-free and a stable endemic steady states are present in Fig. 22 (b).

2.4 Summary

We conclude that in two dimensional extensions of the *SIR* endemic model: R class susceptible in Sect. 2.1; nonlinear transmission class in Sect. 2.2; and exogenous infection class in Sect. 2.3, for $\mathcal{R}_0 > 1$, there is an unstable infection-free steady state and a unique stable endemic steady state, with a forward bifurcation at $\mathcal{R}_0 = 1$ when $\mathcal{P} < \mathcal{P}_{\text{crit}}$. A backward bifurcation occurs at $\mathcal{R}_0 = 1$ when $\mathcal{P} > \mathcal{P}_{\text{crit}}$. We have found some sub-critical endemic steady states when $\mathcal{R}_{\text{saddle}} < \mathcal{R}_0 < 1$ and $\mathcal{P} > \mathcal{P}_{\text{crit}}$. Thus, these models exhibit the dynamics of backward bifurcation; multiple endemic steady states; and the phenomenon of hysteresis for certain values of $\mathcal{R}_0$ less than one.

In Sect. 2.2, the *SIR* model with nonlinear transmission class have a function $h(i)$ that may lead to the presence of a limit cycle about the steady state. From [6], we have applied a theorem that fails to prove the existence of any limit cycles for the function $h(i) = \frac{\mathcal{P}i}{1+\mathcal{P}i}$. However, we have also applied Dulac's criterion which fails to exclude any limit cycles. This criterion can not tell us about the global stability of the non trivial steady state in this case. However, from the calculation of the stability of infection-free and endemic steady states, the bifurcation and the phase-plane analyses, we have found that this model also possess a backward bifurcation phenomena.

3 General Analysis of 2D Models

In this chapter, we will examine several two dimensional extensions of the *SIR* endemic model: R class susceptible; nonlinear transmission class; and exogenous infection class, in a general manner and using a matrix framework.
Consider the ODE system

$$\frac{d\mathbf{y}}{dt} = -M\mathbf{y} + f(\mathbf{y}). \tag{31}$$

where M is a non-singular 2×2 matrix, $\mathbf{y}$ is the vector $\begin{pmatrix} s \\ i \end{pmatrix}$ and $f(\mathbf{y})$ is a vector-valued function. At the endemic steady state $\frac{d\mathbf{y}}{dt} = 0$, $-M\mathbf{y} + f(\mathbf{y}) = 0$, where $\mathcal{R}_0$ is the same parameter used previously. Hence, we calculate M and $f(\mathbf{y})$ in such a manner that $\mathcal{R}_0 = 1$ defines a bifurcation point with either a forward or a backward bifurcation. Given these conditions, we have applied Taylor and binomial expansions to obtain results, using i^* as a small perturbation variable, about the infection-free steady state $\mathbf{y} = \begin{pmatrix} 1 \\ 0 \end{pmatrix}$.

The basic idea in this chapter is to apply a perturbation technique to compare the previous bifurcation analysis for endemic steady states; and to establish that these perturbation results agree with the summary in Chapter 2. This will lay the framework for a general analysis model of these types.

3.1 Susceptible R Class

Consider the ODEs for a susceptible R class as given in Sect. 2.1 (see equations (12)). Taking basic reproduction number $\mathcal{R}_0 = \frac{\beta}{\mu+\gamma}$ and $\mathcal{P}$ is the ratio of transmission probabilities from the recovered and susceptible classes. Rescaling time so that $\mu = 1$ we rewrite equations (12) as

$$\begin{aligned} \frac{ds}{dt} &= 1 - \mathcal{R}_0\mathcal{A}si - s, \\ \frac{di}{dt} &= \mathcal{R}_0\mathcal{A}si + \mathcal{P}\mathcal{R}_0\mathcal{A}(1-s-i)i - \mathcal{A}i, \end{aligned}$$

where $\mathcal{A} = \frac{\mu+\gamma}{\mu}$ (See Table 5). Separating linear and quadratic terms, we have equation (31) where,

$$M = \begin{pmatrix} 1 & 0 \\ 0 & \mathcal{A}(1-\mathcal{P}\mathcal{R}_0) \end{pmatrix},$$

and

$$f(\mathbf{y}) = \begin{pmatrix} 1 - \mathcal{R}_0\mathcal{A}si \\ \mathcal{R}_0\mathcal{A}(si - \mathcal{P}(s+i)i) \end{pmatrix}.$$

Notation	Description
$\mathcal{A}$	$\frac{\mu+\gamma}{\mu}$
$\bar{\mathcal{C}}$	$\frac{\mu+\nu}{\mu}$
$\mathcal{D}$	$\frac{(\mu+\nu)(\mu+\gamma)}{\mu\nu}$
$\bar{\mathcal{D}}$	$\frac{\mu+\nu}{\nu}$
$\bar{B}$	$\frac{\kappa\gamma}{\mu}$
B	$\frac{\mu+\delta}{\mu}$
$\bar{E}$	$\frac{(\mu+\nu)(\mu+\gamma)-\kappa\gamma\nu}{\mu\nu}$
$\mathcal{F}$	$\frac{\gamma}{\mu+\delta}$
x	$\frac{\lambda}{\mu}$

Table 5: Frequently Used Notation in Chapters 3 and 5

Setting time derivatives of this matrix system to zero we have

$$\frac{d}{dt}\begin{pmatrix} s \\ i \end{pmatrix} = 0 \Longrightarrow -M\mathbf{y} + f(\mathbf{y}) = \mathbf{0}. \tag{32}$$

At a steady state when $\mathbf{y}^\star = \begin{pmatrix} s^\star \\ i^\star \end{pmatrix}$, equation (32) becomes

$$\mathbf{y}^\star = M^{-1} f(\mathbf{y}^\star). \tag{33}$$

Thus

$$\mathbf{y}^\star = \begin{pmatrix} s^\star \\ i^\star \end{pmatrix} = \begin{pmatrix} 1 - \mathcal{R}_0 \mathcal{A} s^\star i^\star \\ \mathcal{R}_0(s^\star i^\star - \mathcal{P} s^\star i^\star - \mathcal{P} i^{\star 2})(1 - \mathcal{P}\mathcal{R}_0)^{-1} \end{pmatrix}. \tag{34}$$

Applying a Taylor series expansion about $i^\star = 0$, to $s^\star$ and $\mathcal{R}_0$ we gain quadratics expressions in $i^\star$ and ignore cubic and higher order terms.

$$\begin{aligned} \mathcal{R}_0 &= 1 + i^\star \mathcal{R}_{01} + i^{\star 2}\mathcal{R}_{02} + \mathcal{O}(i^{\star 3}), \\ s^\star &= 1 + i^\star s_1^\star + i^{\star 2} s_2^\star + \mathcal{O}(i^{\star 3}), \\ \mathcal{R}_0 s^\star i^\star &= i^\star + i^{\star 2}(\mathcal{R}_{01} + s_1^\star) + \mathcal{O}(i^{\star 3}). \end{aligned} \tag{35}$$

Substituting these back into equation (34) to get

$$\mathbf{y}^\star = \begin{pmatrix} 1 + i^\star s_1^\star + i^{\star 2} s_2^\star \\ i^\star \end{pmatrix}$$

$$= \begin{pmatrix} 1 - \mathcal{A}(i^\star + i^{\star 2}(\mathcal{R}_{01} + s_1^\star)) \\ [(i^\star + i^{\star 2}(\mathcal{R}_{01} + s_1^\star))(1 - \mathcal{P}) - \mathcal{P} i^{\star 2}] \, (1 - \mathcal{P} - i^\star \mathcal{P}\mathcal{R}_{01} - i^{\star 2}\mathcal{P}\mathcal{R}_{02})^{-1} \end{pmatrix}.$$

Now taking $(1 - \mathcal{P})^{-1}$ out as a factor in row 2, we apply the binomial expansion to the inverse exponent to get

$$\mathbf{y}^\star = \begin{pmatrix} 1 - \mathcal{A}(i^\star + i^{\star 2}(\mathcal{R}_{01} + s_1^\star)) \\ \left(i^\star + i^{\star 2}(\mathcal{R}_{01} + s_1^\star) - \frac{\mathcal{P}}{1-\mathcal{P}} i^{\star 2}\right) (1 - z)^{-1} \end{pmatrix}, \tag{36}$$

where $z = \left(\frac{i^\star \mathcal{P}\mathcal{R}_{01}}{1-\mathcal{P}} + \frac{i^{\star 2}\mathcal{P}\mathcal{R}_{02}}{1-\mathcal{P}}\right)$. Using the Binomial expansion to find an approximation

$$\begin{aligned} (1 - z)^{-1} &= 1 + z + z^2 + \mathcal{O}(z^3) \\ &= 1 + \frac{\mathcal{P}\mathcal{R}_{01} i^\star}{1 - \mathcal{P}} + \frac{\mathcal{P}\mathcal{R}_{02} i^{\star 2}}{1 - \mathcal{P}} + \frac{\mathcal{P}^2 \mathcal{R}_{01}^2 i^{\star 2}}{(1 - \mathcal{P})^2} + \mathcal{O}(i^{\star 3}), \end{aligned}$$

and neglecting higher order terms, we rewrite equation (34) to obtain

$$\mathbf{y}^\star = \begin{pmatrix} 1 + i^\star s_1^\star + i^{\star 2} s_2^\star \\ i^\star \end{pmatrix} = \begin{pmatrix} 1 - \mathcal{A}(i^\star + i^{\star 2}(\mathcal{R}_{01} + s_1^\star)) \\ i^\star + i^{\star\, 2}\left(\frac{\mathcal{P}\mathcal{R}_{01}}{1 - \mathcal{P}} + s_1^\star + \mathcal{R}_{01} - \frac{\mathcal{P}}{1 - \mathcal{P}}\right) \end{pmatrix}.$$

or

$$\begin{pmatrix} 1 \\ 0 \end{pmatrix} + i^\star \begin{pmatrix} s_1^\star \\ 1 \end{pmatrix} + i^{\star 2} \begin{pmatrix} s_2^\star \\ 0 \end{pmatrix}$$

$$= \begin{pmatrix} 1 \\ 0 \end{pmatrix} + i^\star \begin{pmatrix} -\mathcal{A} \\ 1 \end{pmatrix} + i^{\star 2} \begin{pmatrix} -\mathcal{A}(s_1^\star + \mathcal{R}_{01}) \\ \frac{\mathcal{P}\mathcal{R}_{01}}{1-\mathcal{P}} + s_1^\star + \mathcal{R}_{01} - \frac{\mathcal{P}}{1-\mathcal{P}} \end{pmatrix}.$$

Comparing equal powers in terms of the perturbation variable $i^\star$

$$s_1^\star = -\mathcal{A} < 0, s_2^\star = -\mathcal{A}(s_1^\star + \mathcal{R}_{01}),$$

$$s_1^\star = \frac{\mathcal{P}}{1 - \mathcal{P}} - \frac{\mathcal{P}\mathcal{R}_{01}}{1 - \mathcal{P}} - \mathcal{R}_{01}. \tag{37}$$

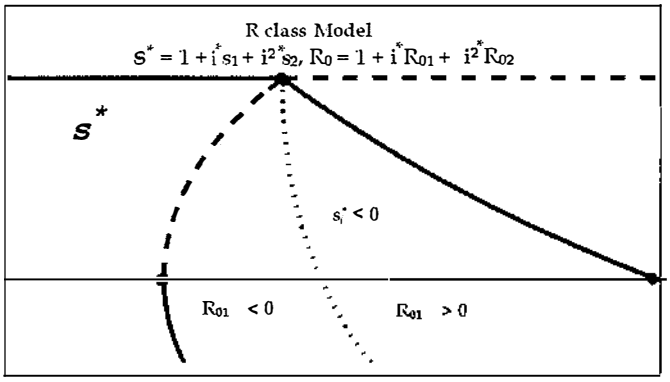

Figure 23: Enlarged top-center part of Figure 5. A clearer view for $s_1^\star < 0$, and the values for $\mathcal{R}_{01}$ as we perturb the variable $i^\star$. Unbroken lines show stable steady states while broken lines signify unstable. The curve $\mathcal{R}_{01} < 0$ when $\mathcal{P} > \mathcal{P}_{\text{crit}}$ and curve $\mathcal{R}_{01} > 0$ when $\mathcal{P} < \mathcal{P}_{\text{crit}}$.

At the critical value of $\mathcal{P}$, $\mathcal{R}_{01} = 0$, $s_1^\star = -\mathcal{A}$ then equation (37) becomes

$$\mathcal{P} = \frac{-\mathcal{A}}{1-\mathcal{A}} = \frac{-\dfrac{\mu+\gamma}{\mu}}{1-\left(\dfrac{\mu+\gamma}{\mu}\right)}.$$

and hence

$$\boxed{\mathcal{P}_{\text{crit}} = 1 + \frac{\mu}{\gamma}}$$

- If $\mathcal{P} > \mathcal{P}_{\text{crit}}$, then $\mathcal{R}_{01} < 0$ and a backward bifurcation occurs.
- If $\mathcal{P} < \mathcal{P}_{\text{crit}}$, then $\mathcal{R}_{01} > 0$ then a forward bifurcation occurs.

This is the same as in Sect. 2.1, and is illustrated in Fig. 23. This sketch shows that using the Taylor series expansion, we have found results consistent with those in Sect. 2.1.

3.2 Nonlinear Transmission Class

In this section, we will investigate the nonlinear transmission model using a general framework. We review the system of ordinary differential equations (18) in Sect. 2.2. with nonlinear force of infection '$\lambda = \beta i(1 + h(i))$' and $h(i) = \frac{\mathcal{P}i}{1+\mathcal{P}i}$. For more details see Sect. 2.2 and Gomes et al. [6]. $\mathcal{R}_0 = \frac{\beta}{(\mu+\gamma)}$ and $\mathcal{P}$ are as in Sect. 2.2. We rewrite the

equations (18) as

$$\begin{aligned}\frac{ds}{dt} &= \mu - \mathcal{R}_0(\mu+\gamma)(1+h(i))si - \mu s,\\ \frac{di}{dt} &= \mathcal{R}_0(\mu+\gamma)(1+h(i))si - (\mu+\gamma)i.\end{aligned}$$

Rescaling time, so that $\mu = 1$ we have

$$\begin{aligned}\frac{ds}{dt} &= 1 - \mathcal{R}_0\mathcal{A}si\left(\frac{1+2\mathcal{P}i}{1+\mathcal{P}i}\right) - s,\\ \frac{di}{dt} &= \mathcal{R}_0\mathcal{A}si\left(\frac{1+2\mathcal{P}i}{1+\mathcal{P}i}\right) - \mathcal{A}i,\end{aligned}$$

where $\mathcal{A} = \frac{\mu+\gamma}{\mu}$ and $1+h(i) = \frac{1+2\mathcal{P}i}{1+\mathcal{P}i}$. In matrix form, we consider equation (31) where

$$M = \begin{pmatrix} 1 & 0 \\ 0 & \mathcal{A} \end{pmatrix},\ \mathbf{y} = \begin{pmatrix} s \\ i \end{pmatrix}, f(\mathbf{y}) = \begin{pmatrix} 1 - \mathcal{R}_0\mathcal{A}si\left(\frac{1+2\mathcal{P}i}{1+\mathcal{P}i}\right) \\ \mathcal{R}_0\mathcal{A}si\left(\frac{1+2\mathcal{P}i}{1+\mathcal{P}i}\right) \end{pmatrix}$$

Setting $\frac{d\mathbf{y}}{dt} = \mathbf{0}$, for a steady state $\mathbf{y}^\star = \begin{pmatrix} s^\star \\ i^\star \end{pmatrix}$, equation (32) becomes

$$\mathbf{y}^\star = M^{-1}f(\mathbf{y}^\star) = \begin{pmatrix} 1 & 0 \\ 0 & \mathcal{A}^{-1} \end{pmatrix}\begin{pmatrix} 1 - \mathcal{R}_0\mathcal{A}s^\star i^\star\left(\frac{1+2\mathcal{P}i^\star}{1+\mathcal{P}i^\star}\right) \\ \mathcal{R}_0\mathcal{A}s^\star i^\star\left(\frac{1+2\mathcal{P}i^\star}{1+\mathcal{P}i^\star}\right) \end{pmatrix}.$$

Hence

$$\mathbf{y}^\star = \begin{pmatrix} \frac{1+\mathcal{P}i^\star - \mathcal{A}\mathcal{R}_0 s^\star i^\star - 2\mathcal{P}\mathcal{A}\mathcal{R}_0 s^\star i^{\star 2}}{1+\mathcal{P}i^\star} \\ \frac{\mathcal{R}_0 s^\star i^\star + 2\mathcal{P}\mathcal{R}_0 s^\star i^{\star 2}}{1+\mathcal{P}i^\star} \end{pmatrix}.$$

Using the binomial expansion $(1+\mathcal{P}i^\star)^{-1} = 1 - \mathcal{P}i^\star + \mathcal{P}^2 i^{\star 2} + \mathcal{O}(i^{\star 3})$ and ignoring higher order terms, we get

$$\mathbf{y}^\star = \begin{pmatrix} s^\star \\ i^\star \end{pmatrix} = \begin{pmatrix} 1 - \mathcal{A}\mathcal{R}_0 s^\star i^\star - \mathcal{P}\mathcal{A}\mathcal{R}_0 s^\star i^{\star 2} \\ \mathcal{R}_0 s^\star i^\star + \mathcal{P}\mathcal{R}_0 s^\star i^{\star 2} \end{pmatrix}. \tag{38}$$

We apply a Taylor series expansion, in equation (38) finding quadratic terms for $s^\star$ and $\mathcal{R}_0$, using a perturbation variable $i^\star$. From equation (35), we have $s^\star$, $\mathcal{R}_0$ and $\mathcal{R}_0 s^\star i^\star$ so we expand $\mathcal{R}_0 s^\star i^{\star 2} = i^\star(i^\star + i^{\star 2}(s_1^\star + \mathcal{R}_{01})) = i^{\star 2} + \mathcal{O}\ (i^{\star 3})$. Ignoring higher order terms,

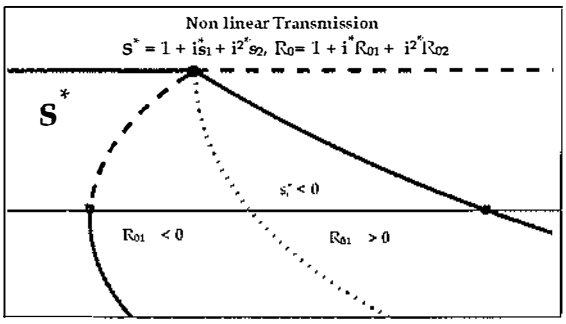

Figure 24: Enlarged diagram taken from Fig. 11. Labels are as in Fig. 23.

we substitute these values back into equation (38) getting

$$\mathrm{y}^\star = \begin{pmatrix} 1 + i^\star s_1^\star + i^{\star 2} s_2^\star \\ i^\star \end{pmatrix} = \begin{pmatrix} 1 - \mathcal{A}(i^\star + i^{\star 2}(s_1^\star + \mathcal{R}_{01} - \mathcal{P})) \\ i^\star + i^{\star 2}(s_1^\star + \mathcal{R}_{01} + \mathcal{P}) \end{pmatrix},$$

or

$$\begin{pmatrix} 1 \\ 0 \end{pmatrix} + i^\star \begin{pmatrix} s_1^\star \\ 1 \end{pmatrix} + i^{\star 2} \begin{pmatrix} s_2^\star \\ 0 \end{pmatrix}$$

=

$$\begin{pmatrix} 1 \\ 0 \end{pmatrix} + i^\star \begin{pmatrix} -\mathcal{A} \\ 1 \end{pmatrix} + i^{\star 2} \begin{pmatrix} -\mathcal{A}(\mathcal{R}_{01} + s_1^\star - \mathcal{P}) \\ \mathcal{R}_{01} + s_1^\star + \mathcal{P} \end{pmatrix}.$$

Comparing terms with equal power of $i^\star$ we get

$$s_1^\star = -\mathcal{A} < 0, s_2^\star = -\mathcal{A}(\mathcal{R}_{01} + s_1^\star - \mathcal{P}),$$

$$s_1^\star = -\mathcal{P} - \mathcal{R}_{01}. \tag{39}$$

At the critical value of $\mathcal{P}$, $\mathcal{R}_{01} = 0$ we have $s_1^\star = -\mathcal{A}$. Thus, equation (39) becomes $\mathcal{P} = -s_1^\star = \mathcal{A}$.

$$\boxed{\mathcal{P}_{\text{crit}} = 1 + \frac{\gamma}{\mu}}$$

- If $\mathcal{P} > \mathcal{P}_{\text{crit}}$, then $\mathcal{R}_{01} < 0$ and a backward bifurcation occurs.
- If $\mathcal{P} < \mathcal{P}_{\text{crit}}$, then $\mathcal{R}_{01} > 0$ and a forward bifurcation occurs.

These results are consistent with those in Sect. 2.2. Fig. (24) shows that a backward bifurcation occurs when $\mathcal{R}_{01} < 0$, while forward bifurcation occurs when $\mathcal{R}_{01} > 0$.

3.3 Exogenous Infection Class

In this section, a system of differential equations for the *SIR* model with exogenous infection class is studied. We consider the ordinary differential equations from Sect. 2.3.

$$\begin{aligned} \frac{ds}{dt} &= \mu - \beta si - \mu s, \\ \frac{di}{dt} &= \mathcal{P}\beta(1-s-i)i + \nu(1-s) - (\mu+\nu)i. \end{aligned} \tag{40}$$

We rescale time to have $\mu = 1$. The transmission rate $\beta = \frac{\mathcal{R}_0(\mu+\nu)\mu}{\nu}$ and the parameter $\mathcal{P}$ are as in Sect. 2.3. Substituting β in equation (40) we get

$$\begin{aligned} \frac{ds}{dt} &= 1 - \mathcal{R}_0\bar{\mathcal{D}}si - s, \\ \frac{di}{dt} &= \mathcal{P}\mathcal{R}_0\bar{\mathcal{D}}(1-s-i)i + \frac{\bar{\mathcal{C}}}{\bar{\mathcal{D}}}(1-s) - \bar{\mathcal{C}}i. \end{aligned}$$

See Table 5 for notations $\bar{\mathcal{D}}$ and $\bar{\mathcal{C}}$. In order to obtain matrix form, we take equation (31), where

$$M = \begin{pmatrix} 1 & 0 \\ \frac{\bar{\mathcal{C}}}{\bar{\mathcal{D}}} & \bar{\mathcal{C}} - \mathcal{P}\mathcal{R}_0\bar{\mathcal{D}} \end{pmatrix}, \ \mathbf{y} = \begin{pmatrix} s \\ i \end{pmatrix}, f(\mathbf{y}) = \begin{pmatrix} 1 - \mathcal{R}_0\bar{\mathcal{D}}si \\ -\mathcal{P}\mathcal{R}_0\bar{\mathcal{D}}(s+i)i + \frac{\bar{\mathcal{C}}}{\bar{\mathcal{D}}} \end{pmatrix}.$$

Setting $\frac{d\mathbf{y}}{dt} = \mathbf{0}$, for a steady state $\mathbf{y}^\star = \begin{pmatrix} s^\star \\ i^\star \end{pmatrix}$, we have equation (33).

$$\mathbf{y}^\star = M^{-1}f(\mathbf{y}^\star) = \begin{pmatrix} 1 - \mathcal{R}_0\bar{\mathcal{D}}s^\star i^\star \\ \frac{(\mathcal{R}_0 s^\star i^\star(\bar{\mathcal{C}} - \mathcal{P}\bar{\mathcal{D}}) - \mathcal{P}\bar{\mathcal{D}}i^{\star 2})}{(\bar{\mathcal{C}} - \mathcal{P}\mathcal{R}_0\bar{\mathcal{D}})} \end{pmatrix}. \tag{41}$$

We apply a Taylor series expansion for $s^\star$ and $\mathcal{R}_0$, using $i^\star$ as a perturbation variable.Ignoring cubic and higher order terms and substituting the quadratic terms from equation (35) back into equation (41) to get

$$\mathbf{y}^\star = \begin{pmatrix} 1 + i^\star s_1^\star + i^{\star 2}s_2^\star \\ i^\star \end{pmatrix}$$

$$= \begin{pmatrix} 1 - \bar{\mathcal{D}}(i^\star + i^{\star 2}(s_1^\star + \mathcal{R}_{01})) \\ \frac{[(i^\star + i^{\star 2}(s_1^\star + \mathcal{R}_{01}))(\bar{\mathcal{C}} - \mathcal{P}\bar{\mathcal{D}}) - \mathcal{P}\bar{\mathcal{D}}\mathcal{R}_{01}i^{\star 2}]}{(\bar{\mathcal{C}} - \mathcal{P}\bar{\mathcal{D}} - i^\star\mathcal{P}\bar{\mathcal{D}}\mathcal{R}_{01} - i^{\star 2}\mathcal{P}\bar{\mathcal{D}}\mathcal{R}_{02})} \end{pmatrix}.$$

Taking $\frac{1}{(\bar{\mathcal{C}}-\mathcal{P}\bar{\mathcal{D}})}$ as a factor from row 2 to have

$$\mathbf{y}^\star = \begin{pmatrix} 1-\bar{\mathcal{D}}(i^\star + i^{\star 2}(s_1^\star + \mathcal{R}_{01})) \\ \left(i^\star + i^{\star 2}(s_1^\star + \mathcal{R}_{01}) - \frac{\mathcal{P}\bar{\mathcal{D}}\mathcal{R}_{01}i^{\star 2}}{\bar{\mathcal{C}}-\mathcal{P}\bar{\mathcal{D}}}\right)(1-z)^{-1} \end{pmatrix}, \tag{42}$$

where

$$z = \left(\frac{\mathcal{P}\bar{\mathcal{D}}\mathcal{R}_{01}i^\star}{\bar{\mathcal{C}}-\mathcal{P}\bar{\mathcal{D}}} + \frac{\mathcal{P}\bar{\mathcal{D}}\mathcal{R}_{02}i^{\star 2}}{\bar{\mathcal{C}}-\mathcal{P}\bar{\mathcal{D}}}\right).$$

At this point, we apply a binomial expansion to obtain an approximation

$$(1-z)^{-1} = 1 + \frac{\mathcal{P}\bar{\mathcal{D}}\mathcal{R}_{01}}{\bar{\mathcal{C}}-\mathcal{P}\bar{\mathcal{D}}}i^\star + \frac{\mathcal{P}\bar{\mathcal{D}}\mathcal{R}_{02}}{\bar{\mathcal{C}}-\mathcal{P}\bar{\mathcal{D}}}i^{\star 2} + \frac{\mathcal{P}^2\bar{\mathcal{D}}^2\mathcal{R}_{01}^2}{(\bar{\mathcal{C}}-\mathcal{P}\bar{\mathcal{D}})^2}i^{\star 2} + \mathcal{O}(i^{\star 3}).$$

Again we ignore cubic and higher order terms and substitute this back in equation (42) to obtain

$$\mathbf{y}^\star = \begin{pmatrix} 1 + i^\star s_1^\star + i^{\star 2}s_2^\star \\ i^\star \end{pmatrix} = \begin{pmatrix} 1-\bar{\mathcal{D}}(i^\star + i^{\star 2}(s_1^\star + \mathcal{R}_{01})) \\ i^\star + i^{\star 2}\left(s_1^\star + \mathcal{R}_{01} + \frac{\mathcal{P}\bar{\mathcal{D}}(\mathcal{R}_{01}-1)}{\bar{\mathcal{C}}-\mathcal{P}\bar{\mathcal{D}}}\right) \end{pmatrix},$$

or

$$\begin{pmatrix} 1 \\ 0 \end{pmatrix} + i^\star \begin{pmatrix} s_1^\star \\ 1 \end{pmatrix} + i^{\star 2} \begin{pmatrix} s_2^\star \\ 0 \end{pmatrix}$$

=

$$\begin{pmatrix} 1 \\ 0 \end{pmatrix} + i^\star \begin{pmatrix} -\bar{\mathcal{D}} \\ 1 \end{pmatrix} + i^{\star 2} \begin{pmatrix} -\bar{\mathcal{D}}(s_1^\star + \mathcal{R}_{01}) \\ s_1^\star + \mathcal{R}_{01} + \frac{\mathcal{P}\bar{\mathcal{D}}(\mathcal{R}_{01}-1)}{\bar{\mathcal{C}}-\mathcal{P}\bar{\mathcal{D}}} \end{pmatrix}.$$

Comparing terms

$$s_1^\star = -\bar{\mathcal{D}} < 0, s_2^\star = -\bar{\mathcal{D}}(s_1 + \mathcal{R}_{01}),$$

$$\frac{\mathcal{P}\bar{\mathcal{D}}\mathcal{R}_{01}}{\bar{\mathcal{C}}-\mathcal{P}\bar{\mathcal{D}}} + s_1^\star + \mathcal{R}_{01} - \frac{\mathcal{P}\bar{\mathcal{D}}}{\bar{\mathcal{C}}-\mathcal{P}\bar{\mathcal{D}}} = 0 \tag{43}$$

At the critical value of $\mathcal{P}$, $\mathcal{R}_{01} = 0$ we have $s_1^\star = -\bar{\mathcal{D}}$ and equation (43) becomes

$$\mathcal{P} = \frac{-\bar{\mathcal{C}}}{1-\bar{\mathcal{D}}} = \frac{-\frac{\mu+\nu}{\mu}}{\frac{-\mu}{\nu}}.$$

$$\boxed{\mathcal{P}_{\text{crit}} = \frac{\nu(\mu+\nu)}{\mu^2}}$$

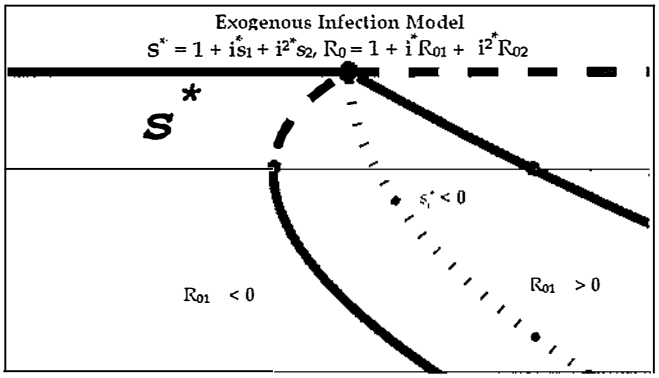

Figure 25: An enlarged top-center portion of the bifurcation fig. (17). Labels are as in Fig. 23.

Thus, we conclude with the following results

- If $\mathcal{P} > \mathcal{P}_{\text{crit}}$, then $\mathcal{R}_{01} < 0$ and a backward bifurcation occurs.
- If $\mathcal{P} < \mathcal{P}_{\text{crit}}$, then $\mathcal{R}_{01} > 0$ and a forward bifurcation occurs.

These results are consistent with those in Sect. 2.3. It is clear from Fig. 25 that $\mathcal{R}_{01} < 0$ gives backward bifurcation, while $\mathcal{R}_{01} > 0$ gives forward bifurcation.

4 3D Extensions

In this chapter, we will investigate four different three dimensional extensions of the *SIR* endemic model. The two dimensional SEI model was examined in Sect. 2.3. Now, we include a recovered R class to make it three dimensional *SEIR* model (see Sect. 4.1, Sect. 4.2 & Sect. 4.3). We will discuss three different *SEIR* models. Firstly, we present the general *SEIR* model then, we investigate two other *SEIR* models that have partial and full recovery respectively. The model in Sect. 4.4 is another three dimensional model which introduces a Carrier class (C), and c(t), a proportion of the population which are carriers.

4.1 *SEIR* model

This model is similar to that which we have discussed in Sect. 2.3 as a two dimensional model. This becomes a three dimensional *SEIR* model when a recovered class is also included. The *SEIR* model postulates long-lasting immunity after infection as there is no transition from the recovered class to the susceptible class [11]. The system of four differential equations describing this model is

$$\begin{aligned} \frac{ds}{dt} &= \mu - \beta si - \mu s, \\ \frac{de}{dt} &= \beta si - \mathcal{P}\beta ei - (\mu+\nu)e, \\ \frac{di}{dt} &= \mathcal{P}\beta ei + \nu e - (\mu+\gamma)i, \\ \frac{dr}{dt} &= \gamma i - \mu r, \end{aligned} \tag{44}$$

with $r(t)$ = 1 - $s(t)$ - $i(t)$ - $e(t)$ to keep equations (44) as a reduced three dimensional system. The parameters μ, γ and ν are as defined in Sect. 2.3. This model is three dimensional and if $\mathcal{P} = 0$, it becomes the classical *SEIR* model [12]. The basic reproduction number $\mathcal{R}_0 = \frac{\beta\nu}{(\mu+\gamma)(\mu+\nu)}$ is independent of $\mathcal{P}$.

Studying the globally stability of the system (44) in the region $\{(s(t), e(t), i(t)) : 0 \leq s(t), e(t), i(t) \leq 1, s+e+i \leq 1\}$ is highly nontrivial. Because, to prove the global stability of such a high dimensional system is not usually possible.

4.1.1 Steady State Solutions

Applying a qualitative approach, we find that the system (44) possess two steady states i.e. infection-free and endemic equilibriums. The infection-free steady state is $(s, e, i) = (1, 0, 0)$. On the other hand, we have endemic steady state: when $\mathcal{P} = 0$; and when $\mathcal{P} \neq 0$. For $\mathcal{P} = 0$, the endemic steady state $(s^*, e^*, i^*) = \left(\frac{1}{\mathcal{R}_0}, \frac{\mu(\mathcal{R}_0-1)}{\mathcal{R}_0(\mu+\nu)}, \frac{\mu(\mathcal{R}_0-1)}{\beta}\right)$.
For $\mathcal{P} \neq 0$, the endemic steady states are

$$s^* = \left(\frac{\mu\nu}{\mathcal{R}_0(\mu+\gamma)(\mu+\nu)i^* + \mu\nu}\right),$$

and

$$e^* = \frac{(\mu+\gamma)\nu i^*}{\mathcal{P}\mathcal{R}_0(\mu+\gamma)(\mu+\nu)i^* + \nu^2},$$

with i^* solves for

$$f(i^*) = \mathcal{P}\mathcal{R}_0 i^{*2} + \rho i^* + \frac{\mu\nu^2(1-\mathcal{R}_0)}{\mathcal{R}_0(\mu+\gamma)^2(\mu+\nu)} = 0, \tag{45}$$

where $\rho = \left(\frac{\mathcal{P}\mu\nu}{(\mu+\gamma)(\mu+\nu)} + \frac{\nu}{\mu+\gamma} - \frac{\mathcal{P}\mathcal{R}_0\mu}{\mu+\gamma}\right)$. We have a unique positive solution $i^* > 0$ for $\mathcal{R}_0 > 1$, as $f(0) < 0$. For $\mathcal{R}_0 < 1$, we solve $f(i^*)$ to find a quadratic solution for i^*

$$i^*_{\pm} = -\frac{\rho(\mu+\gamma)(\mu+\nu) \pm \sqrt{\rho^2(\mu+\nu)^2[2\mu\gamma + (\mu+\gamma)] + 4\mathcal{P}\mu\nu^2(\mathcal{R}_0-1)}}{2\mathcal{P}\mathcal{R}_0(\mu+\gamma)(\mu+\nu)}.$$

For $\mathcal{R}_0 < 1$, we have three possibilities for the solutions of $f(i^*)$. If the discriminant of $f(i^*)$ is positive, then we have two real roots and if it is negative, then we have no real roots. If it is zero, then graphically, the parabola of $f(i^*)$ opens upward and is tangential to the i^*-axis. The value of $\mathcal{R}_0$ causing it to be tangential to the parabola on the i^*-axis is denoted as $\mathcal{R}_{\text{saddle}}$.

4.1.2 Saddle Node Equation

In this section, we will look for the conditions of the critical point for $\mathcal{P}$ where backward bifurcation occurs. We find the critical value for $\mathcal{P}$, therefore we can calculate the saddle node equation for $\mathcal{R}_0$ when $\mathcal{P} > \mathcal{P}_{\text{crit}}$ where backward bifurcation occurs. Treating $\mathcal{R}_0$ as a function of i^* and differentiating equation (45) to get

$$i^* = \frac{\frac{\mathcal{P}\mathcal{R}_0\mu}{\mu+\gamma} - \frac{\nu}{\mu+\gamma}\left(\frac{\mathcal{P}\mu}{\mu+\nu} + 1\right)}{2\mathcal{P}\mathcal{R}_0}.$$

μ	0.02
γ	0.06
ν	0.05
$\mathcal{P}_{\text{crit}}$	8.75
$\mathcal{R}_{\text{saddle}}$	0.977

Table 6: Parameter values for the *SEIR* model.

Setting $(\mathcal{R}_0, i^\star) = (1, 0)$ to obtain the critical value

$$\mathcal{P}_{\text{crit}} = \frac{\nu(\mu+\nu)}{\mu^2}.$$

We calculate the saddle node solution by treating $\mathcal{R}_0$ as a function of $i^\star$ in equation (45), for $\mathcal{P} > \mathcal{P}_{\text{crit}}$; and then at the saddle we have $\frac{d\mathcal{R}_0}{di^\star} = 0$, which defines the minimum value of $\mathcal{R}_0$. Substituting the value of $i^\star$ into equation (45) to get the saddle node equation

$$\mathcal{P}^2\mathcal{R}_0^2 + \left(\frac{2\nu^2}{\mu(\mu+\nu)} - \frac{\mathcal{P}\nu}{\mu+\nu} - \frac{\nu}{\mu}\right) 2\mathcal{P}\mathcal{R}_0 + \left(\frac{\nu}{\mu} - \frac{\mathcal{P}\nu}{(\mu+\nu)}\right)^2 = 0.$$

This equation solves for $\mathcal{R}_{\text{saddle}}$, at which two endemic steady states coincide with each other, at the turning point with $i-$component $i_+^\star = i_-^\star = i^\star$.

4.1.3 Stability

Linearising the ODE system (44), the Jacobian matrix is

$$J = \begin{pmatrix} -\mu - \beta i & 0 & -\beta s \\ \beta i & -\mathcal{P}\beta i - (\mu+\nu) & \beta s - \mathcal{P}\beta e \\ 0 & \mathcal{P}\beta i + \nu & \mathcal{P}\beta e - (\mu+\gamma) \end{pmatrix}. \tag{46}$$

For the infection-free equilibrium $(s, e, i) = (1, 0, 0)$, the Jacobian matrix becomes

$$J_{\text{infection-free}} = \begin{pmatrix} -\mu & 0 & -\beta \\ 0 & -(\mu+\nu) & \beta \\ 0 & \nu & -(\mu+\gamma) \end{pmatrix} \tag{47}$$

The essential sub-matrix is the second 2×2 diagonal block. The stability conditions for τ and Δ read

$$\tau = -(2\mu + \gamma + \nu),$$

$$\Delta = (\mu+\gamma)(\mu+\nu)(1 - \mathcal{R}_0).$$

From this we always have $\tau < 0$ but if $\mathcal{R}_0 < 1$, then $\Delta > 0$ and if $\mathcal{R}_0 > 1$ then, $\Delta < 0$ for all parameters. Hence, we have found that the infection-free steady state is stable when $\mathcal{R}_0 < 1$, and unstable when $\mathcal{R}_0 > 1$.

For the endemic equilibrium, if $\mathcal{P} = 0$, then $(s^\star, e^\star, i^\star) = \left(\frac{1}{\mathcal{R}_0}, \frac{\mu(\mathcal{R}_0-1)}{\mathcal{R}_0(\mu+\nu)}, \frac{\mu(\mathcal{R}_0-1)}{\beta}\right)$,

$$J_{\text{endemic}} = \begin{pmatrix} -\mu\mathcal{R}_0 & 0 & -\frac{(\mu+\gamma)(\mu+\nu)}{\nu} \\ \mu(\mathcal{R}_0-1) & -(\mu+\nu) & \frac{(\mu+\nu)(\mu+\gamma)}{\nu} \\ 0 & \nu & -(\mu+\gamma) \end{pmatrix}.$$

This leads to the characteristic equation $\omega^3 + a_1\omega^2 + a_2\omega + a_3 = 0$, where

$$a_1 = \nu + \gamma + (2 + \mathcal{R}_0)\mu,$$

$$a_2 = \mu\mathcal{R}_0(2\mu + \nu + \gamma),$$

$$a_3 = \mu(\mathcal{R}_0 - 1)[\mu^2 + \mu(\nu + \gamma) + \nu\gamma].$$

From the Routh-Hurwitz theorem, if the conditions (c_1) $a_1 > 0$, (c_2) $a_3 > 0$ and (c_3) $a_1a_2 - a_3 > 0$ are true, then all the roots of the characteristic equation have negative real part which means stable equilibrium. First two conditions are true for $\mathcal{R}_0 > 1$ as a_1 and a_3 are both positive quantities. The third condition

$$c_3 = \mu\left[\mathcal{R}_0\left\{(3\mu + \nu + \mu\mathcal{R}_0)(\nu + \gamma) + \mu^2(3 + 2\mathcal{R}_0) + \gamma^2\right\} + \mu^2 + \mu(\nu + \gamma) + \nu\gamma\right]$$

is greater than zero, for all parameter values in Table 6, hence it is also true. Thus, we say that a stable endemic steady state is present for $\mathcal{R}_0 > 1$, by the Routh-Hurwitz criteria.

Now to find the stability of the endemic steady state when $\mathcal{P} \neq 0$, we substitute the value of $s_+^\star$ and $e_+^\star$ into the Jacobian matrix (46) (in terms of $i_+^\star$) to get

$$J = \begin{pmatrix} -\mu - \beta i_+^\star & 0 & \frac{-\beta\mu}{\mu+\beta i_+^\star} \\ \beta i_+^\star & \ddot{S}_+ & \hat{S}_+ \\ 0 & \mathcal{P}\beta i_+^\star + \nu & S_+ \end{pmatrix}, \tag{48}$$

where, $S_+ = \frac{\mathcal{P}\beta(\mu+\gamma)i_+^\star}{\mathcal{P}\beta i_+^\star + \nu} - (\mu + \gamma)$, $\ddot{S}_+ = -\mathcal{P}\beta i_+^\star - (\mu + \nu)$ and $\hat{S}_+ = \frac{\beta\mu}{\mu+\beta i_+^\star} - \frac{\mathcal{P}\beta(\mu+\gamma)i_+^\star}{\mathcal{P}\beta i_+^\star + \nu}$.
Now we have the characteristic equation $\omega^3 + a_1\omega^2 + a_2\omega + a_3 = 0$, where,

$$a_1 = \frac{(3\mu + \gamma)\nu + (\mathcal{P}\beta i_+^\star + \nu)^2 + \beta i_+^\star(2\mu\mathcal{P} + \beta\mathcal{P}i_+^\star + \nu)}{\mathcal{P}\beta i_+^\star},$$

$$a_2 = S_+\ddot{S}_+ - (S_+ + \ddot{S}_+)(\mu + \beta i_+^*) - \hat{S}_+(\mathcal{P}\beta i_+^* + \nu),$$

$$a_3 = (\mu + \beta i_+^*)[S_+\ddot{S}_+ + \hat{S}_+(\mathcal{P}\beta i_+^* + \nu)] + \frac{\beta^2 i_+^* \mu(\mathcal{P}\beta i_+^* + \nu)}{\mu + \beta i_+^*}.$$

These results are found using **Maple** [5]; for $\mathcal{R}_0 < 1$ and $\mathcal{P} > \mathcal{P}_{\text{crit}}$. We calculate that the conditions (c_1), (c_2) and (c_3) are true for the values of the parameters in Table 6. Therefore, a stable endemic steady state exists for $\mathcal{R}_{\text{saddle}} < \mathcal{R}_0 < 1$ and $\mathcal{P} > \mathcal{P}_{\text{crit}}$.

Now substituting s_-^* and e_-^*, in terms of i_-^*, into the Jacobian matrix (46)

$$J = \begin{pmatrix} -\mu - \beta i_-^* & 0 & \frac{-\beta\mu}{\mu+\beta i_-^*} \\ \beta i_-^* & \ddot{S}_- & \hat{S}_- \\ 0 & \mathcal{P}\beta i_-^* + \nu & S_- \end{pmatrix}, \tag{49}$$

where, $S_- = \frac{\mathcal{P}\beta(\mu+\gamma)i_-^*}{\mathcal{P}\beta i_-^* + \nu} - (\mu + \gamma)$, $\ddot{S}_- = -\mathcal{P}\beta i_-^* - (\mu + \nu)$ and $\hat{S}_- = \frac{\beta\mu}{\mu+\beta i_-^*} - \frac{\mathcal{P}\beta(\mu+\gamma)i_-^*}{\mathcal{P}\beta i_-^* + \nu}$.
We have the characteristic equation $\omega^3 + a_1\omega^2 + a_2\omega + a_3 = 0$, where:

$$a_1 = \frac{(3\mu + \gamma)\nu + (\mathcal{P}\beta i_-^* + \nu)^2 + \beta i_-^*(2\mu\mathcal{P} + \beta\mathcal{P}i_-^* + \nu)}{\mathcal{P}\beta i_-^*};$$

$$a_2 = S_-\ddot{S}_- - (S_- + \ddot{S}_-)(\mu + \beta i_-^*) - \hat{S}_-(\mathcal{P}\beta i_-^* + \nu),$$

$$a_3 = (\mu + \beta i_-^*)[S_-\ddot{S}_- + \hat{S}_-(\mathcal{P}\beta i_-^* + \nu)] + \frac{\beta^2 i_-^* \mu(\mathcal{P}\beta i_-^* + \nu)}{\mu + \beta i_-^*}.$$

We find that conditions (c_1) and (c_3) are true while condition (c_2) is false for the values of parameters as given in Table 6. According to the Routh-Hurwitz criteria, if one of these conditions is false, then we have an unstable steady state.

Hence, we say that we have unstable and stable endemic steady states that give a backward bifurcation when $\mathcal{R}_{\text{saddle}} < \mathcal{R}_0 < 1$ and $\mathcal{P} > \mathcal{P}_{\text{crit}}$. Conversely, for $\mathcal{R}_0 > 1$ and $\mathcal{P} < \mathcal{P}_{\text{crit}}$ a forward bifurcation occurs. These results are similar to those in Sect. 2.3.

4.1.4 Bifurcation Analysis

The bifurcation analysis is summarised in Fig. 26. Observe that, for any value of $\mathcal{P}$, the infection-free steady state is asymptotically stable for $\mathcal{R}_0 < 1$, while it is unstable, for $\mathcal{R}_0 > 1$. However, the endemic steady states depend on $\mathcal{R}_0$ and $\mathcal{P}$. If $\mathcal{P} > \mathcal{P}_{\text{crit}}$, then the steady states leaves the bifurcation point at $\mathcal{R}_0 = 1$, in a backward direction in the region $\mathcal{R}_{\text{saddle}} < \mathcal{R}_0 < 1$, with an unstable equilibrium therefore turns forward at $\mathcal{R}_{\text{saddle}}$ and becomes stable as $\mathcal{R}_0 > \mathcal{R}_{\text{saddle}}$ increases. For $\mathcal{R}_0 > 1$, the endemic steady state is

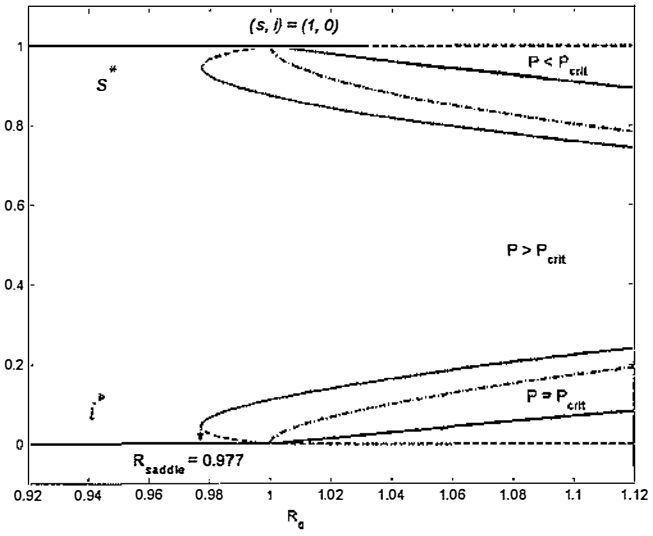

Figure 26: Bifurcation Diagram for the *SEIR* model. Curves are $s^\star$ and $i^\star$ as the functions of $\mathcal{R}_0$. Continuous lines show stable steady state and broken lines are unstable steady states. There are curves for $\mathcal{P} < \mathcal{P}_{\text{crit}}$, $\mathcal{P} = \mathcal{P}_{\text{crit}}$ and $\mathcal{P} > \mathcal{P}_{\text{crit}}$. For this model, $\mathcal{P}_{\text{crit}} = \frac{\nu(\mu+\nu)}{\mu^2}$.

unique and stable for all $\mathcal{P}$. This model also exhibits the phenomenon of hysteresis (see Sect. 2.1).

4.1.5 Phase-Plane Analysis

In this section, we will analyse the phase-planes for the *SEIR* model, showing the trajectories of the three dimensional system onto two dimensions. The valid region in three dimensional space is a tetrahedron, for example $s + e + i \leq 1$. We will look at a two dimensional projection of phase-space where the trajectories are confined to the triangle $s + i \leq 1$. For a projection, trajectories of the solutions may appear to cross but they do not intersect in three dimensional space.

1. $\mathcal{P} = 0$
   - $\mathcal{R}_0 < 1$: A stable infection-free steady state is present in Fig. 27 (a).
   - $\mathcal{R}_0 > 1$: There are one unstable infection-free steady state and a stable endemic equilibrium exist in Fig. 27 (b).
2. $\mathcal{P} = \frac{\mathcal{P}_{\text{crit}}}{2}$
   - $\mathcal{R}_0 < 1$: A stable infection-free steady state exists in Fig. 28 (a).

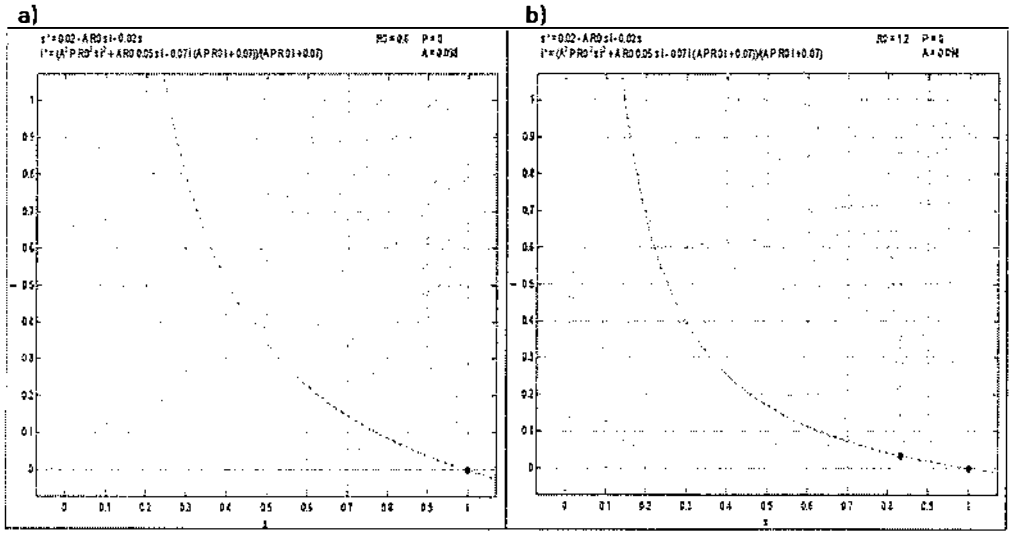

Figure 27: Phase-Planes for the *SEIR* Model for $\mathcal{P} = 0$: when (a) $\mathcal{R}_0 = 0.6 < 1$; (b) $\mathcal{R}_0 = 1.2 > 1$.

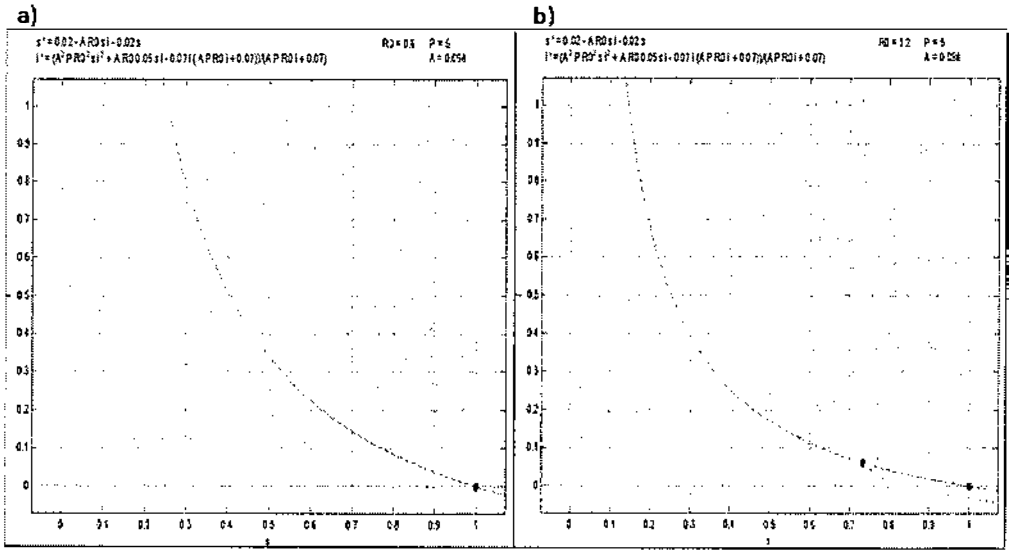

Figure 28: Phase-Planes for the *SEIR* Model for $\mathcal{P} = 5 < \mathcal{P}_{\text{crit}}$ when: (a) $\mathcal{R}_0 = 0.6 < 1$; (b) $\mathcal{R}_0 = 1.2 > 1$.

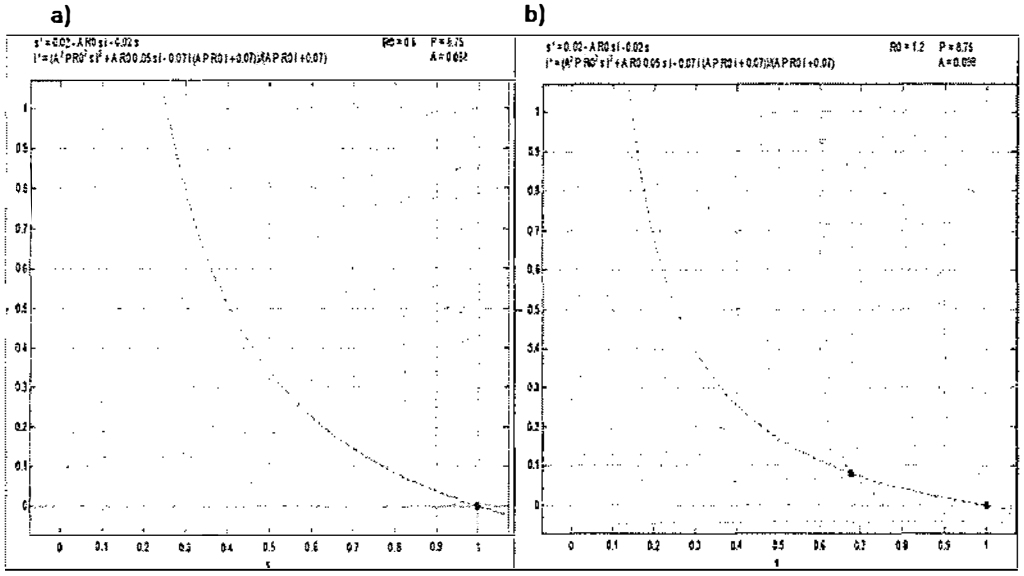

Figure 29: Phase-Planes for the *SEIR* Model for $\mathcal{P} = 8.75 = \mathcal{P}_{\text{crit}}$ when: (a) $\mathcal{R}_0 = 0.6 < 1$; (b) $\mathcal{R}_0 = 1.2 > 1$.

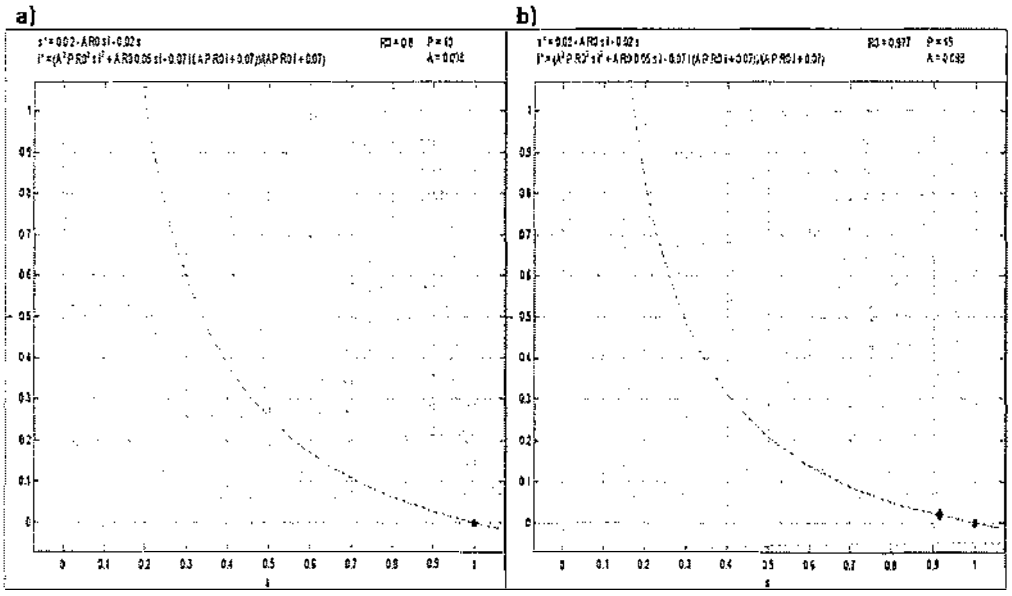

Figure 30: Phase-Planes for the *SEIR* Model for $\mathcal{P} > \mathcal{P}_{\text{crit}}$ when: (a) $\mathcal{R}_0 = 0.8 < \mathcal{R}_{\text{saddle}}$; (b) $\mathcal{R}_{\text{saddle}} = 0.977 < 1$.

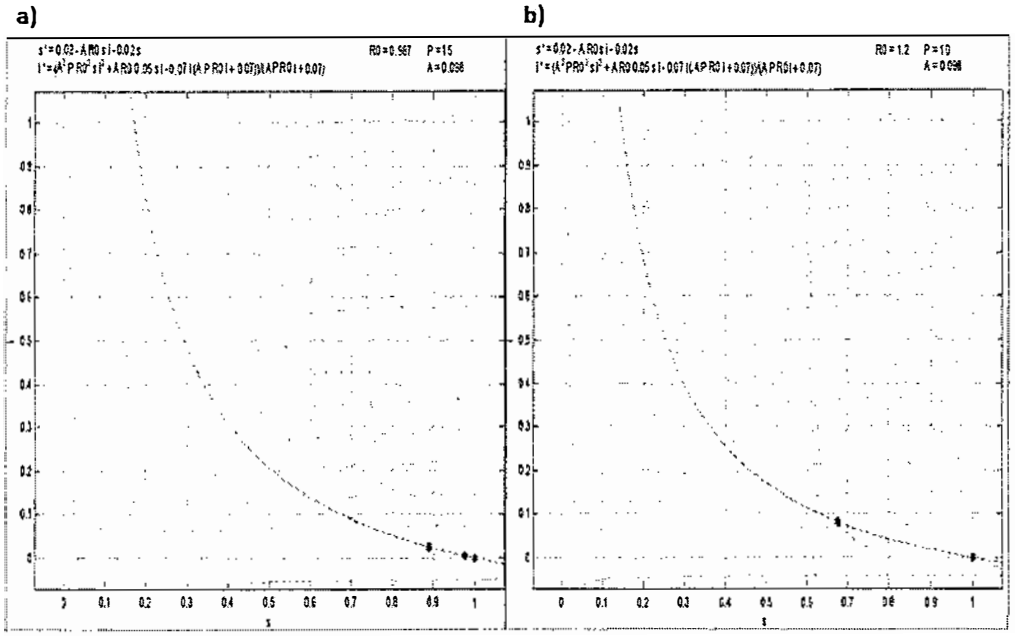

Figure 31: Phase-Planes for the *SEIR* Model for $\mathcal{P} > \mathcal{P}_{\text{crit}}$ when: (a) $\mathcal{R}_0 = 0.987 < 1$; (b) $\mathcal{R}_0 = 1.2 > 1$.

- $\mathcal{R}_0 > 1$: There are one stable endemic and unstable infection-free equilibriums are present in this Fig. 28 (b).

3. $\mathcal{P} = \mathcal{P}_{\text{crit}}$

   - $\mathcal{R}_0 < 1$: A stable infection-free steady state exists in Fig. 29 (a).
   - $\mathcal{R}_0 > 1$: There are an unstable infection-free and a stable endemic steady states in Fig. 29 (b).

4. $\mathcal{P} > \mathcal{P}_{\text{crit}}$

   - $\mathcal{R}_0 < \mathcal{R}_{\text{saddle}}$: Only an infection-free equilibrium is present in Fig. 30 (a).
   - $\mathcal{R}_0 = \mathcal{R}_{\text{saddle}} = 0.977$: A stable infection-free steady state exists. At this point, we have stable and unstable endemic steady states coinciding with each other in Fig. 30 (b).
   - $\mathcal{R}_{\text{saddle}} < \mathcal{R}_0 < 1$: There are multiple endemic steady states: stable; and unstable and a stable infection-free equilibrium in Fig. 31 (a).
   - $\mathcal{R}_0 > 1$: A stable endemic steady state and an unstable infection-free steady state are present in Fig. 31 (b).

4.2 The *SEIR* model with Partial Recovery

A special case of the *SEIR* model with partial recovery is the model by Van den Driessche *et al.* [14]. In this special case, the susceptible and recovered classes enter the exposed class at rates βsi and $\mathcal{P}\beta si$ respectively. The system of four differential equations for this model is

$$\begin{aligned} \frac{ds}{dt} &= \mu - \beta si - \mu s, \\ \frac{de}{dt} &= \beta si + \mathcal{P}\beta ri - (\mu+\nu)e + \kappa\gamma i, \\ \frac{di}{dt} &= \nu e - (\mu+\gamma)i, \\ \frac{dr}{dt} &= -\mathcal{P}\beta ri + (1-\kappa)\gamma i - \mu r, \end{aligned} \tag{50}$$

with $r(t) = 1$ - $s(t)$ - $i(t)$ - $e(t)$ to keep equations (50) as a reduced three dimensional system. A rational number κ represents the unsuccessful recovery of the infectious class which re-approach the exposed class.

We find the basic reproduction number by solving equations in System (50) and considering the standard *SEIR* model when $\mathcal{P} = 0$. Obtain $s^* = \frac{\mu}{\mu+\beta i^*}$ and $e^* = \frac{(\mu+\gamma)i^*}{\nu}$ by setting the right hand side of first three equations to zero, and substituting the values of s^* and e^* to get

$$i^* = \frac{\mu(\beta\nu + \kappa\gamma\nu - (\mu+\gamma)(\mu+\nu))}{\beta((\mu+\gamma)(\mu+\nu) - \kappa\gamma\nu)}.$$

Substituting the value of $i(t)$ into $s(t)$ to get $s^* = \frac{(\mu+\gamma)(\mu+\nu)-\kappa\gamma\nu)}{\beta\nu}$. Now we know that $\mathcal{R}_0$ is the reciprocal of s^*, then the basic reproduction number is $\mathcal{R}_0 = \frac{\beta\nu}{((\mu+\gamma)(\mu+\nu)-\kappa\nu\gamma)}$.

4.2.1 Steady State Solutions

By setting right hand side of system (50) to zero, we find the infection-free steady state is (s, e, i) =(1, 0, 0). The endemic steady state (s^*, e^*, i^*) when $\mathcal{P} = 0$, we have

$$(s^*, e^*, i^*) = \left(\frac{\mu}{\mu+\beta i^*}, \frac{(\mu+\gamma)i^*}{\nu}, \frac{\mu(\mathcal{R}_0 - 1)}{\beta}\right).$$

If $\mathcal{P} \neq 0$, then the endemic steady state for i^* solves

$$f(i^*) = \mathcal{P}\mathcal{R}_0(\mu+\gamma+\nu)i^{*2} + \ddot{M}i^* + \frac{\mu\nu^2\left(\frac{1}{\mathcal{R}_0} - 1\right)}{((\mu+\gamma)(\mu+\nu) - \kappa\nu\gamma)} = 0 \tag{51}$$

μ	0.02
γ	0.05
ν	0.05
κ	0.4
$\mathcal{P}_{\text{crit}}$	2.6
$\mathcal{R}_{\text{saddle}}$	0.9545

Table 7: Parameter values for the *SEIR* model with partial recovery.

where $\ddot{M} = \left(\nu(1-\mathcal{P}\mathcal{R}_0) + \frac{\mathcal{P}\mu\nu(\mu+\nu+\gamma)}{((\mu+\gamma)(\mu+\nu)-\kappa\nu\gamma)}\right)$. The function $f(i^*)$ is a quadratic in i^* and has a unique positive solution when $\mathcal{R}_0 > 1$. For $\mathcal{R}_0 < 1$, we may have a bit more complicated situation, depending on the values of the parameters (see Table 7). The solution of the quadratic equation is

$$i^*_{\pm} = \frac{-\ddot{M} \pm \sqrt{\mathcal{E}}}{2\mathcal{P}\mathcal{R}_0(\iota+\nu+\gamma)},$$

where $\mathcal{E} = \ddot{M}^2 - 4\mathcal{P}\frac{\mu\nu^2(\mu+\nu+\gamma)(1-\mathcal{R}_0)}{((\mu+\gamma)(\mu+\nu)-\kappa\nu\gamma)}$. For $\mathcal{R}_0 < 1$, we may have three solutions. The solutions may be real or complex depending on nature of the discriminant $\mathcal{E}$. If $\mathcal{E} = 0$ then, graphically the parabola of $f(i^*)$ is tangential to the $i-$ axis. This happens when two endemic steady state coincides with each other whenever $\mathcal{R}_0 = \mathcal{R}_{\text{saddle}}$. This is a critical point at which the endemic steady states coincide. In next section, we will calculate the critical conditions for $\mathcal{P}_{\text{crit}}$ and $\mathcal{R}_{\text{saddle}}$.

4.2.2 Saddle Node Equation

Firstly, we find i^* at the critical point, using the equation (51) and forming the implicit derivative $\frac{d\mathcal{R}_0}{di^*} = 0$.

$$i^* = \nu\frac{\left((\mathcal{P}\mathcal{R}_0 - 1) - \frac{\mathcal{P}\mu(\mu+\nu+\gamma)}{((\mu+\gamma)(\mu+\nu)+\kappa\nu\gamma)}\right)}{2\mathcal{P}\mathcal{R}_0(\mu+\nu+\gamma)}.$$

We then calculate the critical value of $\mathcal{P}_{\text{crit}}$ by setting $(\mathcal{R}_0, i^*) = (1,0)$ in i^* to get

$$\mathcal{P}_{\text{crit}} = \frac{[(\mu+\gamma)(\mu+\nu) - \kappa\nu\gamma]}{\gamma\nu(1-\kappa)}.$$

For $\mathcal{P} > \mathcal{P}_{\text{crit}}$, we get the saddle node equation by substituting i^* into equation (51),

$$\mathcal{P}^2\mathcal{R}_0^2 + \left(\frac{2\mathcal{P}\mu(\mu+\nu+\gamma)}{((\mu+\gamma)(\mu+\nu)-\kappa\nu\gamma)}(2-\mathcal{P}) - 2\mathcal{P}\right)\mathcal{R}_0 + \left(\frac{\mathcal{P}\mu(\mu+\nu+\gamma)}{((\mu+\gamma)(\mu+\nu)-\kappa\nu\gamma)} - 1\right)^2 = 0$$

This equation solves for $\mathcal{R}_{\text{saddle}}$. In next section, we will consider the stability of the infection-free and endemic steady states, using the critical values of $\mathcal{P}$ and $\mathcal{R}_{\text{saddle}}$.

4.2.3 Stability

By linearising

$$J = \begin{pmatrix} -\mu-\beta i & 0 & -\beta s \\ \beta i(1-\mathcal{P}) & -\mathcal{P}\beta i-(\mu+\nu) & \beta s+\mathcal{P}\beta(1-s-e-2i)+\kappa\gamma \\ 0 & \nu & -(\mu+\gamma) \end{pmatrix}, \quad (52)$$

for the infection-free equilibrium $(s, e, i) = (1, 0, 0)$, becomes

$$J = \begin{pmatrix} -\mu & 0 & -\beta \\ 0 & -(\mu+\nu) & \beta+\kappa\gamma \\ 0 & \nu & -(\mu+\gamma) \end{pmatrix}. \quad (53)$$

We reduce this matrix to blocks, essential sub-matrix is the second 2×2 diagonal block. The trace and determinant of this sub-matrix are

$$\tau = -(\mu+\nu)-(\mu+\gamma), \Delta = (1-\mathcal{R}_0)[\mu(\mu+\nu+\gamma)+\gamma\nu(1-\kappa)].$$

The trace is always negative while $\Delta < 0$ when $\mathcal{R}_0 > 1$ and $\Delta > 0$ when $\mathcal{R}_0 < 1$. For $\mathcal{R}_0 < 1$, we have a asymptotically stable steady state. For $\mathcal{R}_0 > 1$, the infection-free steady state is unstable.

Now, for the endemic steady state when $\mathcal{P} = 0$, the Jacobian matrix (52) will become

$$J_{\text{endemic}} = \begin{pmatrix} -\mu\mathcal{R}_0 & 0 & -\frac{((\mu+\gamma)(\mu+\nu)-\kappa\nu\gamma)}{\nu} \\ \mu(\mathcal{R}_0-1) & -(\mu+\nu) & \frac{((\mu+\gamma)(\mu+\nu)-\kappa\nu\gamma)}{\nu}+\kappa\gamma \\ 0 & \nu & -(\mu+\gamma) \end{pmatrix}.$$

This leads to the characteristic equation $\omega^3 + a_1\omega^2 + a_2\omega + a_3 = 0$ where

$$a_1 = 2\mu+\gamma+\nu+\mu\mathcal{R}_0,$$

$$a_2 = \mu\mathcal{R}_0(2\mu+\gamma+\nu),$$

$$a_3 = \mu(\mathcal{R}_0-1)[\mu^2+\mu\nu+\mu\gamma-\kappa\nu\gamma].$$

All the roots of this characteristic equation shows a stable steady state if the conditions (c_1), (c_2) and (c_3) are true from the Routh-Hurwitz criteria. It is easy to see that for

$\mathcal{R}_0 > 1$, the conditions (c_1) and (c_2) are both true and third condition (c_3) is also true as $a_1a_2 - a_3 = \mu\mathcal{R}_0[(3\mu + \mu\mathcal{R}_0)(\nu+\gamma) + \nu\gamma(1+\kappa) + \nu^2 + \gamma^2 + (3\mu^2 + 2\mu^2\mathcal{R}_0)] + \mu(\mu^2 + \mu\nu + \mu\gamma - \kappa\nu\gamma)$ is greater than zero. Thus a stable endemic steady state exists for $\mathcal{R}_0 > 1$.

If $\mathcal{P} \neq 0$, then the Jacobian matrix (52) for the endemic steady states $(s_+^\star = \frac{\mu}{\mu+\beta i_+^\star}, e_+^\star = \frac{(\mu+\gamma)i_+^\star}{\nu}, i_+^\star)$ becomes

$$J_{\text{endemic}} = \begin{pmatrix} -\mu - \beta i_+^\star & 0 & -\frac{\beta\mu}{\beta i_+^\star + \mu} \\ \beta i_+^\star(1-\mathcal{P}) & \ddot{S}_+ & \hat{S}_+ \\ 0 & \nu & -(\mu+\gamma) \end{pmatrix}$$

where $\ddot{S}_+ = -\mathcal{P}\beta i_+^\star - (\mu+\nu)$ and $\hat{S}_+ = \frac{\beta\mu}{\beta i_+^\star + \mu} + \mathcal{P}\beta\left(1 - \frac{\mu}{\beta i_+^\star + \mu} - \frac{(\mu+\gamma)i_+^\star}{\nu}\right) - 2\mathcal{P}\beta i_+^\star + \kappa\gamma$. Now from the characteristic equation we find that $\omega^3 + a_1\omega^2 + a_2\omega + a_3 = 0$, where

$$a_1 = 3\mu + \nu + \gamma + (1+\mathcal{P})\beta i_+^\star,$$

$$a_2 = -[\hat{S}_+\nu + \ddot{S}_+(\mu+\gamma) + (\mu + \beta i_+^\star)(\ddot{S}_+ - (\mu+\gamma))],$$

$$a_3 = \frac{\beta^2\mu\nu(1-\mathcal{P})}{\mu + \beta i_+^\star} - (\mu + \beta i_+^\star)[\ddot{S}_+(\mu+\gamma) + \hat{S}_+\nu].$$

Again we check if the conditions (c_1) $a_1 > 0$, (c_2) $a_3 > 0$ and (c_3) $a_1a_2 > a_3$, from the Routh-Hurwitz criteria are true or false in order to find stability of the endemic steady state. By using **Maple** [5], we find that these conditions are true for $\mathcal{R}_{\text{saddle}} < \mathcal{R}_0 < 1$, as a_1 and a_3 are both positive and we calculate that in third condition (c_3) a_1a_2 is greater than a_3 for the parameter values given in Table 7. Thus, we have a stable endemic steady state for $\mathcal{R}_{\text{saddle}} < \mathcal{R}_0 < 1$ and for $\mathcal{P} > \mathcal{P}_{\text{crit}}$.

The Jacobian matrix (52) for the endemic steady states when $s_-^\star = \frac{\mu}{\mu+\beta i_-^\star}$, and $e_-^\star = \frac{(\mu+\gamma)i_-^\star}{\nu}$ in terms of $i_-^\star$ becomes

$$J = \begin{pmatrix} -\mu - \beta i_-^\star & 0 & -\frac{\beta\mu}{\beta i_-^\star + \mu} \\ \beta i_-^\star(1-\mathcal{P}) & \ddot{S}_- & \hat{S}_- \\ 0 & \nu & -(\mu+\gamma) \end{pmatrix},$$

where $\ddot{S}_- = -\mathcal{P}\beta i_-^\star - (\mu+\nu)$ and $\hat{S}_- = \frac{\beta\mu}{\beta i_-^\star + \mu} + \mathcal{P}\beta\left(1 - \frac{\mu}{\beta i_-^\star + \mu} - \frac{(\mu+\gamma)i_-^\star}{\nu}\right) - 2\mathcal{P}\beta i_-^\star + \kappa\gamma$. From the characteristic equation we have $\omega^3 + a_1\omega^2 + a_2\omega + a_3 = 0$, where

$$a_1 = 3\mu + \nu + \gamma + (1+\mathcal{P})\beta i_-^\star,$$

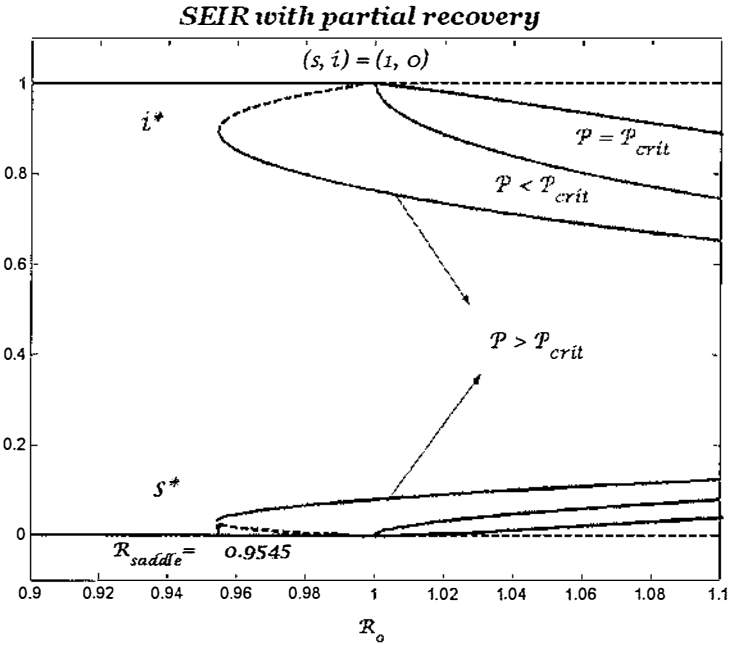

Figure 32: Bifurcation Diagram for the *SEIR* model with partial recovery. Labels are as in Figure 26. This model have $\mathcal{P}_{\text{crit}} = \frac{[(\mu+\gamma)(\mu+\nu)-\kappa\nu\gamma]}{\gamma\nu(1-\kappa)}$.

$$a_2 = -[\hat{S}_-\nu + \ddot{S}_-(\mu+\gamma) + (\mu+\beta i^*_-)(\ddot{S}_- - (\mu+\gamma))],$$
$$a_3 = \frac{\beta^2\mu\nu(1-\mathcal{P})}{\mu+\beta i^*_-} - (\mu+\beta i^*_-)[\ddot{S}_-(\mu+\gamma) + \hat{S}_-\nu].$$

We use **Maple** [5] to calculate these conditions, for $\mathcal{P} > \mathcal{P}_{\text{crit}}$ and $\mathcal{R}_{\text{saddle}} < \mathcal{R}_0 < 1$, the conditions (c_1) and (c_2) are true but condition (c_2) is untrue for parameters in Table 7, thus this endemic steady state is unstable. When $\mathcal{R}_0 > 1$, and for all $\mathcal{P}$, we estimate that the endemic steady state is stable, as all the conditions are true for certain parameters in Table 7.

In general, we understand that there are multiple endemic steady states for $\mathcal{P} > \mathcal{P}_{\text{crit}}$ and $\mathcal{R}_{\text{saddle}} < \mathcal{R}_0 < 1$; stable; and unstable. When $\mathcal{R}_0 > 1$, we have stable endemic steady state for all $\mathcal{P}$.

4.2.4 Bifurcation Analysis

Figure 32 illustrates that this phenomenon exhibits backward bifurcation, this is the same as in Sect. 4.1.4.

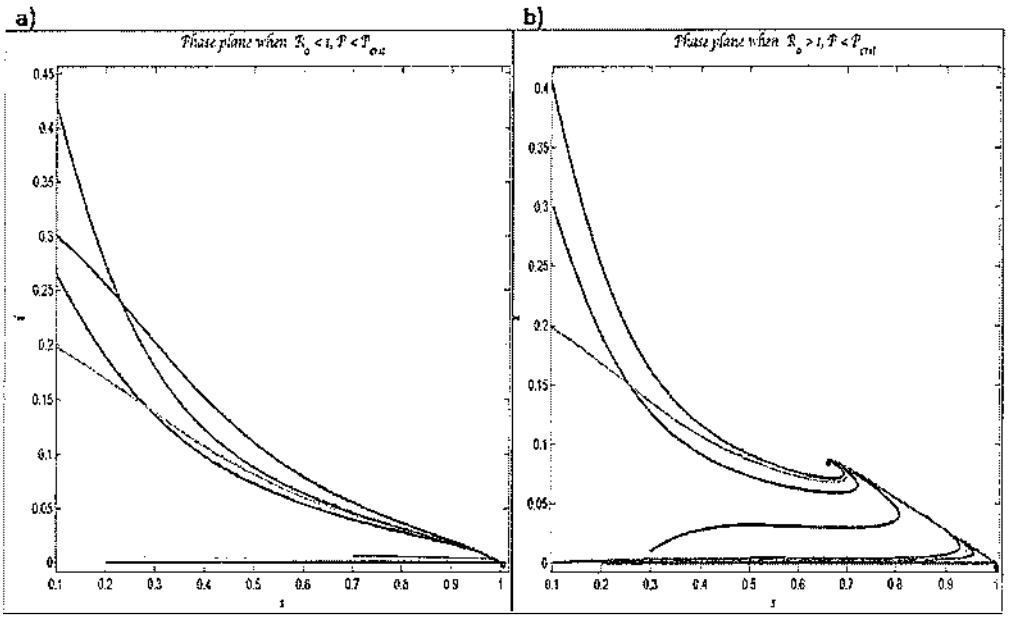

Figure 33: Phase-Plane for the *SEIR* Model with partial recovery for $\mathcal{P} = 0$ when: (a) $\mathcal{R}_0 = 0.7 < 1$; (b) $\mathcal{R}_0 = 1.2 > 1$.

4.2.5 Phase-Plane Analysis

We now study the phase-planes for the *SEIR* model with partial recovery class. In these phase-planes we derive three dimensional information from two dimensional projections ($r(t) = 1 - s(t) - e(t) - i(t)$). The solutions in these phase-planes may appear to cross each other only because of this projection. We use the numerical mathematical package **MATLAB** ODE45 [10] to understand these phase-planes. A number of shades and tints of grey colour are used for different solutions to represent different initial conditions.

1. $\mathcal{P} = 0$

   - $\mathcal{R}_0 < 1$: A stable infection-free steady state exists in Fig. 33 (a).
   - $\mathcal{R}_0 > 1$: There are an unstable infection-free steady state and a stable endemic equilibriums in Fig. 33 (b).

2. $\mathcal{P} = \frac{\mathcal{P}_{\text{crit}}}{2}$

   - $\mathcal{R}_0 < 1$: A stable infection-free steady state exists in Fig. 34 (a).
   - $\mathcal{R}_0 > 1$: There are two stable endemic and an unstable infection-free equilibriums in Fig. 34 (b).

3. $\mathcal{P} = \mathcal{P}_{\text{crit}}$

   - $\mathcal{R}_0 < 1$: A stable infection-free steady state is present in Fig. 35 (a).

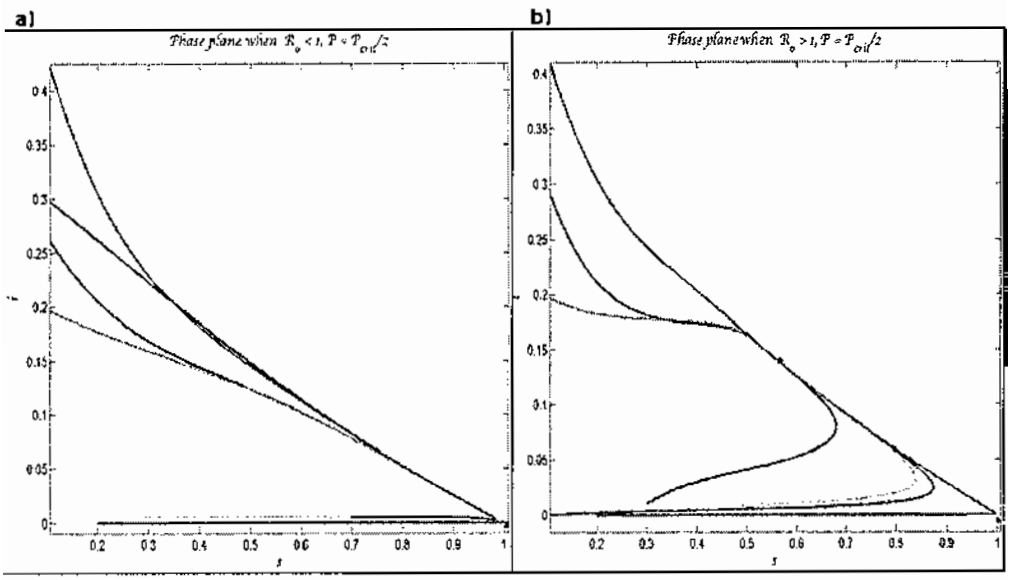

Figure 34: Phase-Plane for the *SEIR* Model with partial recovery for $\mathcal{P} = 1.3 = \frac{\mathcal{P}_{\text{crit}}}{2}$ when: (a) $\mathcal{R}_0 = 0.7 < 1$; (b) $\mathcal{R}_0 = 1.2 > 1$.

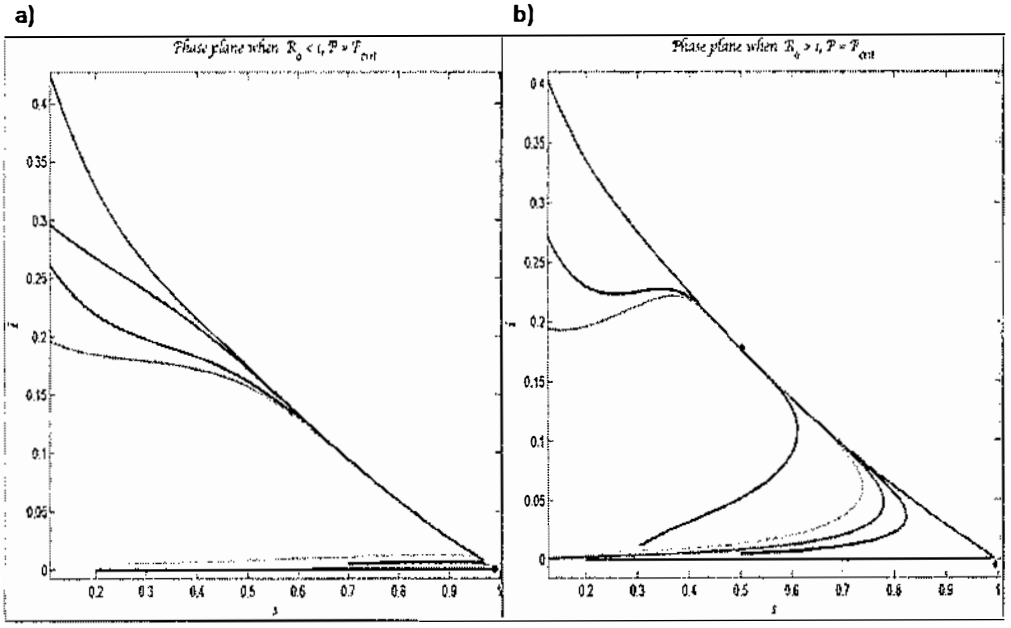

Figure 35: Phase-Plane for the *SEIR* Model with partial recovery for $\mathcal{P} = 2.6 = \mathcal{P}_{\text{crit}}$ when: (a) $\mathcal{R}_0 = 0.7 < 1$; (b) $\mathcal{R}_0 = 1.2 > 1$.

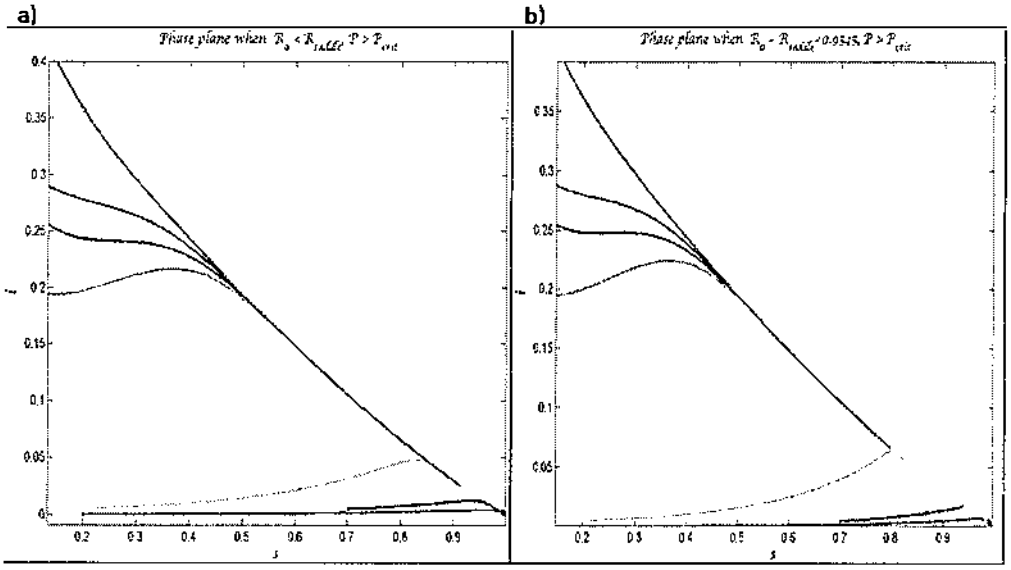

Figure 36: Phase-Plane for the *SEIR* Model with partial recovery for $\mathcal{P} > \mathcal{P}_{\text{crit}}$ when: (a) $\mathcal{R}_0 = 0.7 < \mathcal{R}_{\text{saddle}}$; (b) $\mathcal{R}_{\text{saddle}} = 0.9545 < 1$.

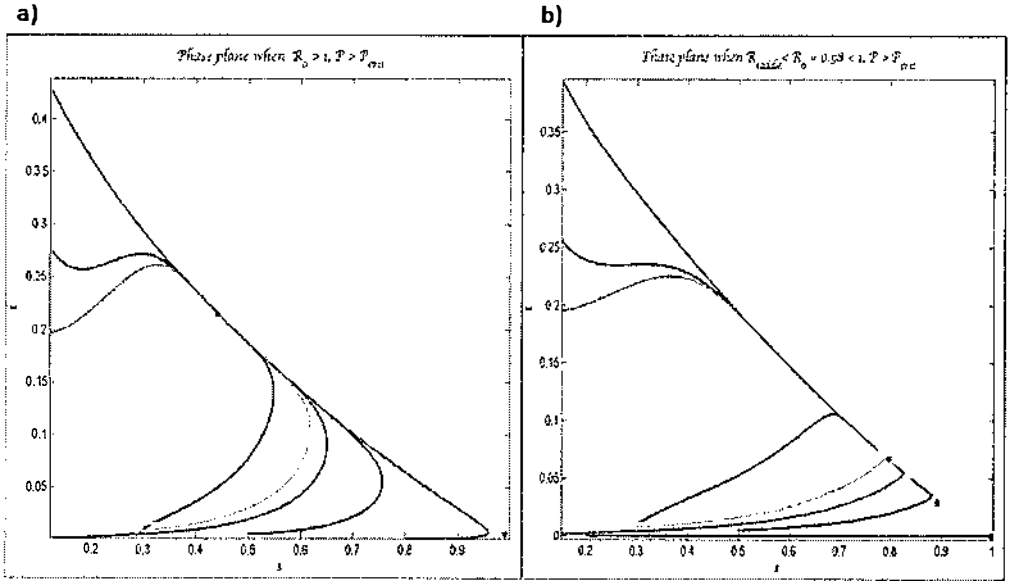

Figure 37: Phase-Plane for the *SEIR* Model with partial recovery for $\mathcal{P} > \mathcal{P}_{\text{crit}}$ when: (a) $\mathcal{R}_{\text{saddle}} < \mathcal{R}_0 = 0.98 < 1$; (b) $\mathcal{R}_0 = 1.2 > 1$.

- $\mathcal{R}_0 > 1$: There are an unstable infection-free and stable endemic steady states in Fig. 35(b).

4. $\mathcal{P} = 5.2 > \mathcal{P}_{\text{crit}}$

   - $\mathcal{R}_0 < \mathcal{R}_{\text{saddle}}$: Only an infection-free equilibrium is present in Fig. 36 (a).
   - $\mathcal{R}_0 = \mathcal{R}_{\text{saddle}} = 0.9545$: A stable infection-free steady state with stable and unstable both endemic steady states coinciding each other in Fig. 36 (b).
   - $\mathcal{R}_{\text{saddle}} < \mathcal{R}_0 < 1$: There are stable and unstable endemic steady states and a stable infection-free equilibrium in Fig. 37 (a).
   - $\mathcal{R}_0 > 1$: There is a stable endemic and unstable infection-free steady states in Fig. 37 (b).

4.3 *SEIR* model with Full Recovery

This model is based on a paper by Van den Driessche [14]. The system of four differential equations for this model is

$$\begin{aligned} \frac{ds}{dt} &= \mu - \beta si - \mu s, \\ \frac{de}{dt} &= \beta si + \mathcal{P}\beta ri - (\mu + \nu)e, \\ \frac{di}{dt} &= \nu e - (\mu + \gamma)i, \\ \frac{dr}{dt} &= -\mathcal{P}\beta ri + \gamma i - \mu r. \end{aligned} \tag{54}$$

with $r(t) = 1 - s(t) - i(t) - e(t)$ to keep equations (54) as a reduced three dimensional system. In this special case, when entering the exposed class there is a successful recovery of infectious class. The basic reproduction number $\mathcal{R}_0$ is the same as in Sect. 4.1. As we have a successful recovery of infectious class thus $\kappa = 0$.

4.3.1 Steady State Solutions

To find the steady state, we set the right hand side of equations (54) to zero. We calculate the infection-free steady state $(s, e, i) = (1, 0, 0)$ and the endemic steady state, when $\mathcal{P} = 0$. They are as in Sect. 4.2. If $\mathcal{P} \neq 0$, then the endemic steady state for i^* is the solution of

$$\mathcal{P}\mathcal{R}_0 i^{*2} + \ddot{N} i^* + \frac{\mu\nu^2\left(\frac{1}{\mathcal{R}_0} - 1\right)}{(\mu + \gamma)(\mu + \nu)(\mu + \nu + \gamma)} = 0. \tag{55}$$

μ	0.02
γ	0.05
ν	0.05
$\mathcal{P}_{\text{crit}}$	1.96
$\mathcal{R}_{\text{saddle}}$	0.9308

Table 8: Parameter values for the *SEIR* model with full recovery.

where $\ddot{N} = \left(\frac{\nu(1-\mathcal{P}\mathcal{R}_0)}{(\mu+\nu+\gamma)} + \frac{\mathcal{P}\mu\nu}{(\mu+\gamma)(\mu+\nu)}\right)$. This equation has a unique positive solution for $\mathcal{R}_0 > 1$. For $\mathcal{R}_0 < 1$, we have more complicated situation which depends on the parameter values. The solution of this quadratic equation is

$$i^*_{\pm} = \frac{-\ddot{N} \pm \sqrt{\ddot{N}^2 - 4\mathcal{P}\frac{\mu\nu^2(1-\mathcal{R}_0)}{(\mu+\gamma)(\mu+\nu)(\mu+\nu+\gamma)}}}{2\mathcal{P}\mathcal{R}_0}.$$

For $\mathcal{R}_0 < 1$, we may have different solutions which may be real or complex. The nature of these solutions is determined by the sign of the discriminant of equation (55). If the discriminant is negative, then we have no real roots; if it is positive, then we get two real roots; and if it is zero, then there is only one real root. In last case, the parabola is concave up and is tangential to the $i-$ axis.
In next section, we will calculate $\mathcal{R}_{\text{saddle}}$, the minimum value of $\mathcal{R}_0$; and $\mathcal{P}_{\text{crit}}$, the critical value for $\mathcal{P}$.

4.3.2 Saddle Node Equation

We find $\mathcal{P}_{\text{crit}}$ from the equation (55) by differentiating $\mathcal{R}_0$ with respect to i^* to get

$$i^* = \frac{\left(\frac{\nu(\mathcal{P}\mathcal{R}_0-1)}{(\mu+\nu+\gamma)} - \frac{\mathcal{P}\mu\nu}{(\mu+\gamma)(\mu+\nu)}\right)}{2\mathcal{P}\mathcal{R}_0}.$$

Then we set $\frac{d\mathcal{R}_0}{di^*}\Big|_{(1,0)} = 0$, in order to define the critical value of $\mathcal{P}$

$$\mathcal{P}_{\text{crit}} = \frac{(\mu+\gamma)(\mu+\nu)}{\gamma\nu}.$$

Thus, we can find the saddle node equation for $\mathcal{R}_0$ when $\mathcal{P} > \mathcal{P}_{\text{crit}}$. Hence, we put the value of i^* back in equation (55) to get the saddle node equation for $\mathcal{R}_0$

$$\mathcal{P}^2\mathcal{R}_0^2 + \left(\frac{2\mathcal{P}\mu(\mu+\nu+\gamma)}{(\mu+\gamma)(\mu+\nu)}(2-\mathcal{P}) - 2\mathcal{P}\right)\mathcal{R}_0 + \left(\frac{\mathcal{P}\mu(\mu+\nu+\gamma)}{(\mu+\gamma)(\mu+\nu)} - 1\right)^2 = 0$$

This equation solves for $\mathcal{R}_{\text{saddle}}$. We will consider the stability of the steady states in next section using the critical values of $\mathcal{P}$ and $\mathcal{R}_{\text{saddle}}$.

4.3.3 Stability

By linearising a system of equations (54)

$$J = \begin{pmatrix} -\mu-\beta i & 0 & -\beta s \\ \beta i(1-\mathcal{P}) & -\mathcal{P}\beta i-(\mu+\nu) & \beta s+\mathcal{P}\beta(1-s-e-i)-\mathcal{P}\beta i \\ 0 & \nu & -(\mu+\gamma) \end{pmatrix}, \quad (56)$$

for the infection-free equilibrium $(s,e,i)=(1,0,0)$, is the same as the Jacobian matrix (47). The eigenvalues are same as for the matrix (47). For $\mathcal{R}_0<1$, we have an asymptotically stable infection-free steady state while for $\mathcal{R}_0>1$, it is unstable.

For an endemic steady state $(s^*,e^*,i^*)=\left(\frac{1}{\mathcal{R}_0},\frac{\mu(\mathcal{R}_0-1)}{\mathcal{R}_0(\mu+\nu)},\frac{\mu(\mathcal{R}_0-1)}{\beta}\right)$, when $\mathcal{P}=0$, we have the same Jacobian matrix (48). This leads to the same characteristic equation $\omega^3+a_1\omega^2+a_2\omega+a_3=0$ of the matrix (48). Thus, a stable endemic steady state is present for $\mathcal{R}_0>1$ when $\mathcal{P}=0$.

Now, when $\mathcal{P}\neq 0$, we put the endemic steady states for $s_+^*=\frac{\mu}{\mu+\beta i_+^*}$, and $e_+^*=\frac{(\mu+\gamma)i_+^*}{\nu}$, in terms of i_+^*, into the Jacobian matrix (56) to have

$$J = \begin{pmatrix} -\mu-\beta i_+^* & 0 & -\frac{\beta\mu}{\beta i_+^*+\mu} \\ \beta i_+^*(1-\mathcal{P}) & \ddot{S}_+ & \hat{S}_+ \\ 0 & \nu & -(\mu+\gamma) \end{pmatrix},$$

where $\ddot{S}_+ = -\mathcal{P}\beta i_+^*-(\mu+\nu)$ and $\hat{S}_+ = \frac{\beta\mu}{\beta i_+^*+\mu}+\mathcal{P}\beta\left(1-\frac{\mu}{\beta i_+^*+\mu}-\frac{(\mu+\gamma)i_+^*}{\nu}\right)-2\mathcal{P}\beta i_+^*$. From the characteristic equation, we find that $\omega^3+a_1\omega^2+a_2\omega+a_3=0$, where

$$a_1 = 3\mu+\nu+\gamma+(1+\mathcal{P})\beta i_+^*,$$

$$a_2 = -[\hat{S}_+\nu+\ddot{S}_+(\mu+\gamma)+(\mu+\beta i_+^*)(\ddot{S}_+-(\mu+\gamma))],$$

$$a_3 = \frac{\beta^2\mu\nu(1-\mathcal{P})}{\mu+\beta i_+^*}-(\mu+\beta i_+^*)[\ddot{S}_+(\mu+\gamma)+\hat{S}_+\nu].$$

We know that, from the Routh-Hurwitz criteria, all the roots of this characteristic equation are stable if the conditions (c_1), (c_2) and (c_3) are true. We calculate that these conditions are true for $\mathcal{R}_0>1$ as a_1 and a_3 both are positive quantities and $a_1a_2-a_3$ is greater than zero using parameter values from the Table 8. Hence, we have a stable

endemic steady state when $\mathcal{R}_0 > 1$, for all $\mathcal{P}$.

Now, for $\mathcal{P} > \mathcal{P}_{\text{crit}}$ and $\mathcal{R}_{\text{saddle}} < \mathcal{R}_0 < 1$, we have calculated that these conditions are true, using **Maple** [5]. Thus we have a stable endemic steady state for $\mathcal{P} > \mathcal{P}_{\text{crit}}$ and $\mathcal{R}_{\text{saddle}} < \mathcal{R}_0 < 1$. Now, we put the endemic steady states for $s^*_- = \frac{\mu}{\mu+\beta i^*_-}$, and $e^*_- = \frac{(\mu+\gamma)i^*_-}{\nu}$, in terms of i^*_- into the Jacobian matrix (56), thus we have

$$J = \begin{pmatrix} -\mu - \beta i^*_- & 0 & -\frac{\beta\mu}{\beta i^*_- + \mu} \\ \beta i^*_-(1-\mathcal{P}) & \ddot{S}_- & \hat{S}_- \\ 0 & \nu & -(\mu+\gamma) \end{pmatrix},$$

where, $\ddot{S}_- = -\mathcal{P}\beta i^*_- - (\mu+\nu)$ and $\hat{S}_- = \frac{\beta\mu}{\beta i^*_- + \mu} + \mathcal{P}\beta\left(1 - \frac{\mu}{\beta i^*_- + \mu} - \frac{(\mu+\gamma)i^*_-}{\nu}\right) - 2\mathcal{P}\beta i^*_-$. This leads to $\omega^3 + a_1\omega^2 + a_2\omega + a_3 = 0$, the characteristic equation, where,

$$a_1 = 3\mu + \nu + \gamma + (1+\mathcal{P})\beta i^*_-,$$

$$a_2 = -[\hat{S}_-\nu + \ddot{S}_-(\mu+\gamma) + (\mu + \beta i^*_-)(\ddot{S}_- - (\mu+\gamma))],$$

$$a_3 = \frac{\beta^2\mu\nu(1-\mathcal{P})}{\mu + \beta i^*_-} - (\mu + \beta i^*_-)[\ddot{S}_-(\mu+\gamma) + \hat{S}_-\nu].$$

When $\mathcal{R}_0 > 1$, and for all $\mathcal{P}$, we have a stable endemic steady state, as conditions (c_1), (c_2) and (c_3) are true for the parameters given in Table 8. For $\mathcal{P} > \mathcal{P}_{\text{crit}}$ and $\mathcal{R}_{\text{saddle}} < \mathcal{R}_0 < 1$, we calculate and use the values in Table 8, that the condition (c_2) is false while rest of the conditions are true by using **Maple** [5]. This implies that an unstable endemic steady state exists for $\mathcal{P} > \mathcal{P}_{\text{crit}}$, $\mathcal{R}_{\text{saddle}} < \mathcal{R}_0 < 1$.

Overall, we conclude that there are two endemic steady states present for $\mathcal{P} > \mathcal{P}_{\text{crit}}$, and in the region of $\mathcal{R}_{\text{saddle}} < \mathcal{R}_0 < 1$. These multiple endemic steady states give a backward bifurcation.

4.3.4 Bifurcation Analysis

Figure 38 summarises that a backward bifurcation occurs at $\mathcal{R}_0 = 1$, this refers to sub-critical endemic steady states (shown as dashed and solid black lines) and a stable infection-free equilibrium. Thus, the dynamics of this system are similar to those of the *SEIR* class, described in Sect. 4.1.

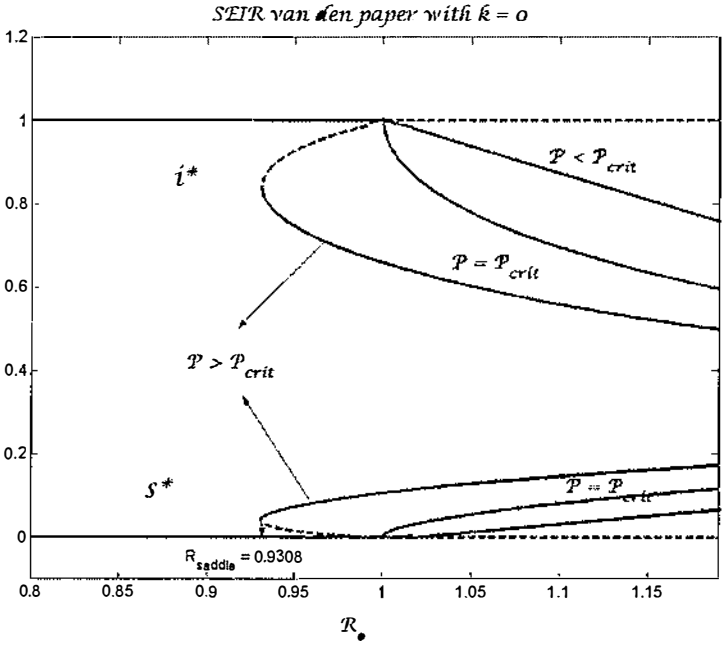

Figure 38: Bifurcation Diagram for the *SEIR* model with full recovery. The critical value of $\mathcal{P}_{\text{crit}} = \frac{(\mu+\gamma)(\mu+\nu)}{\gamma\nu}$.

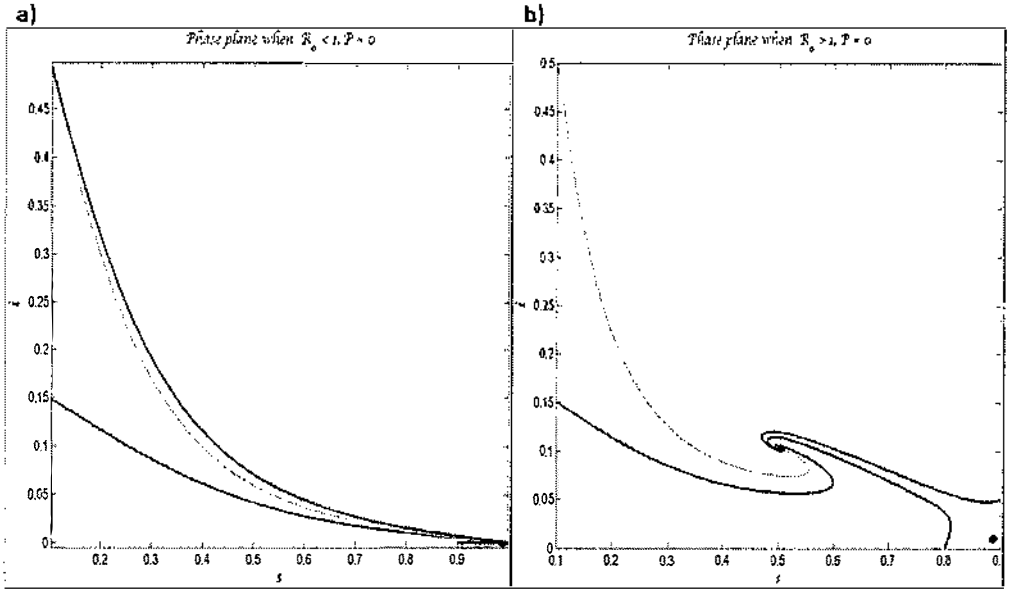

Figure 39: Phase-Planes for the *SEIR* Model with full recovery for $\mathcal{P} = 0$ when: (a) $\mathcal{R}_0 = 0.7 < 1$; (b) $\mathcal{R}_0 > 1$.

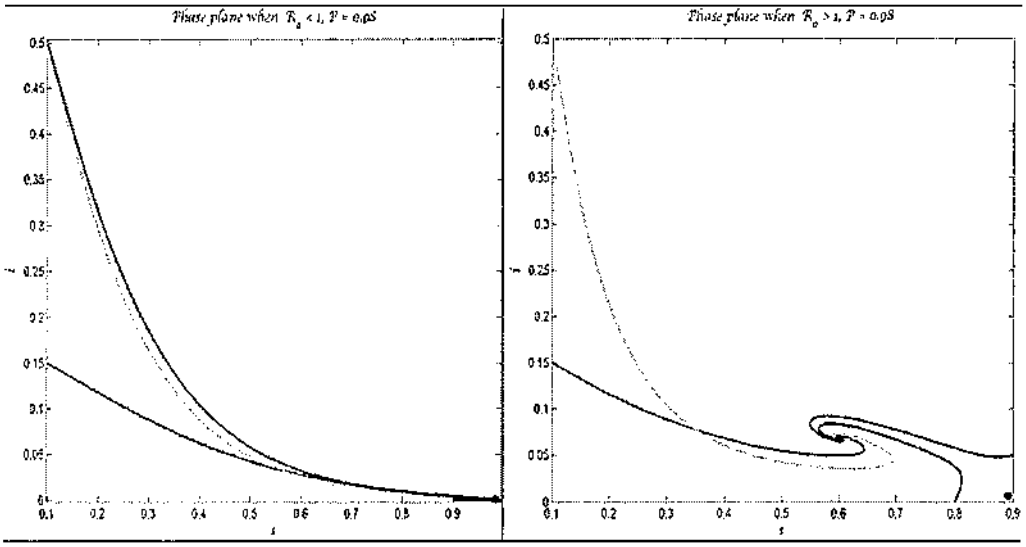

Figure 40: Phase-Planes for the *SEIR* Model with full recovery for $\mathcal{P} = 0.98 = \frac{\mathcal{P}_{\text{crit}}}{2}$ when: (a) $\mathcal{R}_0 = 0.7 < 1$; (b) $\mathcal{R}_0 = 2 > 1$.

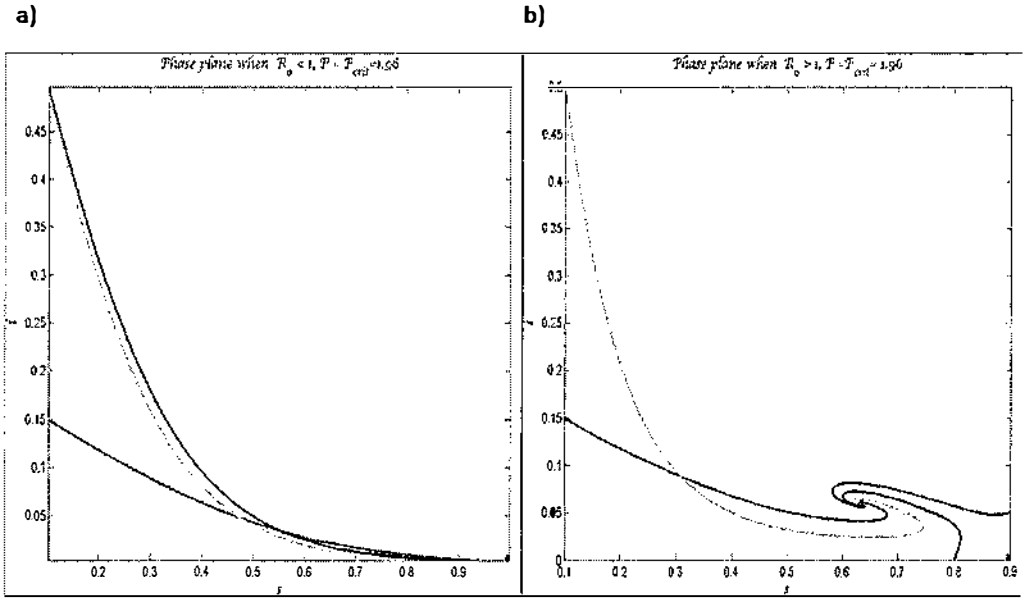

Figure 41: Phase-Plane for the *SEIR* Model with full recovery for $\mathcal{P} = 1.96 = \mathcal{P}_{\text{crit}}$ when: (a) $\mathcal{R}_0 = 0.7 < 1$; (b) $\mathcal{R}_0 = 2 > 1$.

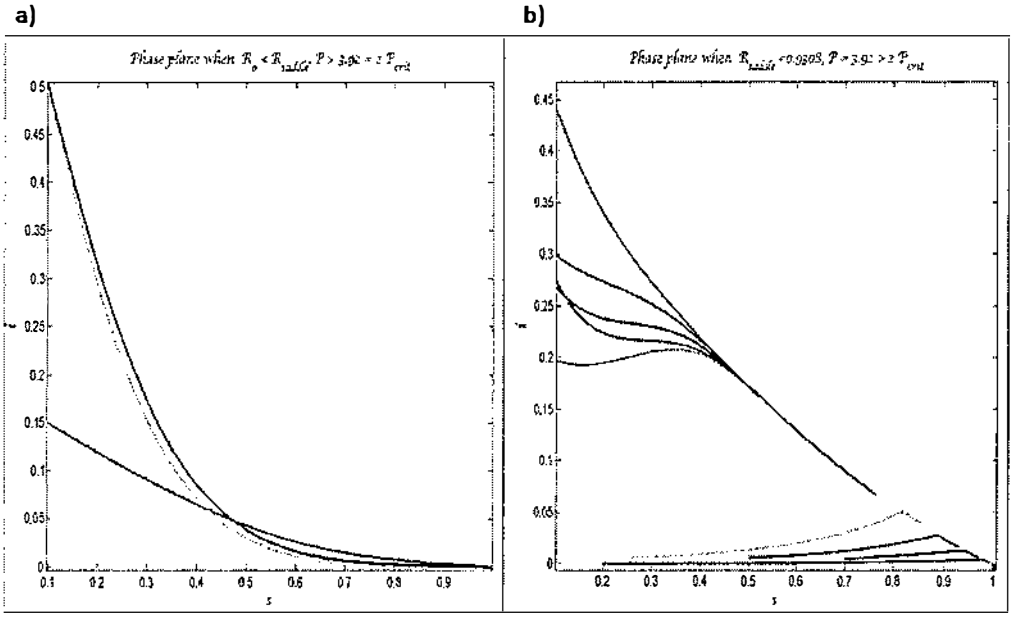

Figure 42: Phase-Plane for the *SEIR* Model with full recovery for $\mathcal{P} > \mathcal{P}_{\text{crit}}$ when: (a) $\mathcal{R}_0 = 0.7 < \mathcal{R}_{\text{saddle}}$; (b) $\mathcal{R}_{\text{saddle}} = 0.9308 < 1$.

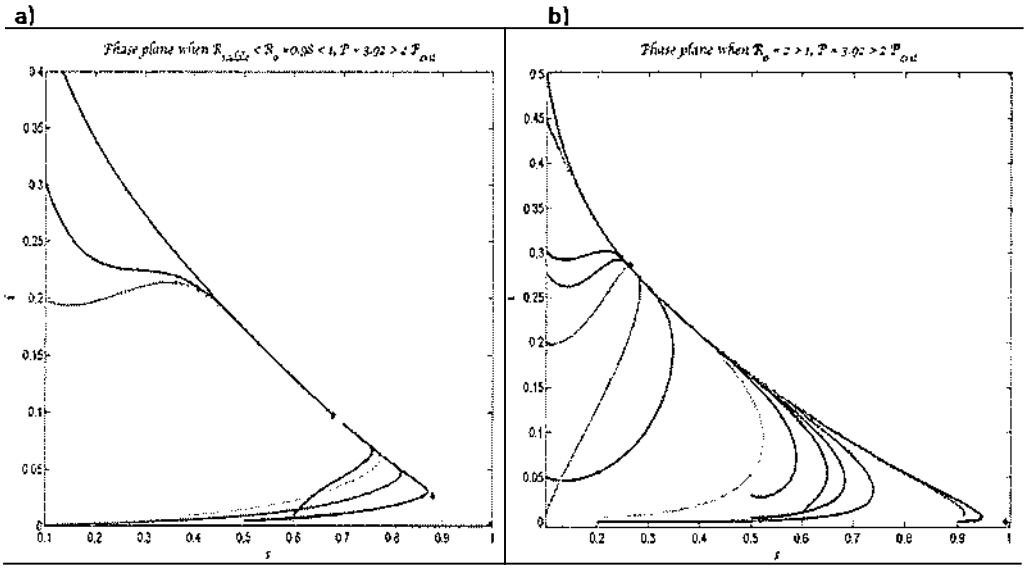

Figure 43: Phase-Plane for the *SEIR* Model with full recovery for $\mathcal{P} > \mathcal{P}_{\text{crit}}$ when: (a) $\mathcal{R}_{\text{saddle}} < \mathcal{R}_0 = 0.98 < 1$; (b) $\mathcal{R}_0 = 2 > 1$.

4.3.5 Phase-Plane Analysis

In this section, we will show the trajectories of the three dimensional system onto two dimensional in the following phase-planes for the *SEIR* model with full recovery. We use the parameter values from Table 8 and different shades and tints of colour grey show different initial conditions.

1. $\mathcal{P} = 0$
   - $\mathcal{R}_0 < 1$: Only a stable infection-free steady state is present in Fig. 39 (a).
   - $\mathcal{R}_0 > 1$: There are one unstable infection-free steady state and stable endemic equilibrium exist in Fig. 39 (b).
2. $\mathcal{P} = \frac{\mathcal{P}_{\text{crit}}}{2}$
   - $\mathcal{R}_0 < 1$: An stable infection-free steady state exists in Fig. 40 (a).
   - $\mathcal{R}_0 > 1$: There are two stable endemic and unstable infection-free equilibriums in Fig. 40 (b).
3. $\mathcal{P} = \mathcal{P}_{\text{crit}}$
   - $\mathcal{R}_0 < 1$: A stable infection-free steady state exists in Fig. 41 (a).
   - $\mathcal{R}_0 > 1$: There are an unstable infection-free and a stable endemic steady states in Fig. 41 (b).
4. $\mathcal{P} = 3.92 > \mathcal{P}_{\text{crit}}$
   - $\mathcal{R}_0 < \mathcal{R}_{\text{saddle}}$: Only an infection-free equilibrium is present in Fig. 42 (a).
   - $\mathcal{R}_0 = \mathcal{R}_{\text{saddle}} = 0.9308$: A stable infection-free steady state and we have stable and unstable endemic steady states on top of each other in Fig. 42 (b).
   - $\mathcal{R}_{\text{saddle}} < \mathcal{R}_0 < 1$: There are locally asymptotically stable and unstable endemic steady states and a stable infection-free equilibrium in Fig. 43 (a).
   - $\mathcal{R}_0 > 1$: A stable endemic and an unstable infection-free steady states are present in Fig. 43 (b).

4.4 The *SIR* Model with Carrier Class

There are some infectious diseases where a carrier may continue to infect others, but not suffer the symptoms of the infection itself. This introduces the Carrier class C. A proportion $q(x)$ join the Carrier class on leaving the infective class when recovered. See,

for example, the model for hepatitis B analysed in Medley et al. [9]. The mathematical model consists of a system of four differential equations as follows

$$\begin{aligned} \frac{ds}{dt} &= -(\lambda+\mu)s+\mu, \\ \frac{di}{dt} &= \lambda s-(\mu+\gamma)i, \\ \frac{dc}{dt} &= q\gamma i-(\mu+\delta)c, \\ \frac{dr}{dt} &= (1-q)\gamma i+\delta c-\mu r. \end{aligned} \tag{57}$$

As $s(t) + i(t) + c(t) + r(t) = 1$, the model is three dimensional. Now, $\lambda = \beta(i + \mathcal{P}c)$, is the force of infection. For this model the constant $\mathcal{P}$ is the infectiousness of carriers relative to acute infectives [9]. Recovery rates of the infectives and carriers are denoted by γ and δ respectively. A proportion $q(x)$ of infectives that move to the carrier class is a function of $x = \frac{\lambda}{\mu}$. In this model we will discuss examples for $q'(x) \geq 0$ where x is a positive quantity. The basic reproduction number is $\mathcal{R}_0 = \frac{\beta}{\mu+\gamma}$.

4.4.1 Steady State Solutions

To study steady states, we solve the differential system (given in equation (57)) by setting $\frac{d.}{dt} = 0$. Solving these equations we find the infection-free and the endemic steady states. The infection-free steady state is $(s, i, c) = (1, 0, 0)$. The endemic steady states for $\mathcal{P} = 0$, we have $s^\star$ and $i^\star$ same as in previous models and $c^\star = \frac{q(x^\star)\gamma\mu(\mathcal{R}_0-1)}{\mathcal{R}_0(\mu+\gamma)(\mu+\delta)}$, where $x^\star = \frac{\beta i^\star}{\mu}$. For $\mathcal{P} \neq 0$, the endemic steady state is

$$(s^\star, i^\star, c^\star) = \left(\frac{1}{1+x^\star}, \frac{x^\star\mu}{(\mu+\gamma)(1+x^\star)}, \frac{\gamma q(x^\star)i^\star}{\mu+\delta}\right), \tag{58}$$

where $x^\star = \frac{\beta(i^\star+\mathcal{P}c^\star)}{\mu}$.

4.4.2 Saddle Node Equation

We find the saddle node equation for $\mathcal{R}_0$ in terms of $x^\star$ which will solve for $\mathcal{R}_{\text{saddle}}$ (which is defined in previous models). We calculate this equation by comparing

$$\beta = \mathcal{R}_0(x^\star)(\mu+\gamma) = \frac{x^\star\mu}{i^\star\left(1+\frac{\mathcal{P}q(x^\star)\gamma}{(\mu+\delta)}\right)}.$$

Now, the steady state for $i^* = \frac{x^*\mu}{(\mu+\gamma)(1+x^*)}$. Thus, substituting the value of i^* and rearranging the above equation, we get the saddle node equation for $\mathcal{R}_0(x^*)$

$$\mathcal{R}_0(x^*) = \frac{(\mu+\delta)(1+x^*)}{\mu+\delta+\mathcal{P}\gamma q(x^*)}. \tag{59}$$

At $(\mathcal{R}_0, i^*) = (1, 0)$, a backward bifurcation occurs for $\mathcal{P} > \mathcal{P}_{\text{crit}} = \frac{\mu+\delta}{q'(0)\gamma}$ (the critical value for $\mathcal{P}$).

4.4.3 Stability

To find the stability of a fixed point we linearise the system (57). The Jacobian matrix is given by

$$J = \begin{pmatrix} -\mu-\beta(i+\mathcal{P}c) & -\beta s & -\mathcal{P}\beta s \\ \beta(i+\mathcal{P}c) & \beta s-(\mu+\gamma) & \mathcal{P}\beta s \\ 0 & q\gamma+q'(x)\gamma\frac{\beta}{\mu}i & -\mu-\delta+q'(x)\gamma\frac{\mathcal{P}\beta}{\mu}i \end{pmatrix}. \tag{60}$$

The Jacobian matrix at the infection-free equilibrium $(s, i, c) = (1, 0, 0)$ is

$$J_{\text{infection-free}} = \begin{pmatrix} -\mu & -\beta & -\mathcal{P}\beta \\ 0 & \beta-(\mu+\gamma) & \mathcal{P}\beta \\ 0 & 0 & -\mu-\delta \end{pmatrix}. \tag{61}$$

The eigenvalues are $\omega_1 = -\mu$, $\omega_2 = (\mathcal{R}_0-1)(\mu+\gamma)$ and $\omega_3 = -(\mu+\delta)$. If $\mathcal{R}_0 < 1$, then all the eigenvalues are negative which shows that there is a stable infection-free steady state while it is unstable for $\mathcal{R}_0 > 1$, as in this case, we find two negative and one positive eigenvalues.

For $\mathcal{P} = 0$, the Jacobian matrix evaluated at the endemic steady state $(s^*, i^*, c^*) = \left(\frac{1}{\mathcal{R}_0}, \frac{(\mathcal{R}_0-1)\mu}{\mathcal{R}_0(\mu+\gamma)}, \frac{q(x^*)(\mathcal{R}_0-1)\mu\gamma}{\mathcal{R}_0(\mu+\gamma)(\mu+\delta)}\right)$ is

$$J_{\text{endemic}} = \begin{pmatrix} -\mu\mathcal{R}_0 & -(\mu+\gamma) & 0 \\ \mu(\mathcal{R}_0-1) & 0 & 0 \\ 0 & q(x^*)\gamma+q'(x^*)\gamma(\mathcal{R}_0-1) & -(\mu+\delta) \end{pmatrix}. \tag{62}$$

We reduce this matrix to blocks to get the essential sub-matrix which is 2×2 diagonal block

$$-(\mu+\gamma)\begin{pmatrix} \mu(\mathcal{R}_0-1) & 0 \\ 0 & -(\mu+\delta) \end{pmatrix}.$$

μ	0.02
γ	0.06
δ	0.025
$\mathcal{P}_{\text{crit}}$ for *Example 1*	0.8333
$\mathcal{R}_{\text{saddle}}$ for *Example 1*	0.8299
$\mathcal{P}_{\text{crit}}$ for *Example 2*	0.9
$\mathcal{R}_{\text{saddle}}$ for *Example 2*	1.09

Table 9: Parameter values for the *SIR* model with carrier class.

This matrix has $\tau = -(\mu+\gamma)[\mu(\mathcal{R}_0-1)-(\mu+\delta)]$ and $\Delta = (\mu+\gamma)(\mu+\delta)(\mathcal{R}_0-1)$. We have negative trace and positive determinant when $\mathcal{R}_0 > 1$, this tells us that if $\mathcal{R}_0 > 1$, then we have a stable endemic steady state whenever $\mathcal{P} = 0$.

When $\mathcal{P} \neq 0$, the Jacobian matrix (60) evaluated at the endemic steady state (equation (58)) in terms of x^*

$$J_{\text{endemic}} = \begin{pmatrix} -\mu(1+x^*) & -\frac{\mathcal{R}_0(\mu+\gamma)}{1+x^*} & -\frac{\mathcal{P}\mathcal{R}_0(\mu+\gamma)}{1+x^*} \\ \mu x^* & \ddot{S} & \frac{\mathcal{P}\mathcal{R}_0(\mu+\gamma)}{1+x^*} \\ 0 & q(x^*)\gamma + \frac{q'(x^*)\gamma\mathcal{R}_0 x^*}{1+x^*} & S \end{pmatrix} \tag{63}$$

where $S = -(\mu+\delta) + \frac{q'(x^*)\gamma\mathcal{P}\mathcal{R}_0 x^*}{1+x^*}$, $\ddot{S} = \frac{(\mu+\gamma)(\mathcal{R}_0-(1+x^*))}{1+x^*}$. Again we find a characteristic equation $\omega^3 + a_1\omega^2 + a_2\omega + a_3 = 0$, where

$$\begin{aligned} a_1 &= \frac{3\mu + 4\mu x^* + (\gamma+\delta)(1+x^*) - q'(x^*)\gamma\mathcal{P}\mathcal{R}_0 x^* - \mathcal{R}_0(\gamma+\mu) + \mu x^{*2}}{1+x^*}, \\ a_2 &= \frac{[(q(x^*)\gamma\mathcal{P} - \mu x^*)(1+x^*) + q'(x^*)\gamma\mathcal{P}\mathcal{R}_0 x^*]\mathcal{R}_0(\mu+\gamma)}{(1+x^*)^2} + \mu(\ddot{S}+S)(1+x^*) - S\ddot{S}, \\ a_3 &= \mu(\mu+\gamma)\left((\mu+\delta)(1+x^*) - q'(x^*)\gamma\mathcal{P}\mathcal{R}_0 x^* - \frac{\mathcal{R}_0(\mu+\delta) - q(x^*)\gamma\mathcal{P}\mathcal{R}_0}{1+x^*}\right). \end{aligned} \tag{64}$$

In the next few sections we will discuss different behaviours by numerically choosing two different examples for the function $q(x^*)$. We will check the conditions (c_1), (c_2) and (c_3) from the Routh-Hurwitz criteria in order to find the stability for different functions $q(x^*)$.

4.4.4 Examples 1, 2

Here we use **Maple** [5] to evaluate steady states solutions, saddle node equations and stability. *Example 1* when $q'(0) > 0$; and *Example 2* when $q'(0) = 0$, both give backward

bifurcations but each leads to a different result. *Example 1* is related to the function $q(x^\star) = 1 - e^{-0.9x^\star}$ for which $q'(0) > 0$ and *Example 2* is for the function $q(x) = \frac{x^{\star 2}}{x^{\star 2}+2}$ for which $q'(0) = 0$.

The main difference in these functions, is that *Example 1* has similar dynamics at $(\mathcal{R}_0, 1 - s^\star) = (1, 0)$ to the extended models in Chapter 2, while *Example 2* gives two backward bifurcations between $\mathcal{R}_{\text{saddle}} < \mathcal{R}_0 < 1.19$.

Example 1

In this section, we will look forward to analyse the steady states and the stability of the endemic steady state when $\mathcal{P} \neq 0$. We will evaluate the Jacobian matrix (63) with $q(x^\star) = 1 - e^{-0.9x^\star}$ and then we will move on to the bifurcation and phase-plane analyses. We will use time- series plots to analyse the qualitative behaviour of the solutions of the system (57) against time, applying different initial conditions.

Steady State Solutions

The infection-free steady state remains the same as that in Sect. 4.4.1 and for the endemic steady states: for $\mathcal{P} = 0$; and $\mathcal{P} \neq 0$ we set $q(x^\star) = 1 - e^{-0.9x^\star}$. Thus in the *Example 1*, we have for: $\mathcal{P} = 0$, the endemic steady state $(s^\star, i^\star, c^\star) = \left(\frac{1}{\mathcal{R}_0}, \frac{(\mathcal{R}_0-1)\mu}{\mathcal{R}_0(\mu+\gamma)}, \frac{(1-e^{-0.9x^\star})(\mathcal{R}_0-1)\mu\gamma}{\mathcal{R}_0(\mu+\gamma)(\mu+\delta)}\right)$, and; for $\mathcal{P} \neq 0$, an endemic steady state $(s^\star, i^\star, c^\star) = \left(\frac{1}{1+x^\star}, \frac{x^\star\mu}{(\mu+\gamma)(1+x^\star)}, \frac{(1-e^{-0.9x^\star})\gamma i^\star}{\mu+\delta}\right)$ exists.

Saddle Node Equation

In Sect. 4.4.2 we set $q(x^\star) = 1 - e^{-0.9x^\star}$ in equation (59), to get the saddle node equation

$$\mathcal{R}_0(x^\star) = \frac{(\mu+\delta)(1+x^\star)}{\mu+\delta+\mathcal{P}\gamma(1-e^{-0.9x^\star})},$$

and the critical value of $\mathcal{P}$ is

$$\mathcal{P}_{\text{crit}} = \frac{\mu+\delta}{0.9\gamma}.$$

Thus, we say that the backward bifurcation at $(\mathcal{R}_0, i^\star) = (1, 0)$ occurs when $\mathcal{P} > \mathcal{P}_{\text{crit}}$ and $\mathcal{R}_{\text{saddle}} < \mathcal{R}_0 < 1$.

Stability

In this section, we will refer to the Jacobian matrix (63) in Sect. 4.4.3 to study the stability of the endemic steady states (s^*, i^*, c^*) for $\mathcal{P} \neq 0$. Equation (64) for $q(x^*) = 1 - e^{-0.9x^*}$ becomes

$$a_1 = \frac{3\mu + 4\mu x^* + (\gamma+\delta)(1+x^*) - 0.9x^* e^{-0.9x^*}\gamma\mathcal{P}\mathcal{R}_0 x^* - \mathcal{R}_0(\gamma+\mu) + \mu x^{*2}}{1+x^*},$$

$$a_2 = \frac{\left[((1-e^{-0.9x^*})\gamma\mathcal{P}\mathcal{R}_0 - \mu x^*\mathcal{R}_0)(1+x^*) + 0.9x^* e^{-0.9x^*}\gamma\mathcal{P}\mathcal{R}_0^2 x^*\right](\mu+\gamma)}{(1+x^*)^2}$$
$$+\mu(\ddot{S}+S)(1+x^*) - S\ddot{S},$$

$$a_3 = \mu(\mu+\gamma)\left((\mu+\delta)(1+x^*) - 0.9\gamma\mathcal{P}\mathcal{R}_0 x^* e^{-0.9x^*} - \frac{\mathcal{R}_0(\mu+\delta) - (1-e^{-0.9x^*})\gamma\mathcal{P}\mathcal{R}_0}{1+x^*}\right),$$

where $S = -(\mu+\delta) + \frac{(1-e^{-0.9x^*})\gamma\mathcal{P}\mathcal{R}_0 x^*}{1+x^*}$, $\ddot{S} = \frac{(\mu+\gamma)(\mathcal{R}_0-(1+x^*))}{1+x^*}$. For this we choose different values of x^*, approximately between 0.025 to 20, for the parameter values given in Table 9. So we find that (c_1), (c_2) and (c_3) are true for $\mathcal{R}_0 > 1$ whenever $\mathcal{P} \geq \mathcal{P}_{\text{crit}}$ for all values of x^*. Thus, there is a stable endemic steady state for $\mathcal{R}_0 > 1$.

When $\mathcal{R}_{\text{saddle}} < \mathcal{R}_0 < 1$ and $\mathcal{P} > \mathcal{P}_{\text{crit}}$, we have conditions (c_1), (c_3) are true but (c_2) is false as $a_3 < 0$ for the values of x^* between 0.025 to 0.8; while for other values, all conditions (c_1), (c_2) and (c_3) are true. Therefore, we have multiple endemic steady states in this region $\mathcal{R}_{\text{saddle}} < \mathcal{R}_0 < 1$, that are stable and unstable, using the values in Table 9. Multiple endemic steady states leads to the phenomenon of backward bifurcation, which occurs at $\mathcal{R}_0 = 1$.

Bifurcation Analysis

Fig. 44 shows a bifurcation diagram of *Example 1*, for certain parameter values. We plot three bifurcation curves against $\mathcal{R}_0$ using infection-free and endemic steady states. We show that a forward bifurcation occurs for $\mathcal{R}_0 > 1$ if $\mathcal{P} \leq \mathcal{P}_{\text{crit}}$, this shows the presence of endemic infection for $\mathcal{R}_0 > 1$.

For $\mathcal{R}_{\text{saddle}} < \mathcal{R}_0 < 1$ and $\mathcal{P} > \mathcal{P}_{\text{crit}} = \frac{\mu+\delta}{\gamma q'(0)}$, there are two sub-critical endemic steady states present, one stable and the other unstable. From $\mathcal{R}_0 = 1$, an unstable endemic steady state *moves backward* until it reaches $\mathcal{R}_{\text{saddle}}$, at which point, it becomes stable and *moves forward*. Thus a backward bifurcation occurs for at $\mathcal{R}_0 = 1$.

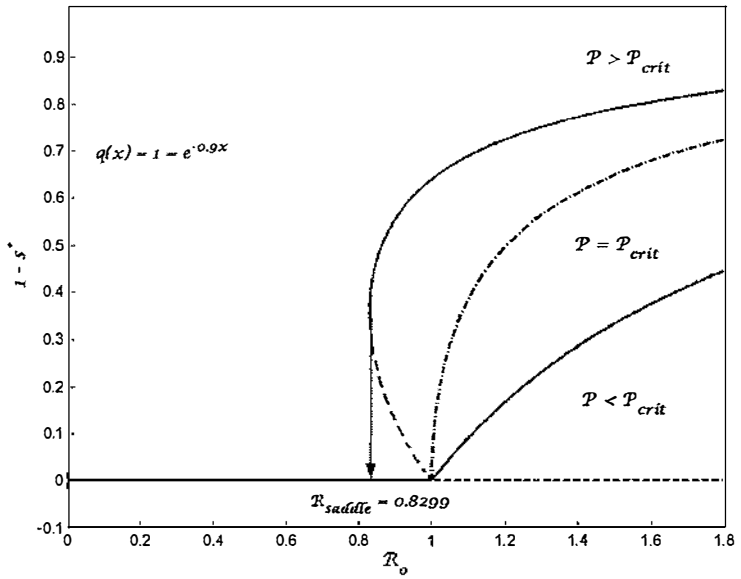

Figure 44: Bifurcation diagram for the *SIR* model with carrier class (*Example 1*) for the function $q(x^\star) = 1 - e^{-0.9x^\star}$. We show 1 - $s^\star$ as a function of $\mathcal{R}_0$. Backward bifurcation occurs when $\mathcal{P} > \mathcal{P}_{\text{crit}} = \frac{\mu+\delta}{\gamma q'(0)}$ at $(\mathcal{R}_0, 1 - s^\star) = (1, 0)$.

Phase-Plane Analysis

We now analyse the phase-planes for the carrier class *Example 1* in a $(s^\star, i^\star)$ plane. The dynamics of these phase-planes, using ODE45 (a numerical integration in **MATLAB** [10]) with different initial conditions (shown by different colours) is consistent with other models as in Chapters 2 and 4 (which are plotted using PPLANE6 application in **MATLAB** [10] as they are in three dimensions and also have a special function $q(x)$ that varies as x varies).

1. $\mathcal{P} = 0$

   - $\mathcal{R}_0 < 1$: A stable infection-free steady state is present in Fig. 45 (a).
   - $\mathcal{R}_0 > 1$: There are an unstable infection-free steady state and a stable endemic steady state in Fig. 45 (b).

2. $\mathcal{P} = \mathcal{P}_{\text{crit}}$

   - $\mathcal{R}_0 < 1$: Only a stable infection-free steady state is present in Fig. 46 (a).
   - $\mathcal{R}_0 > 1$: In Fig. 46 (b), there are unstable infection-free and stable endemic steady states.

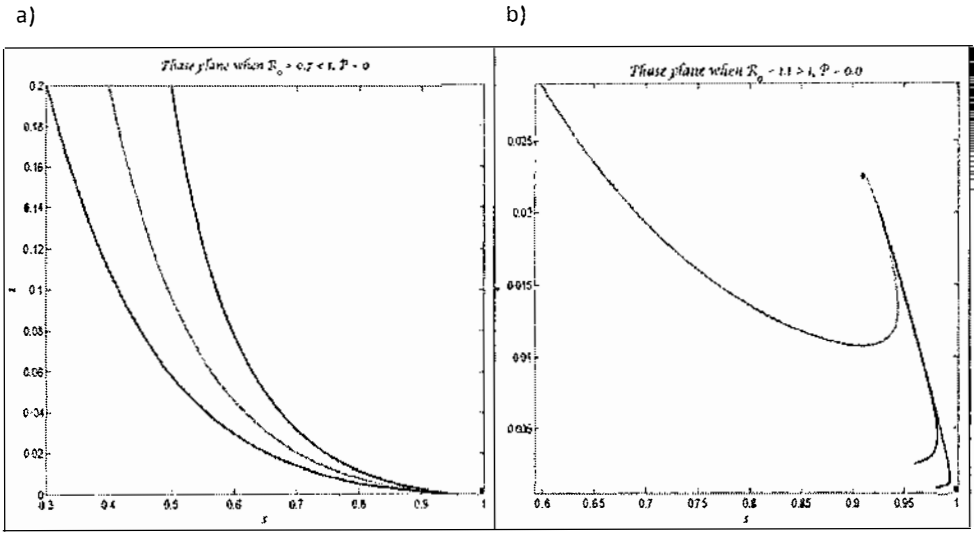

Figure 45: Phase-Plane for the *Example 1* for $\mathcal{P} = 0 < \mathcal{P}_{\text{crit}}$ when: (a) $\mathcal{R}_0 = 0.7$; (b) $\mathcal{R}_0 = 1.1$.

3. $\mathcal{P} > \mathcal{P}_{\text{crit}}$

   - $\mathcal{R}_0 < 1$: We find only a stable infection-free equilibrium in Fig. 47 (a).
   - $\mathcal{R}_0 = \mathcal{R}_{\text{saddle}} = 0.8299$: A stable infection-free steady state exists and endemic steady states coincide with each other as shown in Fig. 47 (b). We see that all the solutions goes to stable infection-free steady state.
   - $\mathcal{R}_{\text{saddle}} < \mathcal{R}_0 = 0.95 < 1$: In Fig. 48, there are stable and unstable endemic steady states and an unstable infection-free equilibrium.
   - $\mathcal{R}_0 > 1$: There is a stable endemic and unstable infection-free steady states are present in Fig. 48.

Time-series plot

In this section, we present a brief time-series analysis for the solutions of the ordinary differential equations (57). The proportions of susceptibles ($s(t)$), infectives ($i(t)$), removed ($r(t)$) and carrier ($c(t)$) classes, in a constant population, move as time (in years) changes and for different values of $\mathcal{P}$ and $\mathcal{R}_0$. We use the initial conditions of $(s^\star, i^\star, c^\star, r^\star) = (0.5, 0.3, 0.2, 0.0)$ in these plots. We also look for the transient part, which depends on the initial condition, and the general part, which gives the steady state. The general part is usually consistent in all time-series plots.

1. $\mathcal{P} = 0$

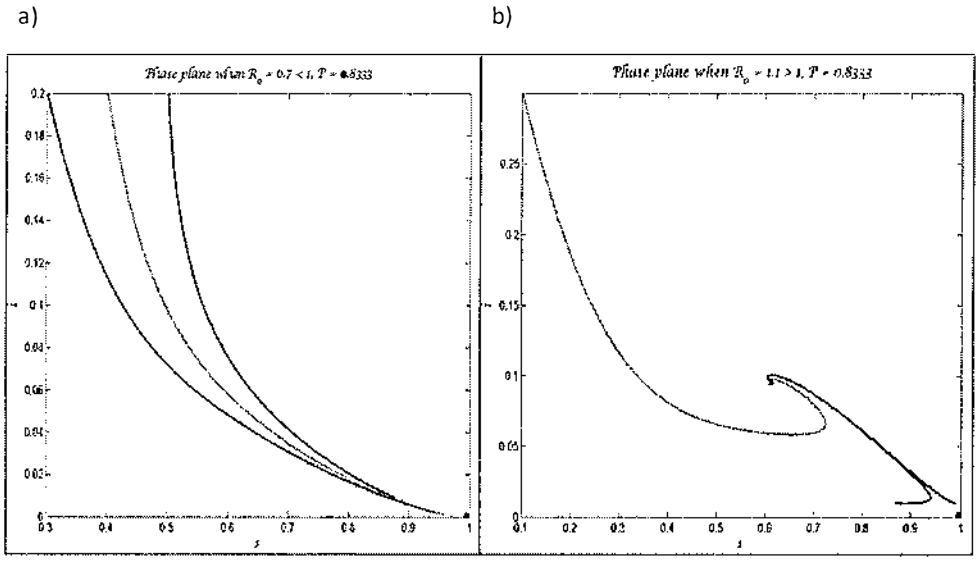

Figure 46: Phase-Plane for the *Example 1* for $\mathcal{P} = 0.8333 = \mathcal{P}_{\text{crit}}$ when: (a) $\mathcal{R}_0 = 0.7$; (b) $\mathcal{R}_0 = 1.1$.

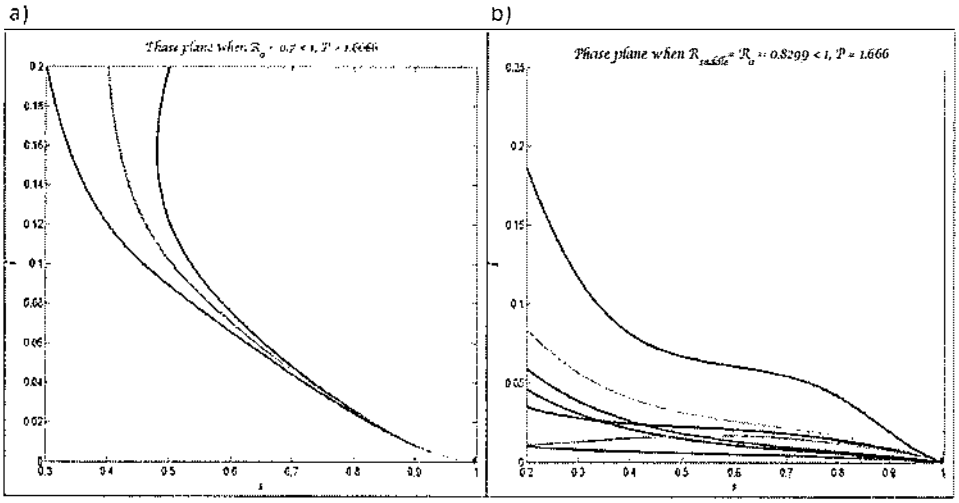

Figure 47: Phase-Plane for the *Example 1* for $\mathcal{P} = 1.6 > \mathcal{P}_{\text{crit}}$ when: (a) $\mathcal{R}_0 = 0.7 < 1$; (b) $\mathcal{R}_0 = \mathcal{R}_{\text{saddle}} = 0.8299 < 1$.

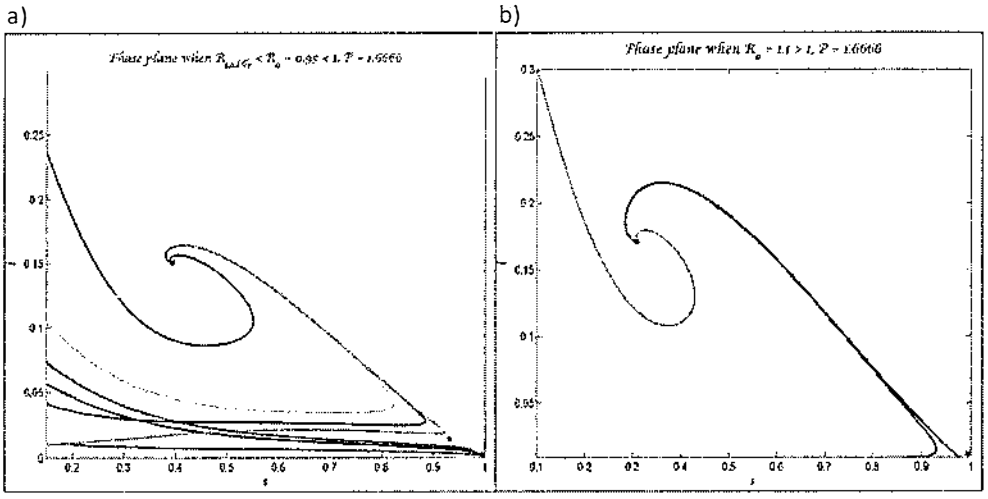

Figure 48: Phase-Plane for the *Example 1*for $\mathcal{P} = 1.6 > \mathcal{P}_{\text{crit}}$ when: (a) $\mathcal{R}_{\text{saddle}} < \mathcal{R}_0 = 0.95 < 1$; (b) $\mathcal{R}_0 = 1.1 > 1$.

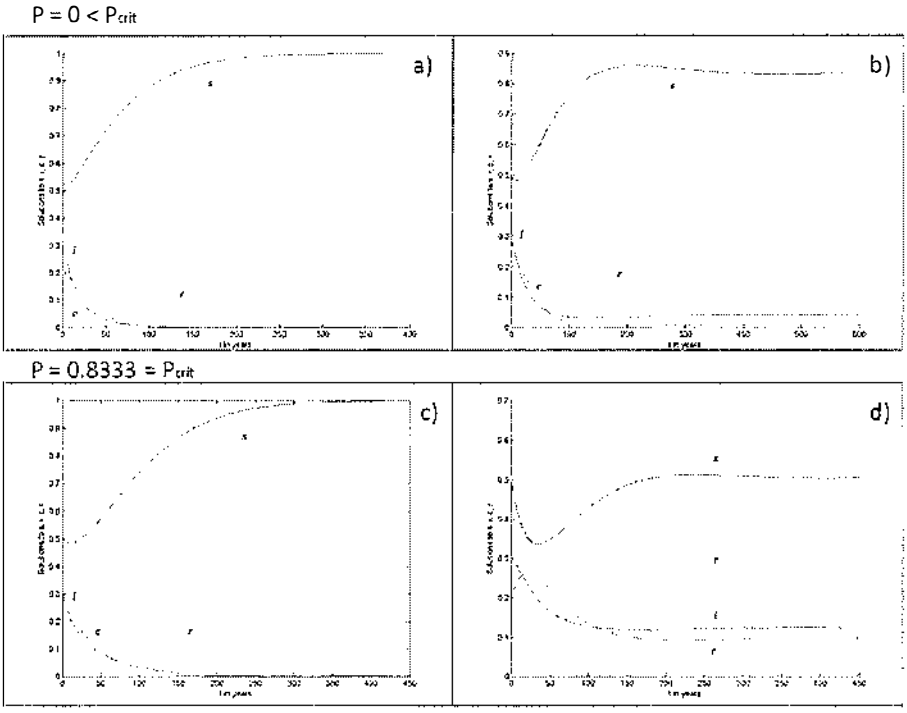

Figure 49: Time-series plots for the carrier class *Example 1.* For $\mathcal{P} = 0 < \mathcal{P}_{\text{crit}}$: (a) $\mathcal{R}_0 = 0.7 < 1$; (b) $\mathcal{R}_0 = 1.1 > 1$ and For $\mathcal{P} = 0.8333 = \mathcal{P}_{\text{crit}}$: (c) $\mathcal{R}_0 = 0.7 < 1$; (d) $\mathcal{R}_0 = 1.1 > 1$.

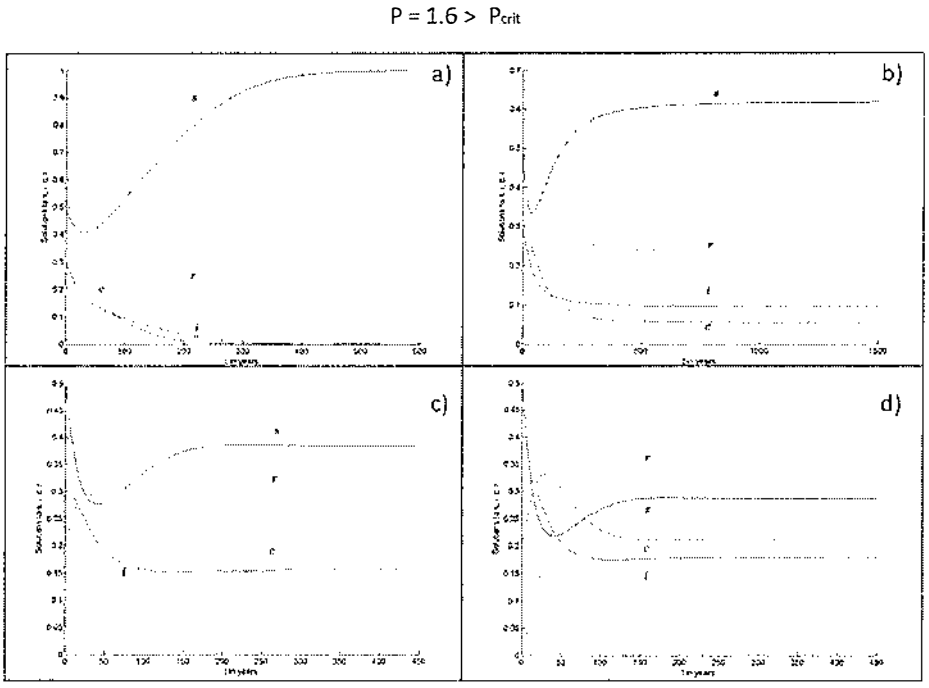

Figure 50: Time-series for $q(x) = 1 - e^{-0.9x}$ the carrier class *Example 1.* For $\mathcal{P} = 1.6 > \mathcal{P}_{\text{crit}}$: (a) $\mathcal{R}_0 = 0.6 < 1$; (b) $\mathcal{R}_{\text{saddle}} = \mathcal{R}_0 = 0.8299 < 1$; (c) $\mathcal{R}_{\text{saddle}} < \mathcal{R}_0 = 0.95 < 1$; (d) $\mathcal{R}_0 = 1.1 > 1$.

- $\mathcal{R}_0 < 1$: In Fig. 49 (a), a stable infection-free steady state is present as $i(t)$ decreases to zero and the proportion $s(t)$ increases and give steady state.
- $\mathcal{R}_0 > 1$: An unstable infection-free steady state and a stable endemic equilibrium exist as $i(t)$ decreases and give steady state. The proportion $s(t)$ decreases and increases rapidly and decreases slowly, then give steady state in Fig. 49 (b).

2. $\mathcal{P} = \mathcal{P}_{\text{crit}}$
   - $\mathcal{R}_0 = 0.5 < 1$: Fig. 49 (c) shows that the proportions $i(t)$, $r(t)$ and $c(t)$ decreases to zero and $s(t)$ increases to 1 which gives a stable infection-free steady state.
   - $\mathcal{R}_0 > 1$: In Fig. 49 (d), we observe that the proportions go to steady states. Thus, there are two steady states: an unstable infection-free; and a stable endemic.
3. $\mathcal{P} > \mathcal{P}_{\text{crit}}$
   - $\mathcal{R}_0 < 1$: The proportion $i(t)$ decreases to zero. Thus only an infection-free equilibrium is present in Fig. 50 (a).

- $\mathcal{R}_0 = \mathcal{R}_{\text{saddle}} = 0.8299$: In Fig. 50 (b), the proportions give steady states for a longer period of time. Only a stable infection-free steady state exists. At this point, we find stable and unstable endemic steady states intersect with each other.
- $\mathcal{R}_{\text{saddle}} < \mathcal{R}_0 < 1$: In Fig. 50 (c), we find all proportions giving steady states in shorter period of time. Thus, there are locally asymptotically stable endemic steady state and a unstable infection-free equilibrium.
- $\mathcal{R}_0 > 1$: There is a stable endemic and unstable infection-free steady states are present as $i(t)$ increases slowly and decreases quickly. On the other hand, $s(t)$ decreases fast and then increases until steady state occurs in Fig. 50 (d).

Example 2

In this section, first we will study the steady states, stability of the endemic steady state when $\mathcal{P} \neq 0$ for $q'(0) = 0$, a *Example 2*. Later, we will analyse bifurcation, phase-planes and time-series plots.

Steady States Solution

The infection-free steady state remains unchanged, see Sect. 4.4.1. For the endemic steady state, we set $q(x^\star) = \frac{x^{\star 2}}{x^{\star 2}+2}$ for all $\mathcal{P}$. Thus in the *Example 2*, we have for: $\mathcal{P} = 0$, the endemic steady state $(s^\star, i^\star, c^\star) = \left(\frac{1}{\mathcal{R}_0}, \frac{(\mathcal{R}_0-1)\mu}{\mathcal{R}_0(\mu+\gamma)}, \frac{x^{\star 2}(\mathcal{R}_0-1)\mu\gamma}{(x^{\star 2}+2)\mathcal{R}_0(\mu+\gamma)(\mu+\delta)}\right)$, and; for $\mathcal{P} \neq 0$, an endemic steady state $(s^\star, i^\star, c^\star) = \left(\frac{1}{1+x^\star}, \frac{x^\star\mu}{(\mu+\gamma)(1+x^\star)}, \frac{x^{\star 2}\gamma i^\star}{(x^{\star 2}+2)\mu+\delta}\right)$.

Saddle Node Equation

The saddle node equation (59) for $q(x^\star) = \frac{x^{\star 2}}{x^{\star 2}+2}$ is

$$\mathcal{R}_0(x^\star) = \frac{(\mu+\delta)(1+x^\star)(x^{\star 2}+2)}{(x^{\star 2}+2)(\mu+\delta)+\gamma\mathcal{P}x^{\star 2}}.$$

This equation solves for $\mathcal{R}_{\text{saddle}}$, but in this example we find two solutions for $\mathcal{R}_{\text{saddle}} > 1$. The critical value for $\mathcal{P}$ is calculated numerically from $q'(0) = 0$. Thus, using **MATLAB** [10], we have $\mathcal{P}_{\text{crit}} = 0.9$.

Stability

We review the Jacobian matrix (63) to study the stability of endemic steady states $(s^\star, i^\star, c^\star)$ for $\mathcal{P} \neq 0$ using **Maple** [5]. At this point we substitute $q(x^\star) = \frac{x^{\star 2}}{x^{\star 2}+2}$ in

equations (64) to get

$$a_1 = \mu(1+x^*) + (\mu+\delta) + (\mu+\gamma) - \left(\frac{4\gamma\mathcal{P}\mathcal{R}_0 x^{*2} + \mathcal{R}_0(\mu+\gamma)(x^{*2}+2)^2}{(1+x^*)(x^{*2}+2)^2}\right),$$

$$a_2 = \frac{x^{*2}\mathcal{R}_0(\mu+\gamma)\left[(x^*+2)(1+x^*)(\gamma\mathcal{P}-\mu x^*)+4\gamma\mathcal{P}\mathcal{R}_0\right]}{(1+x^*)(x^*+2)^2} + \mu(\ddot{S}+S)(1+x^*) - S\ddot{S},$$

$$a_3 = \frac{\mu(\mu+\gamma)\left[(\mu+\delta)(x^*+2)^2((1+x^*)^2-\mathcal{R}_0) - \gamma\mathcal{P}\mathcal{R}_0 x^{*2}(5+4x^*)\right]}{(1+x^*)(x^*+2)^2},$$

where $S = -(\mu+\delta) + \frac{4\gamma\mathcal{P}\mathcal{R}_0 x^{*2}}{(1+x^*)(x^*+2)^2}$, $\ddot{S} = \frac{(\mu+\gamma)(\mathcal{R}_0-(1+x^*))}{1+x^*}$. We have observed that for all $\mathcal{P}$ there is a stable endemic steady state for $\mathcal{R}_0 > 1$. When $\mathcal{R}_{\text{saddle}} < \mathcal{R}_0 < 1.19$ and $\mathcal{P} > \mathcal{P}_{\text{crit}}$, we have a untrue condition (c_2) as $a_3 < 0$ for some values of x^* approximately between 0.5 to 1.2; while for the other values of x^*, all conditions are true.

To calculate these results we use **Maple** [5] with the parameter values given in Table 9. Thus, we find that there are multiple endemic steady states depending on the different values of x^* in this region. For $\mathcal{R}_0 > 1$, we have stable endemic steady state if $\mathcal{P} > \mathcal{P}_{\text{crit}}$, we have sub-critical endemic steady states for $\mathcal{R}_{\text{saddle}} < \mathcal{R}_0 < 1.19$. This means the *Example 2* exhibits different dynamics as there are two backward bifurcations.

This example is discussed in detail in Medley et al. [9] and have a different function $q(\lambda)$ with a constant f, $0 \leq f \leq 1$, in terms of λ, which has unit time^{-1}. However, this function exhibits similar dynamics to our chosen function $q(x^*) = \frac{x^{*2}}{x^{*2}+2}$.

Bifurcation Analysis

In Fig. 51 the bifurcation diagram for example $q'(0) = 0$ is presented. When $\mathcal{P} < \mathcal{P}_{\text{crit}}$ and $\mathcal{R}_0 > 1$, we find a forward bifurcation. At $\mathcal{P}_{\text{crit}}$, there is an inflection in the bifurcation curve, and this separates two qualitatively different behaviours. If $\mathcal{P} > \mathcal{P}_{\text{crit}}$, then we have multiple endemic steady states for some value of $\mathcal{R}_0$. At $\mathcal{R}_0 > 1$ the curve leaves the trivial solution in a forward direction, then at $\mathcal{R}_0 = 1.19$, the curve moves backward and the steady state becomes unstable. Until $\mathcal{R}_{\text{saddle}} = 1.09$, the curve moves in a forward direction again, and the endemic steady state becomes stable.

Clearly, as $q'(0) = 0$, there can be no backward bifurcation at $\mathcal{R}_0 = 1$, thus $\mathcal{R}_0 = 1$ is not a bifurcation point, in this example. We observe that, instead at $\mathcal{R}_0 = 1.19$, there is a backward bifurcation for $\mathcal{P} > \mathcal{P}_{\text{crit}}$, where $\mathcal{P}_{\text{crit}}$ is found numerically. Several multiple endemic steady states are present for $\mathcal{R}_{\text{saddle}} < \mathcal{R}_0 < 1.19$. Thus in this model an

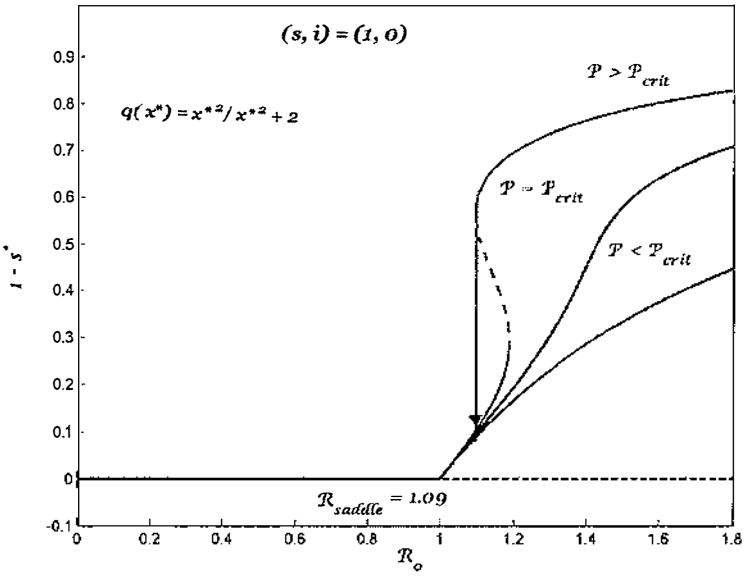

Figure 51: Bifurcation Diagram for the carrier class for the function $q(x^*) = \frac{x^{*2}}{x^{*2}+2}$. In this diagram, 1 - s^* is plotted against $\mathcal{R}_0$. Backward bifurcation occurs when $\mathcal{P} > \mathcal{P}_{\text{crit}} = 0.9$ for $q'(0) = 0$. Multiple endemic steady states exist in the region of $\mathcal{R}_{\text{saddle}} < \mathcal{R}_0 < 1.19$.

endemic infection persists for $\mathcal{R}_0 > 1$, as well as for $\mathcal{R}_0 < 1$. This example of the carrier class model is different from previous model as it exhibits two backward bifurcations.

Phase-Plane Analysis

At this point we analyse the phase-planes for the *Example 2*. We categorise this analyse in three behaviours with respect to; $\mathcal{P} < \mathcal{P}_{\text{crit}}$; $\mathcal{P} = \mathcal{P}_{\text{crit}}$ and; $\mathcal{P} > \mathcal{P}_{\text{crit}}$ for $\mathcal{R}_0 < 1$ and $\mathcal{R}_0 > 1$. The projection of three dimensional (s^*, i^*, c^*)-plane onto two dimensional (s^*, i^*)-plane may show the intersection of possible trajectories.

1. $\mathcal{P} = 0$

   - $\mathcal{R}_0 < 1$: A stable infection-free steady state is present in Fig. 52 (a).
   - $\mathcal{R}_0 > 1$: An unstable infection-free steady state and stable endemic equilibrium exist in Fig. 52 (b).

2. $\mathcal{P} = \mathcal{P}_{\text{crit}}$

   - $\mathcal{R}_0 < 1$: A stable endemic and an unstable infection-free steady states in Fig. 53 (a).

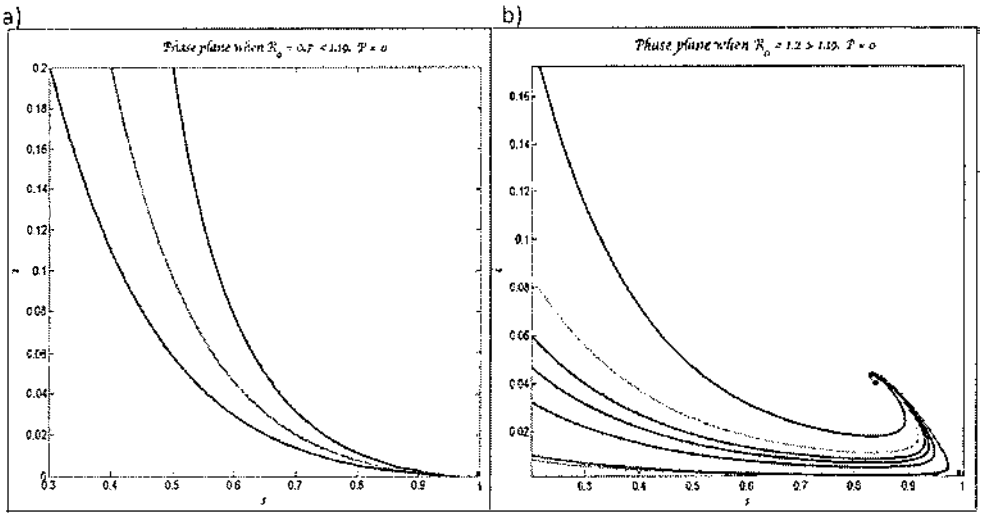

Figure 52: Phase-Planes for the *Example 2* for $\mathcal{P} = 0 < \mathcal{P}_{\text{crit}}$ when: (a) $\mathcal{R}_0 = 0.7 < 1.19$; (b) $\mathcal{R}_0 = 1.2 > 1.19$.

- $\mathcal{R}_0 > 1$: There are an unstable infection-free and a stable endemic steady states in Fig. 53(b).

3. $\mathcal{P} > \mathcal{P}_{\text{crit}}$

   - $\mathcal{R}_0 < \mathcal{R}_{\text{saddle}}$: Only an infection-free equilibrium exists in Fig. 54 (a).
   - $\mathcal{R}_0 = \mathcal{R}_{\text{saddle}} = 1.09$: A stable infection-free steady state exists. There are endemic steady states which seems to be on top of each other in Fig. 54 (b).
   - $\mathcal{R}_{\text{saddle}} < \mathcal{R}_0 < 1.19$: An unstable and a stable endemic steady states and a unstable infection-free equilibrium exist in Fig. 55 (a).
   - $\mathcal{R}_0 > 1$:There is a stable endemic and unstable infection-free steady states are present in Fig. 55(b).

Time-Series Plots

In this section, we will study a brief time series analysis for the solutions of the ordinary differential equations (57), where $q(x) = \frac{x^2}{x^2+2}$. The proportions of susceptibles $(s(t))$, infectives $(i(t))$, recovered $(r(t))$ and carriers $(c(t))$, in a constant population changes as time increases. This behaviour is similar to the behaviour shown in the time-series plot for $q(x) = 1 - e^{-0.9x}$. We apply the initial conditions $(s^\star, i^\star, c^\star, r^\star) = (0.5, 0.2, 0.2, 0.1)$ to all plots.

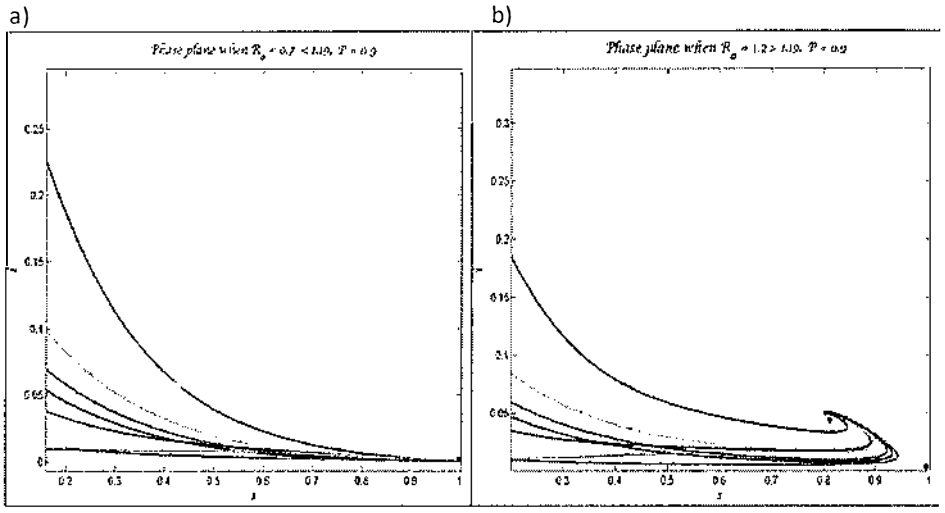

Figure 53: Phase-Planes for the *Example 2* for $\mathcal{P} = 0.9 = \mathcal{P}_{\text{crit}}$ when: (a) $\mathcal{R}_0 = 0.7 < 1.19$; (b) $\mathcal{R}_0 = 1.2 > 1.19$.

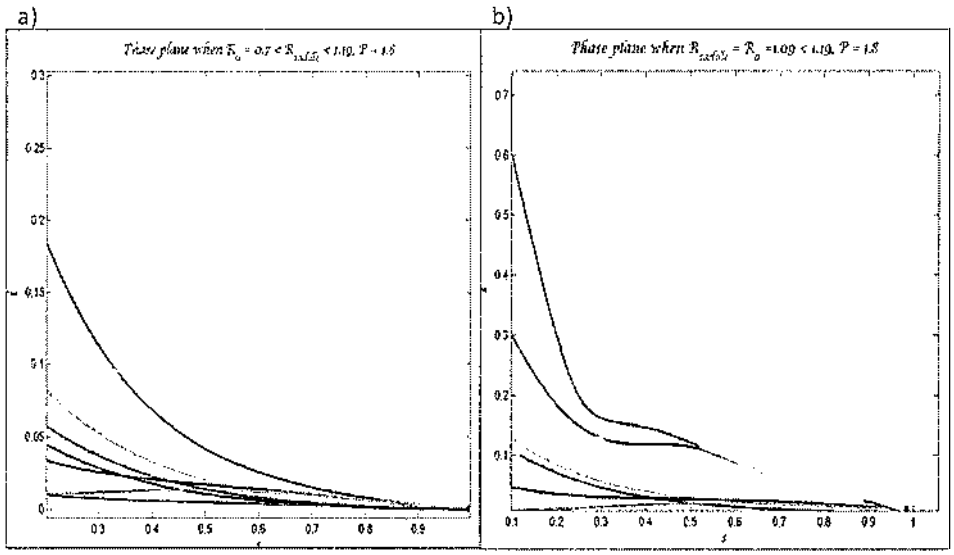

Figure 54: Phase-Planes for the *Example 2* for $\mathcal{P} = 1.8 > \mathcal{P}_{\text{crit}}$ when: (a) $\mathcal{R}_0 = 0.7 < 1.19$; (b) $\mathcal{R}_{\text{saddle}} = \mathcal{R}_0 = 1.09 < 1.19$.

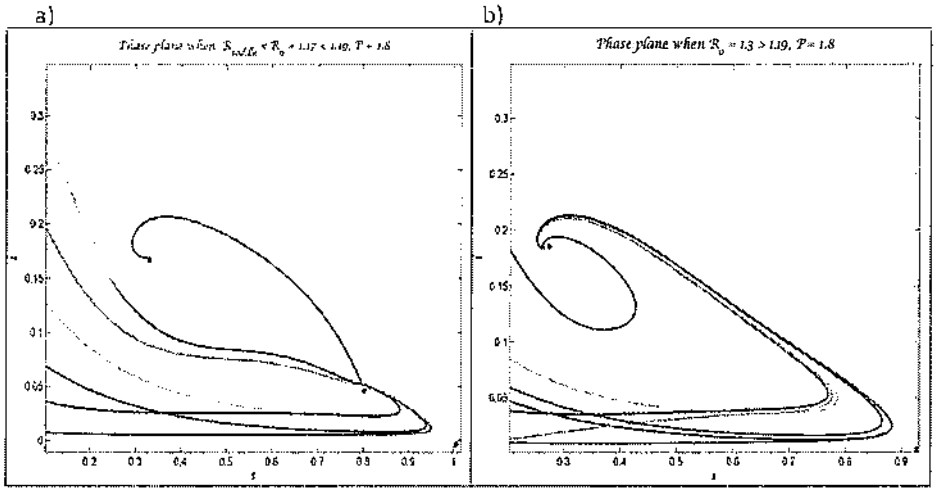

Figure 55: Phase-Planes for the *Example 2* for $\mathcal{P} = 1.8 > \mathcal{P}_{\text{crit}}$ when: (a)$\mathcal{R}_{\text{saddle}} < \mathcal{R}_0 = 1.17 < 1.19$; (b) $\mathcal{R}_0 = 1.2 > 1.19$.

1. $\mathcal{P} = 0$

   - $\mathcal{R}_0 < 1$: In Fig. 56 (a), the proportion $i(t)$ decreases till zero. Thus there is stable infection-free steady state.
   - $\mathcal{R}_0 > 1$: There are an unstable infection-free steady state and stable endemic equilibrium exist as the proportions $i(t)$ and $s(t)$ decreases and increases respectively (see Fig. 56 (b)).

2. $\mathcal{P} = \mathcal{P}_{\text{crit}}$

   - $\mathcal{R}_0 < 1$: Fig. 56 (c) gives a stable infection-free steady state.
   - $\mathcal{R}_0 > 1$: In Fig. 56 (d), there are two steady states: an unstable infection-free; and a stable endemic. The proportions $i(t)$ goes to steady state after decreasing.The proportion $s(t)$ decreases first and then increases and then goes to steady state.

3. $\mathcal{P} > \mathcal{P}_{\text{crit}}$

   - $\mathcal{R}_0 < 1$: Only an infection-free equilibrium is present in Figure 57 (a). The proportion $i(t)$ decreases to zero.
   - $\mathcal{R}_0 = \mathcal{R}_{\text{saddle}} = 1.09$: A stable infection-free steady state exists. The proportion $i(t)$ increases and decreases until steady state occurs. Conversely, $s(t)$

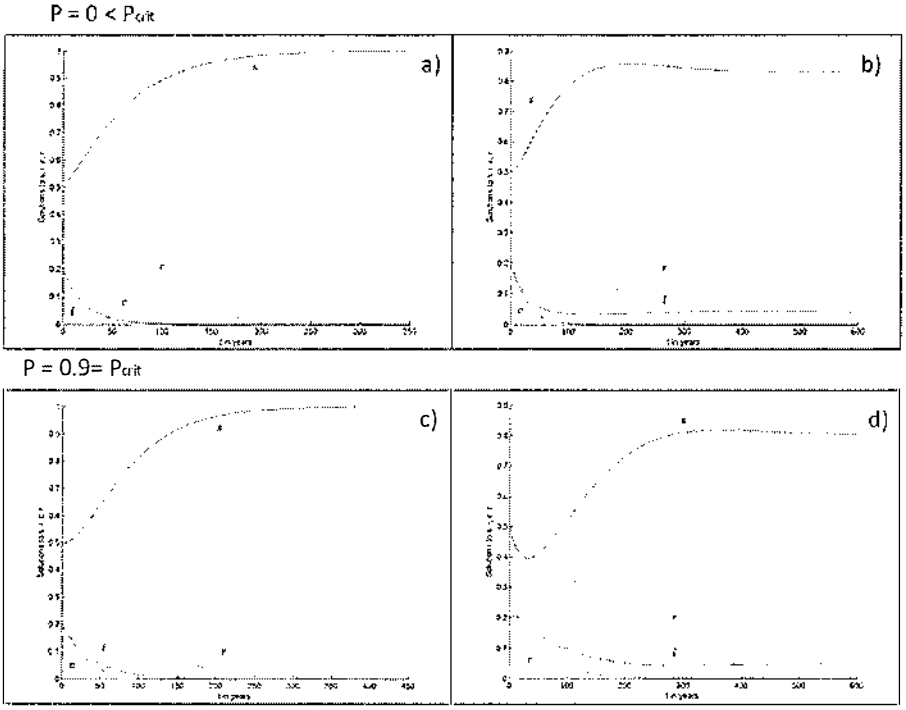

Figure 56: Time-series plots for the carrier class *Example 2*. For $\mathcal{P} = 0 < \mathcal{P}_{\text{crit}}$: (a) $\mathcal{R}_0 = 0.7 < 1$; (b) $\mathcal{R}_0 = 1.2 > 1$ and For $\mathcal{P} = 0.9 = \mathcal{P}_{\text{crit}}$: (c) $\mathcal{R}_0 = 0.7 < 1$; (d) $\mathcal{R}_0 = 1.2 > 1$.

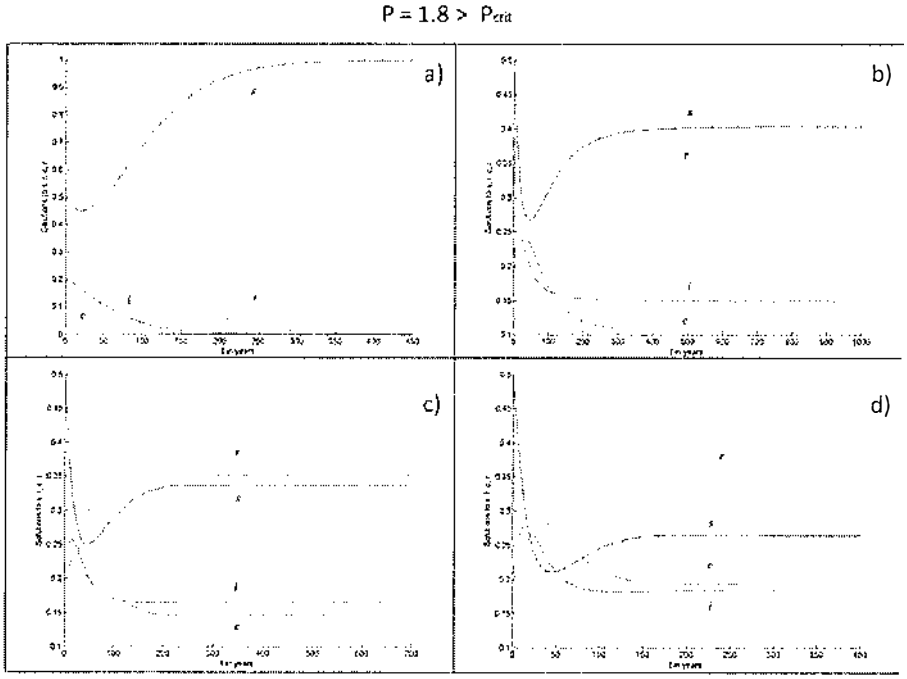

Figure 57: Time-series plots for the carrier class *Example 2* for $\mathcal{P} = 1.8 > \mathcal{P}_{\text{crit}}$: (a) $\mathcal{R}_0 = 0.7 < 1$; (b) $\mathcal{R}_0 = \mathcal{R}_{\text{saddle}} = 1.09 < 1.19$; (c)$\mathcal{R}_{\text{saddle}} < \mathcal{R}_0 = 1.16 < 1.19$; (d) $\mathcal{R}_0 = 1.2 > 1$.

decreases and then increases before going to the steady state. This show the presence of two endemic steady states coincides (see in Fig. 57 (b))

- $\mathcal{R}_{\text{saddle}} < \mathcal{R}_0 < 1.19$: In Fig. 57 (c), there are an unstable and a stable endemic steady states and an unstable infection-free equilibrium.
- $\mathcal{R}_0 > 1$: There are a stable endemic and an unstable infection-free steady states as the proportions $i(t)$ and $s(t)$ goes to steady states (see Fig. 57 (d)).

4.5 Summary

Even for three dimensional extensions of the *SIR* model: the *SEIR* model in Sect. 4.1; the *SEIR* model with partial recovery in Sect. 4.2; the *SEIR* model with full recovery in Sect. 4.3; and a carrier class *Example 1* in Sect. 4.4.4, we conclude that an endemic infection persists for some values of $\mathcal{R}_0 < 1$ when $\mathcal{P} > \mathcal{P}_{\text{crit}}$. The infection-free steady state is locally asymptotically stable for $\mathcal{R}_0 < 1$ and unstable for $\mathcal{R}_0 > 1$ as before.

The carrier class *Example 2*, for $q'(0) = 0$ in Sect. 4.4.4, we have different dynamics compared to the other models we study so far. A forward and two backward bifurcations show the persistence of an endemic infection for both $\mathcal{R}_0 > 1$ and $Ro < 1$ when $\mathcal{P} > \mathcal{P}_{\text{crit}}$.

5 General Analysis of 3D Models

This section focuses on the three dimensional extensions of the *SIR* endemic models: the exogenous infection model which has already been discussed as a two dimensional model in Sect. 2.3; and a model with a carrier class. We study these models in a general manner under a matrix framework. This method was applied to the two dimensional models in Sect. 3.

We consider the ordinary differential equation

$$\frac{d\mathbf{y}}{dt} = -M\mathbf{y} + f(\mathbf{y}), \tag{65}$$

where M is a non-singular 3×3 matrix, $\mathbf{y}$ is a vector and $f(\mathbf{y})$ is a vector-valued function. We calculate M and $f(\mathbf{y})$ to find the direction of the bifurcation using a bifurcation parameter $\mathcal{R}_0$ at a steady state $\mathbf{y} = \begin{pmatrix} 1 \\ 0 \\ 0 \end{pmatrix}$. We use $i^\star$ as a perturbation variable, and apply Taylor series and Binomial expansions to obtain our results.

5.1 The *SEIR* model

Consider the *SEIR* model reported in [12] and described in §4.1. We consider equation (44), omitting $\frac{dr}{dt}$, taking $\beta = \mathcal{R}_0 \frac{(\mu+\nu)(\mu+\gamma)}{\nu}$, and rescaling time so that $\mu = 1$, equation (44) becomes

$$\begin{aligned} \frac{ds}{dt} &= 1 - \mathcal{R}_0\mathcal{D}si - s, \\ \frac{de}{dt} &= \mathcal{R}_0\mathcal{D}si - \mathcal{P}\mathcal{R}_0\mathcal{D}ei - \bar{\mathcal{C}}e, \\ \frac{di}{dt} &= \mathcal{P}\mathcal{R}_0\mathcal{D}ei + \frac{\bar{\mathcal{C}}}{\bar{\mathcal{D}}}e - \mathcal{A}i. \end{aligned}$$

See Table 5 for the notations of $\mathcal{D}$, $\bar{\mathcal{C}}$, $\bar{\mathcal{D}}$ and $\mathcal{A}$.

Now we write this equation with the form of system (65), by setting $\mathbf{y} = \begin{pmatrix} s \\ e \\ i \end{pmatrix}$.

Here $M = \begin{pmatrix} 1 & 0 & 0 \\ 0 & \bar{\mathcal{C}} & 0 \\ 0 & -\frac{\bar{\mathcal{C}}}{\bar{\mathcal{D}}} & \mathcal{A} \end{pmatrix}$, $f(\mathbf{y}) = \begin{pmatrix} 1 - \mathcal{R}_0\mathcal{D}si \\ \mathcal{R}_0\mathcal{D}si - \mathcal{P}\mathcal{R}_0\mathcal{D}ei \\ \mathcal{P}\mathcal{R}_0\mathcal{D}ei \end{pmatrix}$

At steady state $\mathbf{y}^\star = \begin{pmatrix} s^\star \\ e^\star \\ i^\star \end{pmatrix}$ is solved to be

$$\mathbf{y}^\star = M^{-1} f(\mathbf{y}^\star) = \begin{pmatrix} 1 & 0 & 0 \\ 0 & \bar{\mathcal{C}}^{-1} & 0 \\ 0 & \mathcal{D}^{-1} & \mathcal{A}^{-1} \end{pmatrix} \begin{pmatrix} 1 - \mathcal{R}_0 \mathcal{D} s^\star i^\star \\ \mathcal{R}_0 \mathcal{D} s^\star i^\star - \mathcal{P}\mathcal{R}_0 \mathcal{D} e^\star i^\star \\ \mathcal{P}\mathcal{R}_0 \mathcal{D} e^\star i^\star \end{pmatrix}.$$

Hence,

$$\mathbf{y}^\star = \begin{pmatrix} s^\star \\ e^\star \\ i^\star \end{pmatrix} = \begin{pmatrix} 1 - \mathcal{D}\mathcal{R}_0 s^\star i^\star \\ \mathcal{D}\bar{\mathcal{C}}^{-1}(\mathcal{R}_0 s^\star i^\star - \mathcal{P}\mathcal{R}_0 e^\star i^\star) \\ \mathcal{R}_0(s^\star i^\star - \mathcal{P} e^\star i^\star) + \mathcal{D}\mathcal{A}^{-1}\mathcal{P}\mathcal{R}_0 e^\star i^\star \end{pmatrix}. \tag{66}$$

We apply a Taylor expansion to get

$$\begin{aligned} \mathcal{R}_0 &= 1 + i^\star \mathcal{R}_{01} + i^{\star 2}\mathcal{R}_{02} + \mathcal{O}(i^{\star 3}), \\ s^\star &= 1 + i s_1^\star + i^{\star 2} s_2^\star + \mathcal{O}(i^{\star 3}), \\ e^\star &= i^\star e_1^\star + i^{\star 2} e_2^\star + \mathcal{O}(i^{\star 3}). \end{aligned} \tag{67}$$

Thus

$$\begin{aligned} \mathcal{R}_0 s^\star i^\star &= i^\star + i^{\star 2}(s_1^\star + \mathcal{R}_{01}) + \mathcal{O}(i^{\star 3}), \\ \mathcal{R}_0 e^\star i^\star &= i^{\star 2} e_1^\star + \mathcal{O}(i^{\star 3}), \\ \mathcal{R}_0 i^{\star 2} &= i^{\star 2} + \mathcal{O}(i^{\star 3}). \end{aligned} \tag{68}$$

Ignoring higher order terms and substituting equation (68) back into equation (66), we have

$$\mathbf{y}^\star = \begin{pmatrix} 1 + i^\star s_1^\star + i^{\star 2} s_2^\star \\ i^\star e_1^\star + i^{\star 2} e_2^\star \\ i^\star \end{pmatrix} = \begin{pmatrix} 1 - \mathcal{D} i^\star - \mathcal{D}(s_1^\star + \mathcal{R}_{01}) i^{\star 2} \\ \mathcal{D}\bar{\mathcal{C}}^{-1} i^\star + \mathcal{D}\bar{\mathcal{C}}^{-1}(s_1^\star + \mathcal{R}_{01} - e_1^\star) i^{\star 2} \\ i^\star + (s_1^\star + \mathcal{R}_{01} - \mathcal{P} e_1^\star + \mathcal{D}\mathcal{A}^{-1}\mathcal{P} e_1^\star) i^{\star 2} \end{pmatrix}. \tag{69}$$

Comparing terms in the same power of $i^\star$

$$\begin{pmatrix} 1 \\ 0 \\ 0 \end{pmatrix} + i^\star \begin{pmatrix} s_1^\star \\ e_1^\star \\ 1 \end{pmatrix} + i^{\star 2} \begin{pmatrix} s_2^\star \\ e_2^\star \\ 0 \end{pmatrix}$$

$$= \begin{pmatrix} 1 \\ 0 \\ 0 \end{pmatrix} + i^* \begin{pmatrix} -\mathcal{D} \\ \mathcal{D}\bar{\mathcal{C}}^{-1} \\ 1 \end{pmatrix} + i^{*2} \begin{pmatrix} -\mathcal{D}(s_1^* + \mathcal{R}_{01}) \\ \mathcal{D}\bar{\mathcal{C}}^{-1}(s_1^* + \mathcal{R}_{01} - e_1^*) \\ (s_1^* + \mathcal{R}_{01} - \mathcal{P}e_1^* + \mathcal{D}\mathcal{A}^{-1}\mathcal{P}e_1^*) \end{pmatrix},$$

We get

$$s_1^* = -\mathcal{D} < 0,$$

$$e_1^* = \mathcal{D}\bar{\mathcal{C}}^{-1},$$

$$s_2^* = -\mathcal{D}(s_1^* + \mathcal{R}_{01}),$$

$$e_2^* = \mathcal{D}\bar{\mathcal{C}}^{-1}(s_1^* + \mathcal{R}_{01} - e_1^*),$$

$$s_1^* + \mathcal{R}_{01} - \mathcal{P}e_1^* + \mathcal{D}\mathcal{A}^{-1}\mathcal{P}e_1^* = 0.$$

To get the critical value for $\mathcal{P}$, we substitute into the last equation $\mathcal{R}_{01} = 0$, $s_1^* = -\mathcal{D}$ and $e_1^* = \mathcal{D}\bar{\mathcal{C}}^{-1}$. Thus,

$$\mathcal{P} = \frac{\bar{\mathcal{C}}\mathcal{A}}{\mathcal{D} - \mathcal{A}}.$$

Now, substituting from Table 5 for $\bar{\mathcal{C}}$, $\mathcal{D}$ and $\mathcal{A}$, we get

$$\mathcal{P} = \frac{\frac{(\mu+\nu)(\mu+\gamma)}{\mu^2}}{\frac{(\mu+\nu)(\mu+\gamma)-\nu(\mu+\gamma)}{\mu\nu}}.$$

Thus,

$$\boxed{\mathcal{P}_{\text{crit}} = \frac{\nu(\mu+\nu)}{\mu^2}}.$$

- If $\mathcal{P} > \mathcal{P}_{\text{crit}}$, then $\mathcal{R}_{01} < 0$ and a backward bifurcation occurs.
- If $\mathcal{P} < \mathcal{P}_{\text{crit}}$, then $\mathcal{R}_{01} > 0$ and a forward bifurcation occurs.

These results are consistent with Sect. 4.1.

5.2 *SEIR* model with Partial Recovery

This model is based on the paper of [14]. The system of four differential equations for this model have already been mentioned in Sect. 4.2. Taking $\beta = \mathcal{R}_0 \frac{((\mu+\nu)(\mu+\gamma) - \kappa\gamma\nu)}{\nu}$ and rescaling time so that $\mu = 1$, equation (50) becomes

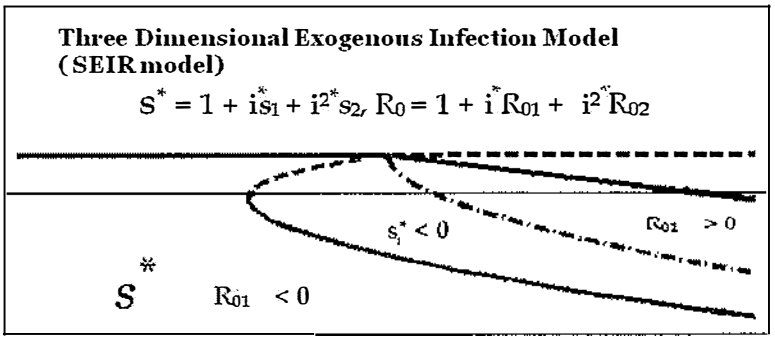

Figure 58: An enlarged top-center portion of Fig. 26. In this sketch, it is clearly shown that $s_1^* < 0$, and $\mathcal{R}_{01} < 0$ give backward bifurcation, while $\mathcal{R}_{01} > 0$ give forward bifurcation.

$$\begin{aligned}
\frac{ds}{dt} &= 1 - \mathcal{R}_0\bar{E}si - s, \\
\frac{de}{dt} &= \mathcal{R}_0\bar{E}si - \mathcal{P}\mathcal{R}_0\bar{E}(s+e+i)i - \bar{\mathcal{C}}e + \mathcal{P}\mathcal{R}_0\mathcal{D}i + \bar{B}(1-\mathcal{P}\mathcal{R}_0)i, \\
\frac{di}{dt} &= \frac{\bar{\mathcal{C}}}{\bar{\mathcal{D}}}e - \mathcal{A}i,
\end{aligned}$$

where $\bar{B} = \frac{\kappa\gamma}{\mu}$, $\bar{E} = \mathcal{D} - \bar{B}$. (see Table 5). We rewrite this equation in a ODE system (65) by setting $\mathbf{y} = \begin{pmatrix} s \\ e \\ i \end{pmatrix}$.

Here

$$M = \begin{pmatrix} 1 & 0 & 0 \\ 0 & \bar{\mathcal{C}} & -\mathcal{P}\mathcal{R}_0\mathcal{D} - \bar{B}(1-\mathcal{P}\mathcal{R}_0) \\ 0 & -\frac{\bar{\mathcal{C}}}{\bar{\mathcal{D}}} & \mathcal{A} \end{pmatrix}, \; f(\mathbf{y}) = \begin{pmatrix} 1 - \mathcal{R}_0\bar{E}si \\ \mathcal{R}_0\bar{E}si - \mathcal{P}\mathcal{R}_0\bar{E}(s+e+i)i \\ 0 \end{pmatrix}.$$

At the steady state, $\mathbf{y}^\star = \begin{pmatrix} s^\star \\ e^\star \\ i^\star \end{pmatrix}$ solves

$$\mathbf{y}^\star = M^{-1}f(\mathbf{y}^\star)$$

$=$

$$\begin{pmatrix} 1 & 0 & 0 \\ 0 & \frac{\mathcal{D}}{\bar{C}(\mathcal{D}-B)(1-\mathcal{P}\mathcal{R}_0)} & \frac{\mathcal{D}(\mathcal{P}\mathcal{R}_0\bar{E}+\bar{B})}{\mathcal{A}\bar{C}(\mathcal{D}-(\mathcal{P}\mathcal{R}_0\bar{E}+\bar{B}))} \\ 0 & \frac{1}{(\mathcal{D}-B)(1-\mathcal{P}\mathcal{R}_0)} & \frac{\mathcal{D}}{\mathcal{A}(\mathcal{D}-(\mathcal{P}\mathcal{R}_0 E+B))} \end{pmatrix} \begin{pmatrix} 1-\mathcal{R}_0\bar{E}s^*i^* \\ \mathcal{R}_0\bar{E}s^*i^* - \mathcal{P}\mathcal{R}_0\bar{E}(s^*+e^*+i^*)i^* \\ 0 \end{pmatrix}.$$

Hence,

$$\mathbf{y}^* = \begin{pmatrix} s^* \\ e^* \\ i^* \end{pmatrix} = \begin{pmatrix} 1-\bar{E}\mathcal{R}_0 s^*i^* \\ \frac{\bar{E}\mathcal{D}}{(\mathcal{D}-\bar{B})\bar{C}}(1-\mathcal{P}\mathcal{R}_0)^{-1}\left[\mathcal{R}_0 s^*i^*(1-\mathcal{P}) - \mathcal{P}\mathcal{R}_0(e^*+i^*)i^*\right] \\ \frac{\bar{E}}{(\mathcal{D}-\bar{B})}(1-\mathcal{P}\mathcal{R}_0)^{-1}\left[\mathcal{R}_0 s^*i^*(1-\mathcal{P}) - \mathcal{P}\mathcal{R}_0(e^*+i^*)i^*\right] \end{pmatrix}. \quad (70)$$

At this point, a Taylor expansion is applied as in Sect. 5.1, from equation (67). Thus, substituting equation (68) back into equation (70), and ignoring higher order terms, we get

$$\mathbf{y}^* = \begin{pmatrix} 1-\bar{E}(i^*+i^{*2}(s_1^*+\mathcal{R}_{01})) \\ \frac{\bar{E}\mathcal{D}}{(\mathcal{D}-\bar{B})\bar{C}}\left[i^*+i^{*2}(s_1^*+\mathcal{R}_{01}-\frac{\mathcal{P}}{1-\mathcal{P}}(e_1^*+1))\right]\left(1-\frac{i^*\mathcal{P}\mathcal{R}_{01}}{1-\mathcal{P}}-\frac{i^{*2}\mathcal{P}\mathcal{R}_{02}}{1-\mathcal{P}}\right)^{-1} \\ \frac{\bar{E}}{(\mathcal{D}-\bar{B})}\left[i^*+i^{*2}(s_1^*+\mathcal{R}_{01}-\frac{\mathcal{P}}{1-\mathcal{P}}(e_1^*+1))\right]\left(1-\frac{i^*\mathcal{P}\mathcal{R}_{01}}{1-\mathcal{P}}-\frac{i^{*2}\mathcal{P}\mathcal{R}_{02}}{1-\mathcal{P}}\right)^{-1} \end{pmatrix}.$$

Taking $(1-\mathcal{P})^{-1}$ out as a factor in row 2, and then we applying the binomial expansion to the inverse exponent. Then we have

$$\mathbf{y}^* = \begin{pmatrix} 1-\bar{E}(i^*+i^{*2}(s_1^*+\mathcal{R}_{01})) \\ \frac{\bar{E}\mathcal{D}}{(\mathcal{D}-\bar{B})\bar{C}}\left[i^*+i^{*2}(s_1^*+\mathcal{R}_{01}-\frac{\mathcal{P}}{1-\mathcal{P}}(e_1^*+1))\right](1-z)^{-1} \\ \frac{\bar{E}}{(\mathcal{D}-\bar{B})}\left[i^*+i^{*2}(s_1^*+\mathcal{R}_{01}-\frac{\mathcal{P}}{1-\mathcal{P}}(e_1^*+1))\right](1-z)^{-1} \end{pmatrix},$$

where

$$z = \left(\frac{i^*\mathcal{P}\mathcal{R}_{01}}{1-\mathcal{P}} + \frac{i^{*2}\mathcal{P}\mathcal{R}_{02}}{1-\mathcal{P}}\right).$$

Expanding

$$(1-z)^{-1} = 1+z+z^2+\mathcal{O}(z^3) = 1+\frac{\mathcal{P}\mathcal{R}_{01}i^*}{1-\mathcal{P}} + \frac{\mathcal{P}\mathcal{R}_{02}i^{*2}}{1-\mathcal{P}} + \frac{\mathcal{P}^2\mathcal{R}_{01}^2 i^{*2}}{(1-\mathcal{P})^2} + \mathcal{O}(i^{*3}).$$

We ignore cubic and higher order terms and rewrite equation (70) to get

$$\mathbf{y}^* = \begin{pmatrix} 1+i^*s_1^*+i^{*2}s_2^* \\ i^*e_1^*+i^{*2}e_2^* \\ i^* \end{pmatrix} = \begin{pmatrix} 1-\bar{E}i^*-\bar{E}(s_1^*+\mathcal{R}_{01})i^{*2} \\ \frac{\bar{E}\mathcal{D}}{(\mathcal{D}-\bar{B})\bar{C}}\left[i^*+i^{*2}(s_1^*+\mathcal{R}_{01}-\frac{\mathcal{P}}{1-\mathcal{P}}(e_1^*+1-\mathcal{R}_{01})\right] \\ \frac{\bar{E}}{(\mathcal{D}-\bar{B})}\left[i^*+i^{*2}(s_1^*+\mathcal{R}_{01}-\frac{\mathcal{P}}{1-\mathcal{P}}(e_1^*+1-\mathcal{R}_{01}))\right] \end{pmatrix}$$

Hence comparing equal powers of the perturbation variable i^* to find the critical value for $\mathcal{P}$.

$$\begin{pmatrix} 1 \\ 0 \\ 0 \end{pmatrix} + i^* \begin{pmatrix} s_1^* \\ e_1^* \\ 1 \end{pmatrix} + i^{*2} \begin{pmatrix} s_2^* \\ e_2^* \\ 0 \end{pmatrix}$$

=

$$\begin{pmatrix} 1 \\ 0 \\ 0 \end{pmatrix} + i^* \begin{pmatrix} -\bar{E} \\ \frac{\bar{E}\mathcal{D}}{(\mathcal{D}-\bar{B})\bar{\mathcal{C}}} \\ \frac{\bar{E}}{(\mathcal{D}-\bar{B})} \end{pmatrix} + i^{*2} \begin{pmatrix} -\bar{E}(s_1^* + \mathcal{R}_{01}) \\ \frac{\bar{E}\mathcal{D}}{(\mathcal{D}D-\bar{B})\bar{\mathcal{C}}} \left[s_1^* + \mathcal{R}_{01} - \frac{\mathcal{P}}{1-\mathcal{P}}(e_1^* + 1 - \mathcal{R}_{01})\right] \\ \frac{\bar{E}}{(\mathcal{D}-\bar{B})} \left[s_1^* + \mathcal{R}_{01} - \frac{\mathcal{P}}{1-\mathcal{P}}(e_1^* + 1 - \mathcal{R}_{01})\right] \end{pmatrix}.$$

We have

$$s_1^* = -\bar{E} < 0,$$

$$e_1^* = \frac{\bar{E}\mathcal{D}}{(\mathcal{D}-\bar{B})\bar{\mathcal{C}}},$$

$$\frac{\bar{E}}{\mathcal{D}-\bar{B}} = 1,$$

$$s_2^* = -\bar{E}(s_1^* + \mathcal{R}_{01}),$$

$$e_2^* = \frac{\bar{E}\mathcal{D}}{(\mathcal{D}-\bar{B})\bar{\mathcal{C}}} \left[s_1^* + \mathcal{R}_{01} - \frac{\mathcal{P}}{1-\mathcal{P}}(e_1^* + 1 - \mathcal{R}_{01})\right],$$

$$\frac{\bar{E}}{(\mathcal{D}-\bar{B})} \left[s_1^* + \mathcal{R}_{01} - \frac{\mathcal{P}}{1-\mathcal{P}}(e_1^* + 1 - \mathcal{R}_{01})\right] = 0.$$

At the critical value for $\mathcal{P}$, set $\mathcal{R}_{01} = 0$, $s_1^* = -\bar{E}$ and $e_1^* = \frac{\mathcal{D}}{\bar{\mathcal{C}}}$. Thus we solve $s_1^* + \mathcal{R}_{01} - \frac{\mathcal{P}}{1-\mathcal{P}}(e_1^* + 1 - \mathcal{R}_{01}) = 0$ to get $\mathcal{P}_{\text{crit}}$

$$\mathcal{P}_{\text{crit}} = \frac{\bar{E}\bar{\mathcal{C}}}{\bar{E}\bar{\mathcal{C}} - \mathcal{D} - \bar{\mathcal{C}}}.$$

Substituting from Table 5, the values for $\bar{\mathcal{C}}$, $\mathcal{D}$ and $\bar{E}$, we get

$$\boxed{\mathcal{P}_{\text{crit}} = \frac{(\mu+\gamma)(\mu+\nu) - \kappa\gamma\nu}{\nu\gamma(1-\kappa)}}.$$

- If $\mathcal{P} > \mathcal{P}_{\text{crit}}$ then $\mathcal{R}_{01} < 0$ and a backward bifurcation occurs.
- If $\mathcal{P} < \mathcal{P}_{\text{crit}}$ then $\mathcal{R}_{01} > 0$ and a forward bifurcation occurs.

These results are consistent with Sect. 4.2.

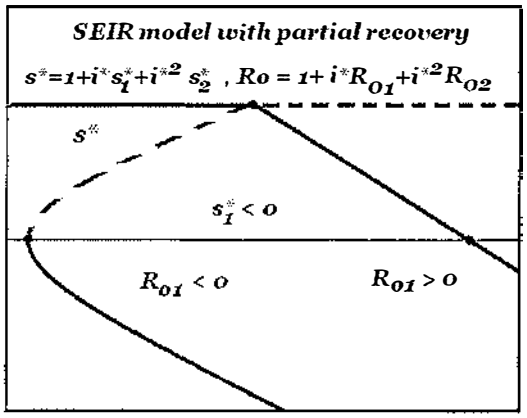

Figure 59: Enlarged top-center portion of Bifurcation diagram 32. The critical value $\mathcal{P}_{\text{crit}} = \dfrac{(\mu+\gamma)(\mu+\nu)-\kappa\gamma\nu}{\nu\gamma(1-\kappa)}$.

5.3 *SEIR* model with Full Recovery

This model is based on the paper of [14]. The system of four differential equations for this model are already mentioned in Sect. 4.3. The basic reproduction number $\mathcal{R}_0$ is same as in Sect. 4.1. Thus rescaling time so that $\mu = 1$, equation (54) becomes

$$\begin{aligned}
\frac{ds}{dt} &= 1 - \mathcal{R}_0\mathcal{D}si - s, \\
\frac{de}{dt} &= \mathcal{R}_0\mathcal{D}si - \mathcal{P}\mathcal{R}_0\mathcal{D}(1-s-e-i)i - \bar{\mathcal{C}}e, \\
\frac{di}{dt} &= \frac{\bar{\mathcal{C}}}{\bar{\mathcal{D}}}e - \mathcal{A}i.
\end{aligned}$$

See Table 5 for notations. We write this equation in a matrix framework system (65) by setting $\mathbf{y} = \begin{pmatrix} s \\ e \\ i \end{pmatrix}$.

Here $M = \begin{pmatrix} 1 & 0 & 0 \\ 0 & \bar{\mathcal{C}} & -\mathcal{P}\mathcal{R}_0 D \\ 0 & -\dfrac{\bar{\mathcal{C}}}{\bar{\mathcal{D}}} & \mathcal{A} \end{pmatrix}$, $f(\mathbf{y}) = \begin{pmatrix} 1 - \mathcal{R}_0\mathcal{D}si \\ \mathcal{R}_0\mathcal{D}si - \mathcal{P}\mathcal{R}_0\mathcal{D}(s+e+i)i \\ 0 \end{pmatrix}$.

At the steady state $\mathbf{y}^\star = \begin{pmatrix} s^\star \\ e^\star \\ i^\star \end{pmatrix}$, we have

$$\mathbf{y}^\star = M^{-1} f(\mathbf{y}^\star)$$

$$= \begin{pmatrix} 1 & 0 & 0 \\ 0 & \frac{1}{\bar{\mathcal{C}}(1-\mathcal{P}\mathcal{R}_0)} & \frac{\mathcal{P}\mathcal{R}_0\mathcal{D}}{\mathcal{A}\bar{\mathcal{C}}(1-\mathcal{P}\mathcal{R}_0)} \\ 0 & \frac{1}{\mathcal{D}(1-\mathcal{P}\mathcal{R}_0)} & \frac{1}{\mathcal{A}(1-\mathcal{P}\mathcal{R}_0)} \end{pmatrix} \begin{pmatrix} 1-\mathcal{R}_0\mathcal{D}s^\star i^\star \\ \mathcal{R}_0\mathcal{D}s^\star i^\star - \mathcal{P}\mathcal{R}_0\mathcal{D}(s^\star+e^\star+i^\star)i^\star \\ 0 \end{pmatrix}.$$

Hence,

$$\mathbf{y}^\star = \begin{pmatrix} s^\star \\ e^\star \\ i^\star \end{pmatrix} = \begin{pmatrix} 1-\mathcal{D}\mathcal{R}_0 s^\star i^\star \\ \mathcal{D}\bar{\mathcal{C}}^{-1}(1-\mathcal{P}\mathcal{R}_0)^{-1}\left[\mathcal{R}_0 s^\star i^\star(1-\mathcal{P}) - \mathcal{P}\mathcal{R}_0(e^\star+i^\star)i^\star\right] \\ (1-\mathcal{P}\mathcal{R}_0)^{-1}\left[\mathcal{R}_0 s^\star i^\star(1-\mathcal{P}) - \mathcal{P}\mathcal{R}_0(e^\star+i^\star)i^\star\right] \end{pmatrix}. \quad (71)$$

In equation (67), we apply a Taylor expansion using the perturbation variable $i^\star$. Substituting equation (68) back into equation (71), we get

$$\mathbf{y}^\star = \begin{pmatrix} 1-\mathcal{D}(i^\star + i^{\star 2}(s_1^\star + \mathcal{R}_{01})) \\ \mathcal{D}\bar{\mathcal{C}}^{-1}\left[i^\star + i^{\star 2}(s_1^\star + \mathcal{R}_{01} - \frac{\mathcal{P}}{1-\mathcal{P}}(e_1^\star+1))\right]\left(1 - \frac{i^\star\mathcal{P}\mathcal{R}_{01}}{1-\mathcal{P}} - \frac{i^{\star 2}\mathcal{P}\mathcal{R}_{02}}{1-\mathcal{P}}\right)^{-1} \\ \left[i^\star + i^{\star 2}(s_1^\star + \mathcal{R}_{01} - \frac{\mathcal{P}}{1-\mathcal{P}}(e_1^\star+1))\right]\left(1 - \frac{i^\star\mathcal{P}\mathcal{R}_{01}}{1-\mathcal{P}} - \frac{i^{\star 2}\mathcal{P}\mathcal{R}_{02}}{1-\mathcal{P}}\right)^{-1} \end{pmatrix}.$$

Again, as in Sect. 5.2, we apply a binomial expansion

$$z = \left(\frac{i^\star\mathcal{P}\mathcal{R}_{01}}{1-\mathcal{P}} + \frac{i^{\star 2}\mathcal{P}\mathcal{R}_{02}}{1-\mathcal{P}}\right).$$

substituting z into $\mathbf{y}^\star$ to have

$$\mathbf{y}^\star = \begin{pmatrix} 1-\mathcal{D}(i^\star + i^{\star 2}(s_1^\star + \mathcal{R}_{01})) \\ \mathcal{D}\bar{\mathcal{C}}^{-1}\left[i^\star + i^{\star 2}(s_1^\star + \mathcal{R}_{01} - \frac{\mathcal{P}}{1-\mathcal{P}}(e_1^\star+1))\right](1-z)^{-1} \\ \left[i^\star + i^{\star 2}(s_1^\star + \mathcal{R}_{01} - \frac{\mathcal{P}}{1-\mathcal{P}}(e_1^\star+1))\right](1-z)^{-1} \end{pmatrix}$$

Expanding $(1-z)^{-1} = 1 + z + z^2 + \mathcal{O}(z^3)$ and ignoring cubic and higher order terms, we rewrite equation (71) to get

$$\mathbf{y}^\star = \begin{pmatrix} 1 + i^\star s_1^\star + i^{\star 2} s_2^\star \\ i^\star e_1^\star + i^{\star 2} e_2^\star \\ i^\star \end{pmatrix} = \begin{pmatrix} 1-\mathcal{D}i^\star - \mathcal{D}(s_1^\star + \mathcal{R}_{01})i^{\star 2} \\ \mathcal{D}\bar{\mathcal{C}}^{-1}\left[i^\star + i^{\star 2}(s_1^\star + \mathcal{R}_{01} - \frac{\mathcal{P}}{1-\mathcal{P}}(e_1^\star + 1 - \mathcal{R}_{01})\right] \\ \left[i^\star + i^{\star 2}(s_1^\star + \mathcal{R}_{01} - \frac{\mathcal{P}}{1-\mathcal{P}}(e_1^\star + 1 - \mathcal{R}_{01}))\right] \end{pmatrix}$$

Comparing equal powers of the perturbation variable $i^\star$, we have

$$\begin{pmatrix} 1 \\ 0 \\ 0 \end{pmatrix} + i^* \begin{pmatrix} s_1^* \\ e_1^* \\ 1 \end{pmatrix} + i^{*2} \begin{pmatrix} s_2^* \\ e_2^* \\ 0 \end{pmatrix}$$

$$= \begin{pmatrix} 1 \\ 0 \\ 0 \end{pmatrix} + i^* \begin{pmatrix} -\mathcal{D} \\ \frac{\mathcal{D}}{\bar{\mathcal{C}}} \\ 1 \end{pmatrix} + i^{*2} \begin{pmatrix} -\mathcal{D}(s_1^* + \mathcal{R}_{01}) \\ \frac{\mathcal{D}}{\bar{\mathcal{C}}} \left[s_1^* + \mathcal{R}_{01} - \frac{\mathcal{P}}{1-\mathcal{P}}(e_1^* + 1 - \mathcal{R}_{01}) \right] \\ s_1^* + \mathcal{R}_{01} - \frac{\mathcal{P}}{1-\mathcal{P}}(e_1^* + 1 - \mathcal{R}_{01}) \end{pmatrix}.$$

We get

$$s_1^* = -\mathcal{D} < 0,$$

$$e_1^* = \frac{\mathcal{D}}{\bar{\mathcal{C}}},$$

$$s_2^* = -\mathcal{D}(s_1^* + \mathcal{R}_{01}),$$

$$e_2^* = \frac{\mathcal{D}}{\bar{\mathcal{C}}} \left[s_1^* + \mathcal{R}_{01} - \frac{\mathcal{P}}{1-\mathcal{P}}(e_1^* + 1 - \mathcal{R}_{01}) \right],$$

$$s_1^* + \mathcal{R}_{01} - \frac{\mathcal{P}}{1-\mathcal{P}}(e_1^* + 1 - \mathcal{R}_{01}) = 0.$$

At the critical value of $\mathcal{P}$, set $\mathcal{R}_{01} = 0$, $s_1^* = -\mathcal{D}$ and $e_1^* = \frac{\mathcal{D}}{\bar{\mathcal{C}}}$. Thus we solve $s_1^* + \mathcal{R}_{01} - \frac{\mathcal{P}}{1-\mathcal{P}}(e_1^* + 1 - \mathcal{R}_{01}) = 0$ for $\mathcal{P}_{\text{crit}}$.

$$\mathcal{P}_{\text{crit}} = \frac{\mathcal{D}\bar{\mathcal{C}}}{\mathcal{D}\bar{\mathcal{C}} - \mathcal{D} - \bar{\mathcal{C}}}.$$

From Table 5, we substitute the values for $\bar{\mathcal{C}}$ and $\mathcal{D}$

$$\mathcal{P}_{\text{crit}} = \frac{(\mu+\nu)^2(\mu+\gamma)}{(\mu+\nu)^2(\mu+\gamma) - \mu(\mu+\nu) - \mu\nu(\mu+\nu)}$$

Thus,

$$\boxed{\mathcal{P}_{\text{crit}} = \frac{(\mu+\gamma)(\mu+\nu)}{\nu\gamma}}$$

- If $\mathcal{P} > \mathcal{P}_{\text{crit}}$ then $\mathcal{R}_{01} < 0$ and a backward bifurcation occurs.
- If $\mathcal{P} < \mathcal{P}_{\text{crit}}$ then $\mathcal{R}_{01} > 0$ and a forward bifurcation occurs.

These results are consistent with Sect. 4.3.

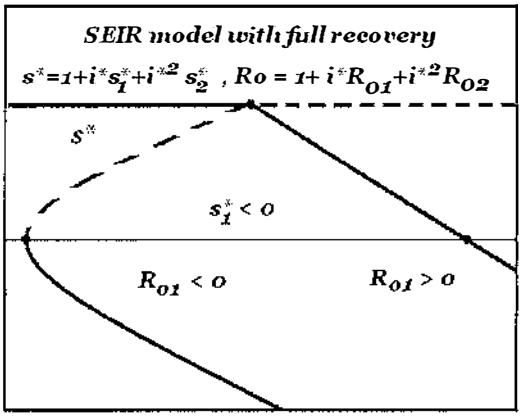

Figure 60: Blow up of the bifurcation diagram 38. Labels are as in Fig. 26. The critical value of $\mathcal{P}$ for this class is $\mathcal{P}_{\text{crit}} = \frac{(\mu+\gamma)(\mu+\nu)}{\nu\gamma}$.

5.4 The *SIR* Model with Carrier Class

Consider the ordinary differential equations (57), as discussed in Sect. 4.4. Rescaling time so that $\mu = 1$, equations (57) become

$$\begin{aligned} \frac{ds}{dt} &= 1 - xs - s \\ \frac{di}{dt} &= xs - \mathcal{A}i \\ \frac{dc}{dt} &= q(x)\frac{\gamma}{\mu}i - Bc. \end{aligned}$$

See Table 5 for notation. We know from Sect. 4.4 that $q(x)$ is a function of x. If we rewrite this in a matrix framework system (65) by setting $\mathrm{y} = \begin{pmatrix} s \\ i \\ c \end{pmatrix}$, then we have

$$M = \begin{pmatrix} 1 & 0 & 0 \\ 0 & \mathcal{A} & 0 \\ 0 & 0 & B \end{pmatrix}, \; f(\mathrm{y}) = \begin{pmatrix} 1 - xs \\ xs \\ q(x)\frac{\gamma}{\mu}i \end{pmatrix}.$$

At the steady state $\mathbf{y}^\star = \begin{pmatrix} s^\star \\ i^\star \\ c^\star \end{pmatrix}$ solves

$$\mathbf{y}^\star = M^{-1} f(\mathbf{y}^\star) = \begin{pmatrix} 1 & 0 & 0 \\ 0 & A^{-1} & 0 \\ 0 & 0 & B^{-1} \end{pmatrix} \begin{pmatrix} 1 - x^\star s^\star \\ x^\star s^\star \\ q(x^\star)\frac{\gamma}{\mu} i^\star \end{pmatrix}.$$

Setting $\mathcal{F} = \frac{\gamma}{\mu + \delta}$

$$\mathbf{y}^\star = \begin{pmatrix} s^\star \\ i^\star \\ c^\star \end{pmatrix} = \begin{pmatrix} 1 - x^\star s^\star \\ \mathcal{A}^{-1} x^\star s^\star \\ q(x^\star)\mathcal{F} i^\star \end{pmatrix}. \tag{72}$$

From Chapter 4, we know that

$$x^\star = \frac{\lambda^\star}{\mu} = \mathcal{A}\mathcal{R}_0(i^\star + \mathcal{P}c^\star).$$

We use equation (67) to apply a Taylor expansion using $i^\star$ as the perturbation variable. In this model, we have the proportion of the carrier class $c(t)$ instead of the proportion of the exogenous class $e(t)$. Thus, we keep $\mathcal{R}_0$ and $s^\star$ from equation (67) and expand $c^\star$, $x^\star$ and $q(x^\star)$ to have.

$$c^\star = i^\star c_1^\star + i^{\star 2} c_2^\star + \mathcal{O}(i^{\star 3}),$$

$$x^\star = i^\star x_1^\star + i^{\star 2} x_2^\star + \mathcal{O}(i^{\star 3})$$

$$= \mathcal{A}[i^\star(1 + \mathcal{P}c_1^\star) + i^{\star 2}(\mathcal{P}c_2^\star + \mathcal{R}_{01} + \mathcal{P}\mathcal{R}_{01}c_1^\star)] + \mathcal{O}(i^{\star 3}),$$

$$q(x^\star) = x^\star q_1 + x^{\star 2} q_2 = i^\star x_1^\star q_1 + i^{\star 2}(x_2^\star q_1 + x_1^{\star 2} q_2) + \mathcal{O}(i^{\star 3}).$$

Ignoring all cubics and higher order terms, we get

$$x^\star s^\star = i^\star x_1^\star + i^{\star 2}(x_1^\star s_1^\star + x_2^\star),$$

$$q(x^\star) i^\star = i^{\star 2} x_1^\star q_1,$$

Substituting the values of $x^\star s^\star$ and $q(x^\star)i^\star$ in equation (72) to get

$$\mathbf{y}^\star = \begin{pmatrix} 1 + i^\star s_1^\star + i^{\star 2} s_2^\star \\ i^\star \\ i^\star c_1^\star + i^{\star 2} c_2^\star \end{pmatrix} = \begin{pmatrix} 1 - i x_1^\star - i^{\star 2} x_2^\star \\ \mathcal{A}^{-1}(i^\star x_1^\star + i^{\star 2} x_2^\star) \\ \mathcal{F} i^{\star 2} x_1^\star q_1 \end{pmatrix}$$

or

$$\begin{pmatrix} 1 \\ 0 \\ 0 \end{pmatrix} + i^* \begin{pmatrix} s_1^* \\ 1 \\ c_1^* \end{pmatrix} + i^{*2} \begin{pmatrix} s_2^* \\ 0 \\ c_2^* \end{pmatrix} = \begin{pmatrix} 1 \\ 0 \\ 0 \end{pmatrix} + i^* \begin{pmatrix} -x_1^* \\ \mathcal{A}^{-1}x_1^* \\ 0 \end{pmatrix} + i^{*2} \begin{pmatrix} -(x_1^* s_1^* + x_2^*) \\ \mathcal{A}^{-1}(x_1^* s_1^* + x_2^*) \\ \mathcal{F}x_1^* q_1 \end{pmatrix}$$

where,

$$x_1^* = \mathcal{A}(1 + \mathcal{P}c_1^*),$$

$$x_2^* = \mathcal{A}(\mathcal{P}c_2^* + \mathcal{R}_{01} + \mathcal{P}\mathcal{R}_{01}c_1^*).$$

We now substitute the values of x_1^* and x_2^* and comparing equal powers of i^* to have

$$s_1^* = -x_1^* = -\mathcal{A}(1 + \mathcal{P}c_1^*) < 0,$$

$$c_1^* = 0,$$

$$s_2^* = -\mathcal{A}[(1 + \mathcal{P}c_1^*)s_1^* + \mathcal{P}c_2^* + \mathcal{R}_{01} + \mathcal{P}\mathcal{R}_{01}c_1^*],$$

$$\begin{aligned} s_1^*(1 + \mathcal{P}c_1^*) + \mathcal{P}c_2^* + \mathcal{R}_{01} + \mathcal{P}\mathcal{R}_{01}c_1^* &= 0. \qquad (73) \\ c_2^* = \mathcal{F}\mathcal{A}q_1(1 + \mathcal{P}c_1^*). & \end{aligned}$$

At the critical value for $\mathcal{P}$, $\mathcal{R}_{01} = 0$, and substituting values s_1^*, c_1^* and c_2^*, equation (73) becomes

$$\mathcal{P} = \frac{1}{\mathcal{F}q_1}.$$

We know that $\mathcal{F} = \frac{\gamma}{\mu + \delta}$, hence

$$\boxed{\mathcal{P}_{\text{crit}} = \frac{\mu + \delta}{\gamma q_1}}$$

- If $\mathcal{P} > \mathcal{P}_{\text{crit}}$ then $\mathcal{R}_{01} < 0$ and a backward bifurcation occurs.
- If $\mathcal{P} < \mathcal{P}_{\text{crit}}$ then $\mathcal{R}_{01} > 0$ and a forward bifurcation occurs.

These results are consistent with Sect. 4.4. This concludes that a backward bifurcation occurs when $\mathcal{R}_{01} < 1$, and for $\mathcal{R}_{01} > 1$, a forward bifurcation occurs. These results are consistent with the carrier class given in Sect. 4.4, and are only valid when $q(0) = 0$ and $q'(0) = q_1 > 0$ (as discussed in Sect. 4.4). This general analysis only works for functions such as

$$q(x) = \frac{q_1 x}{1 + x}, q'(x) = \frac{q_1}{(1 + x)^2}$$

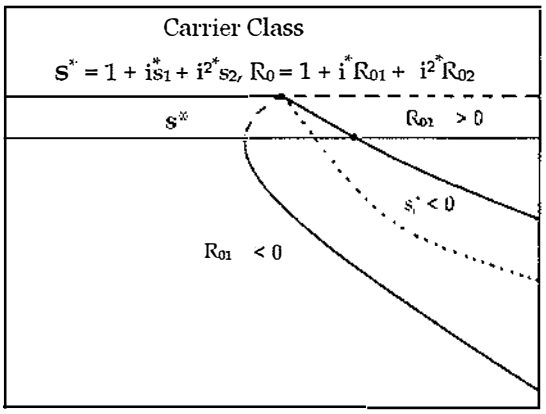

Figure 61: A top-center blow up of Bifurcation diagram 44. Labels are as in Fig. 26. The critical value for $\mathcal{P}$ is $\mathcal{P}_{\text{crit}} = \frac{\mu + \delta}{\gamma q'(x^*)}$.

$$q(x) = 1 - e^{-q_1 x}, q'(x) = q_1 e^{-q_1 x}.$$

6 Discussion

The infection-free steady state, in the renowned *SIR* endemic model, is globally stable for $\mathcal{R}_0 < 1$ and unstable for $\mathcal{R}_0 > 1$. This gives rise to a forward bifurcation at $\mathcal{R}_0 = 1$. Asymptotic stability in the *SIR* endemic model shows that there is an infection that persists endemically when $\mathcal{R}_0 > 1$. We considered the basic reproduction number $\mathcal{R}_0$ as a main bifurcation parameter, which has been used to determine the stability of the steady states of the *SIR* endemic model. In this thesis we mainly focused on the two and three dimensional extensions, of the *SIR* endemic model, for which a backward bifurcation occurs at $\mathcal{R}_0 = 1$. For this we chose some reasonable biological factors that lead to the phenomena of the backward bifurcation, multiple endemic steady states and hysteresis with some parameter values. We applied analytical and numerical tools to investigate these phenomena.

Furthermore we presented a general classification of the two and three dimensional extensions of the *SIR* endemic model in which we expanded steady state solutions, in terms of a small perturbation variable i^*. We used Taylor and Binomial expansions in order to establish a matrix framework. Moreover, we showed that the results given in the general classification are consistent with the results deduced in the qualitative approach.

Accordingly in Chapter 1, we gave a brief background of the *SIR* model and its two main examples i.e. the *SIR* epidemic model and the *SIR* endemic model. In two short segments Sect. 1.2 and Sect. 1.3 we discussed these examples. We also studied and reproduced the bifurcation analysis which is done in [12]. In Sect. 1.2, we briefly looked at the *SIR* epidemic model while in the Sect. 1.3 we thoroughly investigated the steady state solutions, their stability and their phase-plane analysis. The purpose of this thesis is to closely investigate the *SIR* endemic model and its extensions.

In the extended models we used $\mathcal{P}$ as a secondary bifurcation parameter, whose precise definition differs between the models. In Chapter 2, we examined two dimensional extensions of the *SIR* endemic model which are: the *SIR* with a susceptible R class (Sect. 2.1); non-linear transmission (Sect. 2.2); and exogenous infection (Sect. 2.3). We classified these models in five steps. Firstly we used a Dulac's criteria to rule out limit cycles and then we evaluated the steady state solutions of these models by setting the right-hand side of the differential equations to zero. Then we found the critical value for $\mathcal{P}$ and a saddle node equation of $\mathcal{R}_0$ which solved for $\mathcal{R}_{\text{saddle}}$, the minimum value of $\mathcal{R}_0$ for which a steady state exists. Thirdly, we linearised the system to find the local stability of these steady state solutions. We used PPLANE, the numerical program of **MATLAB** [10] to

plot bifurcation and phase-plane diagrams for a variety of parameter values given in each section. We analysed bifurcations and the phase-planes using a threshold parameter $\mathcal{R}_0$ and a secondary parameter $\mathcal{P}$, adopting the idea from [12]. The secondary parameter $\mathcal{P}$ has different definition for each model.

In Sect. 2.1, we studied a model from [13]. We found that, for $\mathcal{R}_0 > 1$, a forward bifurcation exists at $\mathcal{R}_0 = 1$, when there is an unstable infection-free steady state and a unique endemic steady state independent of $\mathcal{P}$. A backward bifurcation occurs, when a stable infection-free steady state and multiple endemic steady states exist for $\mathcal{R}_{\text{saddle}} < \mathcal{R}_0 < 1$ and $\mathcal{P} > \mathcal{P}_{\text{crit}}$. This also causes the hysteresis phenomenon.

Usually it is assumed that with nonlinear transmission, we find only a forward bifurcation. Instead we discovered in Sect. 2.2, a function $h(i)$ that depends on the infectives and satisfies certain biological conditions. We also used a theorem from the paper of Gomes [6] that fails to prove the existence of any limit cycle for this function. We also observed that this model exhibits a backward bifurcation and hysteresis phenomena.

In Sect. 2.3, we have investigated a model, introduced by [4], in which the recovered class is replaced from the exposed class. This model also exhibited the backward bifurcation phenomenon.

Now, in Chapter 3, we applied a general classification for the two dimensional extensions of the *SIR* endemic model. We investigated the different dynamics applying Taylor and Binomial expansions by a perturbation variable $i^\star$ near the bifurcation point i.e. near $\mathcal{R}_0 = 1$. We checked if the results at the turning points are consistent with the results found in Chapter 2.

Chapter 4 took account of three dimensional extensions of the *SIR* endemic model. We considered the same strategy as in Chapter 2 except for the following: we cannot use Dulac's criteria with the three dimensional differential equations; we linearised the 3×3 Jacobian matrices using **Maple** [5]; we checked the stability using the Routh-Hurwitz Criteria; and we used ODE45, a numerical package of **MATLAB** [10], to plot phase-plane diagrams. These phase-planes plotted, by putting three dimensions onto the two dimensional projection, hence the trajectories may appear to coincide. We studied four three dimensional extensions: *SEIR* model (Sect. 4.1); *SEIR* model with full recovery class (Sect. 4.2); *SEIR* model with partial recovery class (Sect. 4.3); and *SIR* model with a carrier class (Sect. 4.4).

In Sect. 4.1, Sect. 4.2, Sect. 4.3, the models are similar to the two dimensional *SIR* model with exogenous infection in Sect. 2.3. These models have a recovered class as well as the exposed class. Sections 4.2 and 4.3 were proposed in a paper by [14]. We checked with our qualitative approach that these models are consistent with the techniques used in [14]. We also proved that these models exhibit backward bifurcation.

In Sect. 4.4, we considered a carrier class instead of exogenous class. In this model we had a proportion $q(x)$ which is a function of $x = \frac{\beta(i+\mathcal{P}c)}{\mu}$ that become carriers. We assumed that for $q(x) = 0$, $q'(x) \geq 0$ when $x \geq 0$. This assumption led to the two examples of carrier class; *Example 1* had a function $q(x) = 1 - e^{0.9x}$ and; *Example 2* had a function $q(x) = \frac{x^2}{x^2+2}$. *Example 1* exhibited the same phenomenon i.e. backward bifurcation occurs at $\mathcal{R}_0 = 1$ as in Sect. 4.1, Sect. 4.2, Sect. 4.3. On the other hand, *Example 2* exhibited two backward bifurcations. The bifurcation at $\mathcal{R}_0 = 1$ is forward but the locus of steady state turns backward for some $\mathcal{R}_0 > 1$.

Lastly in Chapter 5, we have a similar general classification for three dimensional extensions as in Chapter 3. We found that these models are consistent with the results we had deduced in Chapter 4. In Sect. 5.4, we showed that the results are compatible only for certain function $q(x)$ such as in *Example 1*.

Finally we conclude that the calculations contained in this thesis will be useful in developing an understanding of both numerical and analytical methods using **MATLAB** [10] and **Maple** [5] respectively, and our results in Chapters 2 and 4 are consistent with those in Chapters 3 and 5.

References

[1] Diekmann, O., J. A. P. Heesterbeek. 2000. *Mathematical epidemiology of infectious disease: model building, analysis and interpretation. Wiley series in mathematical and computational biology.* Wiley, Chichester, UK.

[2] Edelstein-Keshet, L. 2005. *Mathematical Models in Biology.* Society for Industrial and Applied Mathematics, Philadelphia PA.

[3] Ellner, S. P. and J. Guckenheimer. 2006. *Differential equation models for infectious disease.* Princeton University Press, Princeton, NJ.

[4] Feng, Z., C. Castillo-Chavez and A. F. Capurro. 2000. A Model for tuberculosis with exogenous reinfection. *Theoretical Population Biology* 57: 235-247.

[5] Garvan, Frank. 2001. The Maple Book. Chapman & Hall/CRC Press. `http://www.maplesoft.com` (accessed November 28, 2001).

[6] Gomes, M. G. M., A. Margheri, G. F. Medley and C. Rebelo. 2005. Dynamical behaviour of epidemiological models with sub-optimal immunity and nonlinear incidence. *Journal of Mathematical Biology* 51: 414-430.

[7] Kermack, W. O. and A. G. McKendrick. 1927. A Contribution to the mathematical theory of epidemics **I**. *Proc. Roy. Soc. London A*115: 700-721.

[8] Korobeinikov, A. 2001. *Stability and Bifurcation of Deterministic Infectious Disease.* ResearchSpace@Auckland.

[9] Medley, G. F., N. A. Lindop, W. J. Edmunds and D. J. Nokes. 2001. Hepatitis-B virus endemicity: heterogeneity, catastrophic dynamics and control. *Nature Medicine.* 5: 619-624.

[10] Moler, Cleve B. 2004. Numerical Computing with MATLAB. Cambridge University Press. `http://www.mathworks.com` (accessed January 1, 2004).

[11] Rhodes, A. J. and E. S. Allman. 2004. *Mathematical Models in Biology: An Introduction.* Cambridge University Press, Cambridge, UK.

[12] Roberts, M. G. 2007. The pluses and minuses of $\mathcal{R}_0$. *Journal of the Royal Society Interface* 4: 949-961.

[13] Safan, M., J. A. P. Heesterbeek and K. Dietz. 2006. The minimum effort required to eradicate infections in models with backward bifurcation. *Journal of Mathematical Biology* 53: 703-718.

[14] van den Driessche, P. and J. Watmough. 2002. Reproduction numbers and subthreshold endemic equilibria for computational models of disease transmission. *Mathematical Biosciences* 180: 29-48.

Massey University

Declaration Confirming Content of Digital Version of Thesis

I confirm that the content of the digital version of this thesis

Title: BACKWARD BIFURCATION IN SIR ENDEMIC MODELS

is the final amended version following the examination process and is identical to this hard bound paper copy.

Student's Name: SAMEEHA QAISER SIDDIQUI

Student's Signature:

Date: 9th April 09